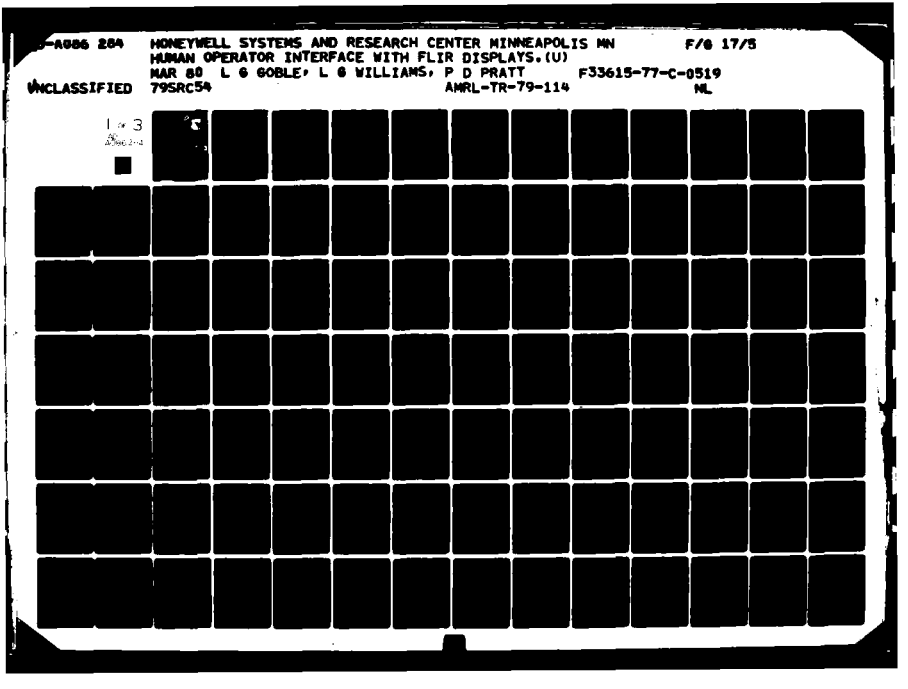
-A086 284
HONEYWELL SYSTEMS AND RESEARCH CENTER MINNEAPOLIS MN
F/G 17/5
HUMAN OPERATOR INTERFACE WITH FLIR DISPLAYS.(U)
MAR 80 L G GOBLE, L G WILLIAMS, P D PRATT
F33615-77-C-0519
UNCLASSIFIED
79SRC54
AMRL-TR-79-114
NL
1 of 3

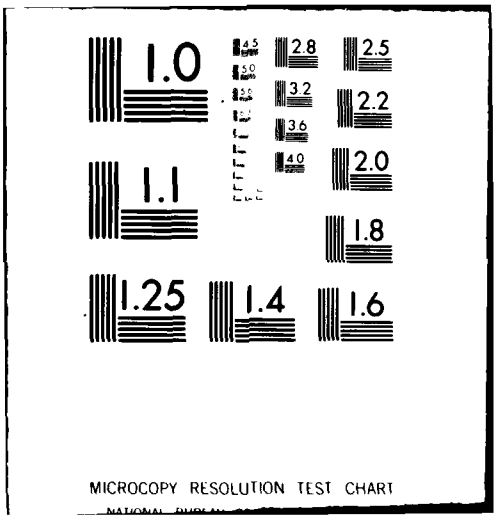
1.0
1.1
1.25
1.4
1.6
1.8
2.0
2.2
2.5
2.8
3.2
3.6
4.0
MICROCOPY RESOLUTION TEST CHART

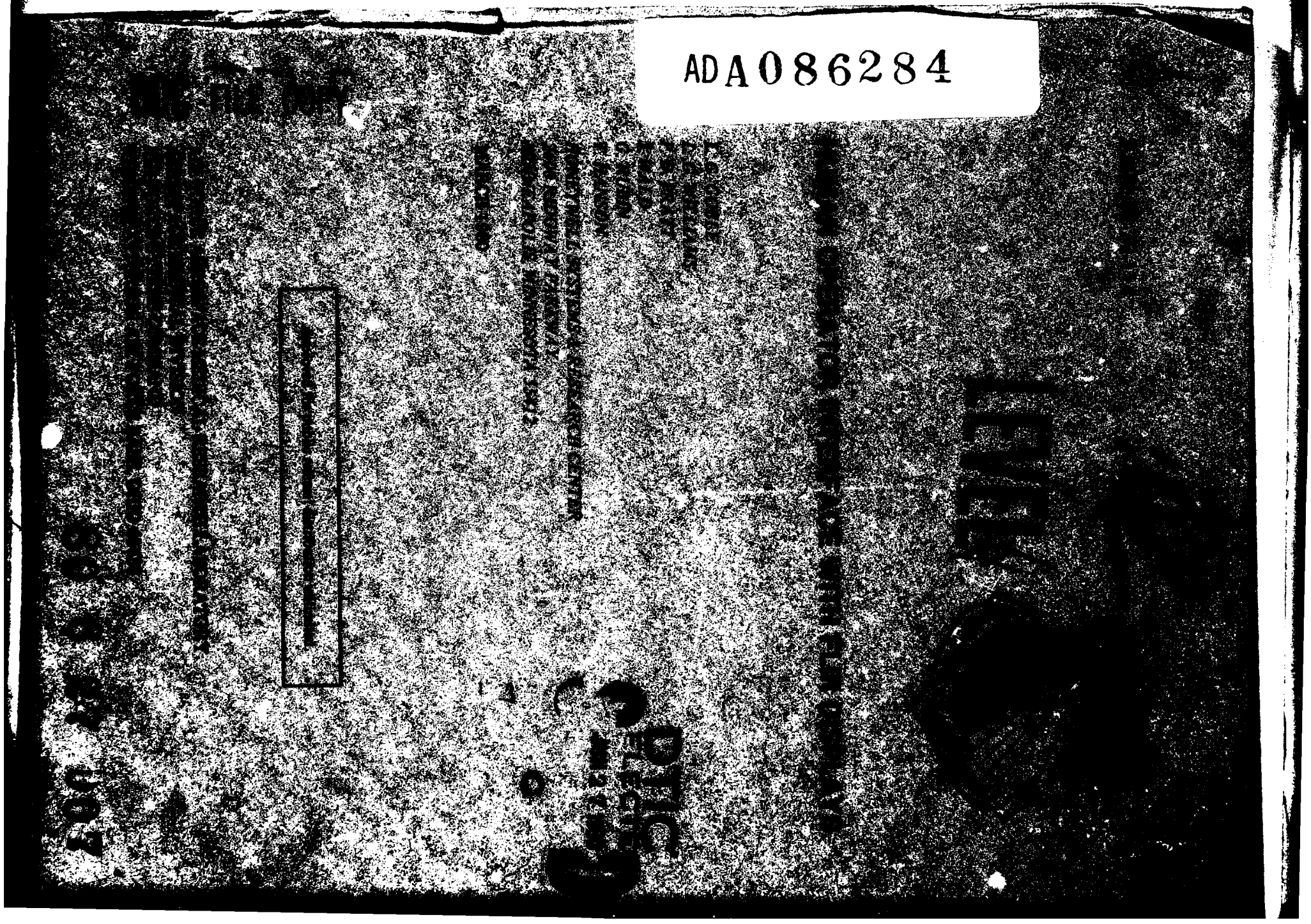

[illegible]

[illegible]

[illegible] copies of this report from Air Force Aerospace Medical Research Laboratory. [illegible]

National Technical Information Service
5285 Port Royal Road
Springfield, Virginia 22161

Federal Government agencies and their contractors registered with Defense Documentation Center should direct requests for copies of this report to:

Defense Documentation Center
Cameron Station
Alexandria, Virginia 22314

TECHNICAL REVIEW AND APPROVAL

AMRL-TR-79-114

This report has been reviewed by the Office of Public Affairs (PA) and is releasable to the National Technical Information Service (NTIS). At NTIS, it will be available to the general public, including foreign nations.

This technical report has been reviewed and is approved for publication.

FOR THE COMMANDER

[illegible]
Chief
[illegible] Division
Air Force Aerospace Medical Research Laboratory

[illegible]

SECURITY CLASSIFICATION OF THIS PAGE (When Data Entered)

REPORT DOCUMENTATION PAGE

READ INSTRUCTIONS BEFORE COMPLETING FORM

1. REPORT NUMBER: AMRL-TR-79-114	2. GOVT ACCESSION NO.: AD-A086 284
3. RECIPIENT'S CATALOG NUMBER:	
4. TITLE (and Subtitle): HUMAN OPERATOR INTERFACE WITH FLIR DISPLAYS.	5. TYPE OF REPORT & PERIOD COVERED: Final Report, Jun 1977 — Sep 1979
	6. PERFORMING ORG. REPORT NUMBER: 79SRC54
7. AUTHOR(s): G. Goble, L. G. Williams, P. D. Pratt, J. Wald, G. Rubin, T. Hanson	8. CONTRACT OR GRANT NUMBER(s): F33615-77-C-0519
9. PERFORMING ORGANIZATION NAME AND ADDRESS: Honeywell Systems and Research Center, 2600 Ridgway Parkway, Minneapolis, Minnesota 55413	10. PROGRAM ELEMENT, PROJECT, TASK AREA & WORK UNIT NUMBERS: 62202F, 7184-11-28
11. CONTROLLING OFFICE NAME AND ADDRESS: Air Force Aerospace Medical Research Laboratory, Aerospace Medical Division, Air Force Systems Com, Wright-Patterson Air Force Base, Ohio 45433	12. REPORT DATE: Mar 1980
	13. NUMBER OF PAGES: 251
14. MONITORING AGENCY NAME & ADDRESS (if different from Controlling Office): 251	15. SECURITY CLASS. (of this report): Unclassified
	15a. DECLASSIFICATION/DOWNGRADING SCHEDULE:

16. DISTRIBUTION STATEMENT (of this Report)

Approved for public release; distribution unlimited.

17. DISTRIBUTION STATEMENT (of the abstract entered in Block 20, if different from Report)

18. SUPPLEMENTARY NOTES

19. KEY WORDS (Continue on reverse side if necessary and identify by block number)

Digital Image processing	Human factors
Modulation transfer function	Noise-equivalent delta temperature
Minimum resolvable temperature	Image quality
Night Vision Laboratory Model	Mathematical modeling
	Infrared system model

20. ABSTRACT (Continue on reverse side if necessary and identify by block number)

This report presents an extensive review of factors which limit performance of forward-looking infrared (FLIR) systems. Two critical variables of system performance, modulation transfer function (MTF) and noise equivalent delta temperature (NEΔT), were chosen for further experimental analysis. The experiment used a digital simulation of the minimum resolvable temperature (MRT) paradigm to test two modeled FLIR systems.

(Cont'd)

DD FORM 1 JAN 73 1473 EDITION OF 1 NOV 65 IS OBSOLETE

SECURITY CLASSIFICATION OF THIS PAGE (When Data Entered)

AD-A086 284

20. Abstract (Cont'd)

Detection and recognition data were collected for two targets (four-bar and square) in trials with varying levels of size, contrast, noise, and MTF. The test results were compared with the NVL predictive model (Ratches, et al., 1975) used to evaluate FLIR system performance.

PREFACE

The research described in this report was funded by the Air Force Aerospace Medical Research Laboratory, Human Engineering Division, Visual Display Systems Branch of the United States Air Force under Contract F33615-77-C-0519, monitored by William N. Kama. The authors thank W. N. Kama, H. L. Task, and W. Martin for their useful suggestions, careful review, and continuing interest in this work. The authors thank C. P. Graf for his timely suggestions and M. Voth for the development and debugging of software. The Principal Investigator for Honeywell was Mr. Larry Goble.

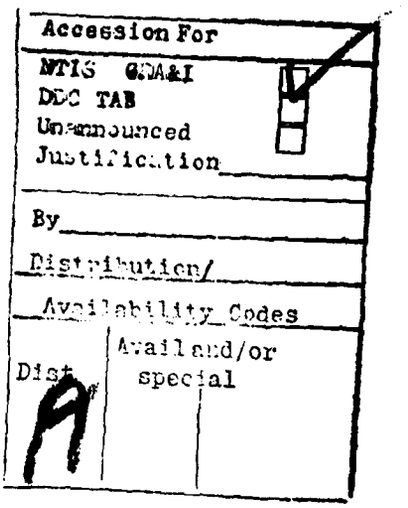

SUMMARY

The purpose of this report is twofold: first, to review the literature on factors which limit forward-looking infrared (FLIR) systems and their use in a European setting; and second, to evaluate empirically a current and second-generation system in terms of some of the system parameters surveyed. The structure of the report reflects these aims.

The first major section of this report provides a synthesis of a wide variety of literature that most heavily deals with the following:

1) FLIR system uses within the military, focusing on Air Force requirements in Europe
2) FLIR system design considerations
3) Recent FLIR system developments and analyses
4) Human operator performance using FLIR imagery

The second section of the report describes an experiment undertaken by Honeywell Systems and Research Center personnel. Two critical variables of system performance, modulation transfer function (MTF) and noise equivalent delta temperature (NEΔT), were chosen for experimental analysis. The experiment used a digital simulation of the minimum resolvable temperature (MRT) paradigm to test two modeled FLIR systems. Twelve male subjects with 20/20 uncorrected vision served as subjects for a forced-choice psychophysical procedure. Detection and recognition data were collected for two targets (four-bar and square) in trials with varying

levels of size, contrast, noise, and MTF. The test results were compared with the NVL predictive model (Ratches, et al., 1975) used to evaluate FLIR system performance. The empirically derived data agreed with the NVL predictive predictive MRT function with some important differences. Namely, the subjects' MRTs fell consistently below the predicted function values: also experimental MRTs showed a leveling at lower spatial frequencies (larger targets).

CONTENTS

CONTENTS (concluded)

LIST OF ILLUSTRATIONS

LIST OF ILLUSTRATIONS (continued)

LIST OF ILLUSTRATIONS (continued)

LIST OF ILLUSTRATIONS (continued)

LIST OF ILLUSTRATIONS (concluded)

LIST OF TABLES

LIST OF TABLES (concluded)

SECTION I

FLIR LITERATURE REVIEW

INTRODUCTION

Within the military, FLIR systems enjoy wide use. Applications are numerous and far-ranging. For example, FLIR systems are used for tank fire control, high-speed aircraft target acquisition, nighttime surveillance, and nighttime target classification (Klass, 1973; Maldonato, 1974). Each of these uses takes advantage of the unique capabilities that FLIR systems afford: the ability to detect objects with temperatures significantly different from their backgrounds (for example, warm tanks that stand out from their cooler nighttime backgrounds), the daytime potential to sense camouflaged objects not readily seen or differentiated by TV sensors or human observers, and the capability to penetrate fog, haze, and smoke conditions that generally limit the utility of microwave and visual sensors (Miller, 1973a; Lloyd, 1975a). Under these conditions, the infrared range can be three to six times that of the visual range (Miller, 1973a).

Unfortunately, each use of FLIR requires that a different set of conditions be satisfied and raises unique problems. Resolution requirements vary, depending on whether target detection or recognition is desired; fields of view must be larger or smaller, depending on the area to be covered in order to accomplish a mission (compare pinpointing a target to landing a helicopter in an unimproved field at night); system size and weight must be limited to the extent that the system should be portable or cost and power efficient; and so on.

The FLIR community's initial response was to design a separate FLIR system for each application. In the early 1970's, the Department of Defense, Research and Engineering studied the situation and suggested that a modular approach to FLIR design be followed. The idea was to identify classes of FLIR use and to design a family of FLIR night-vision systems for each kind of use. As Klass (1973) wrote at the time,

> Each class of FLIR would include a family of modular subsystems to enable the needs of any specific weapons system to be met by appropriate selection of subsystems, rather than designing a new FLIR for almost every new application as in the past (p. 17).

The modular concept has influenced FLIR design ever since (see, for example, Kruse, 1976).

Among the families of modular systems identified were those required for high-speed aircraft and for general surveillance. The rest of this review will focus on FLIR systems intended for these uses. This is necessary, modular commonality notwithstanding, since different FLIR uses still have different system requirements.

FLIR USES IN A EUROPEAN SETTING

Analyses of the European scenarios for a 1985-1990 time frame indicate a variety of uses for FLIR systems. Those for advanced fighter/attack aircraft missions will be dealt with here.

Representative of the advanced fighter aircraft missions that are projected for a European theatre are the air-to-ground missions discussed in a recent document written at Honeywell, Incorporated (Hanson, Jones, Macek, Peters, and Sandvig, 1978). The document analyzes specific types of missions, among them deep strike and battlefield interdiction. These missions use FLIR systems in some capacity.

In the case of the deep-strike mission, it is anticipated that FLIR systems might be used as one of a variety of alternative sensor and weapon combinations. For example, a FLIR sensor (with data link) might be used with a GBU-15 type weapon in conjunction with a global positioning satellite (CPS) controlled launch point (Hanson, Jones, Macek, Peters, and Sandvig, 1978). In the case of the battlefield interdiction mission, FLIR systems will enjoy a more prominent role as the primary ground search sensor. If the FLIR devices used in these missions are to perform adequately, they must be able to operate under the sets of constraints determined by each mission's purpose and the conditions under which it is flown.

The purposes of the two missions differ. Deep-strike missions attack primary targets and installations at known and relatively fixed positions. Synthetic aperture radar is used as the primary ground search sensor. In addition, target imagery is available in advance of the mission. In contrast, the battlefield interdiction mission is conducted against weapons, personnel, transportation, and ground force supplies. Typically, the targets are in a known, but not fixed, position. Consequently, target identification is required using aerial reconnaissance and surveillance sensors such as those provided by a FLIR system.

Some of the conditions under which the two missions will have to be flown are different; notably, their flight profiles: during the attack phase of the deep-strike mission, high altitudes (60,000 ft) and supersonic speeds are attained. During the comparable phase of the battlefield interdiction mission, however, a low altitude and somewhat slower speed (100 ft; M 1.2) (Hanson, Jones, Macek, Peters, and Sandvig, 1978).*

There are other conditions under which the two missions will have to be flown that are comparable and require a FLIR sensor's capabilities. Each requires operational capabilities for day and night missions and each has to be flown in less than optimal weather much of the time. In Europe, in particular, one expects to have to operate under conditions of limited visibility characterized by a low ceiling (low clouds) and haze (see below). However, these environmental conditions, along with system parameters and operator characteristics, limit FLIR system's performance. The remainder of this review identifies the more important of these system and operator factors and discusses their influences on FLIR system performance.

SURVEY OF FACTORS INFLUENCING FLIR PERFORMANCE

Background

FLIR systems are designed to detect long-wavelength infrared radiation that is received at the sensor. The image produced by the FLIR system is a function of the variations in the radiation received.

---

*Altitude and speed change with the phase of the missions.

There are four sources of radiation in the environment: background, foreground, atmosphere, and target objects. These sources can contribute to the variation of radiation in three ways: through emissivity, through reflection, and through assorption. These aspects of infrared radiation cause some of the special problems associated with FLIR systems and some of the difficulties encountered in the interpretation and processing of FLIR imagery.

Some of these problems are best illuminated by a comparison of FLIR systems with other electro-optical devices. Active and passive TV systems,* for example, make use of the visible spectrum, sometimes in the near-infrared region. These systems primarily detect reflected light. Given the constant reflectivity of the surfaces present, as the ambient illumination changes the modulation of the overall scene changes proportionately. As a result, the dynamic range requirements of TV systems remain proportionately the same. This is not the case when one turns to an infrared system. Because the radiation within this region comes not only from the relative reflectivity of the environmental surfaces viewed by an infrared sensor, but also from the emissivity of the objects themselves, the infrared modulation of the scene does not change proportionately with an overall average change (that is, with ambient coolings and warmings). Because of

---

*The term active implies that an auxiliary scene irradiator, located near or at the television sensor, is used. Passive systems do not use such auxiliary irradiators, relying instead on natural sources of irradiation (Sendall and Rosell, 1973).

this, dynamic range considerations remain important.* Large areas may have extreme modulations but at the same time contain important smaller modulations that must be detected (Sendall and Rosell, 1973).†

Associated with the lack of an invariant background-object relationship is another difference between electro-optical and infrared sensors that has potential perceptual significance. Because TV sensors make use of the same sources of information that the human visual system does, the imagery

---

*Lloyd writes,

> The dynamic range of a system is described by a temperature difference dynamic range and by a luminance dynamic range... The dynamic range of ΔT is the maximum scene ΔT which is displayed unclipped for a particular condition of control settings. The maximum dynamic range of ΔT is the maximum unclipped ΔT for the lowest gain setting. The luminance dynamic range gives the maximum luminance the system produces (p. 432, 1975b).

†Narendra, Tack, and Joseph (1977) note the following:

> Thermal imagers have a high inherent scene dynamic range. For example, the dynamic range of a FLIR scene with a cold sky and hot ground background can be as high as 1000:1, with a 100 deg temperature range and 0.1 deg MRT (the minimum resolvable temperature, which is discussed in the text below). With the advent of higher-sensitivity detectors the dynamic range could be even greater. This high dynamic range video information must be displayed on an imager display that has a luminance range typically of 15:1 to 30:1. If saturation in some part of the display and blackout in others is to be avoided, the gain of the display should be set very low. This means that low contrast (temperature difference) information in the scheme is translated to even smaller luminance (brightness) differences on the display, and cannot be perceived by the operator as it falls below the contrast sensitivity threshold (p. 53).

produced corresponds to what an observer of that scene would see. Infrared sensors provide a different image of the scene. This image has both advantages and disadvantages for the operator. Fundamental advantages derive from the following two facts: (1) within the infrared range a target object acts as its own source and (2) the object's radiation is not blocked by such things as brush, camouflage, or haze to the extent that radiation in the visible spectrum is. Consequently, object outlines remain relatively intact when viewed by an infrared sensor. Coupled with this outcome is the further fact that objects viewed by an infrared sensor do not produce real-time shadows, but only shadows that are temperature gradients built up over time. Taken together, these characteristics of infrared imagery mean that the objects imaged appear more distinctive when viewed by an infrared sensor than when viewed by its electro-optical counterpart (Sendall and Rosell, 1973).

However, the very distinctiveness of infrared imagery can present problems insofar as the infrared signatures are perceptually different from the objects as they are seen visually or as they might appear on the display of an electro-optical system. The problem is discussed in the following terms by Sendall and Rosell (1973):

> For the various natural objects, the IR scene varies with aspect angle, foreground, and background as well as atmosphere. The following summarizes the important parameters and their general relationships. The emissivity of the various objects is constant with time (except for dew, etc.) but a function of aspect angle. Therefore, it is a function of time when the sensor is moving. The temperature is a strong function of time as sky conditions, air temperature, and the effects of the sun vary with time. The apparent temperature of various areas of the scene is a strong function of the actual temperature, emissivity, and background. Man-made objects

> exhibit similar but different characteristics. They often have their temperature determined by heat sources other than the sun. When the sun and natural conditions determine the temperature variations on man-made objects, they present a very natural TV-like image. When they have temperature differences due to localized heating, the image can be very unnatural (pp. 22-23).

Regardless of the natural or unnatural appearances of objects, their detection and recognition is of fundamental military importance. Therefore, in order to anticipate FLIR requirements for their use in Europe, it is worth enumerating various variables associated with FLIR systems that affect system/operator performance in general. Each variable can be assigned to one of three broad categories: environmental, system, or operator. In turn, each category can be broken down further. This has been done in Table 1.

The influence of each of these variable categories may be characterized as follows:

Environmental

1) Establishes the dynamic range that must be handled by the system

2) Determines the windows that transmit useful amounts of information and the spectral characteristics of transmittance through these windows

3) May indirectly influence resolution requirements of the system since amount of detail required for target detection or recognition varies as a function of clutter and contrast

TABLE 1. BREAKDOWN OF SOME OF THE VARIABLE CATEGORIES THAT AFFECT FLIR SYSTEM/OPERATOR PERFORMANCE

ENVIRONMENTAL VARIABLES	
Atmosphere	**Scene**
Humidity	Target characteristics
Aerosol content	Background characteristics
Cloud cover	Clutter
Haze, smoke, fog (and other atmospheric suspensions)	

SYSTEM VARIABLES		
Sensor	**Image Processing**	**Display**
Bandwidth	Static & dynamic enhancements (for example, edge and contrast enhancements)	Luminance
Number of scan lines		Size
MTF		Number of scan lines
Field of view		MTF
Field/frame rate		Contrast
Aspect ratio		Dynamic range
Signal-to-noise ratio	Spatial filtering	Scene movement
Integration time		Signal-to-noise ratio
Scan mode: serial, parallel		Aspect ratio
Detector detectivity		Gamma
Detector architecture		Field of view
		Bandwidth

OPERATOR VARIABLES	
Perceptual	**Situational**
Spatial integration	Task (for example, identification vs recognition)
Temporal integration	Briefing
Contrast sensitivity	Lighting
MTF	Display vibration stress
Signal-to-noise ratio	
Light/dark adaptation level	

4) Can set sensitivity requirements in that atmosphere will attenuate signal transmission and reduce contrast

System

1) Influences bandwidth of signal transmitted

2) Affects bandpass characteristics of the signal transmitted

3) Affects signal-to-noise ratio and contrast of the signal transmitted

4) Affects display of information that can influence operator performance.

Operator

1) Can limit which signals are detectable

2) Can determine which signals are sufficient to accomplish particular tasks

3) Can influence the interpretability of particular signals

Aspects of each variable category will now be examined in more detail.

Environmental Factors

Probably the most important set of environmental variables that will influence FLIR performance in Central Europe has to do with the atmospheric conditions found there. Winter months are often characterized by low ceilings and limited visibility. During summer months, visibility is much improved and cloud cover is not as great a problem. These conditions are shown graphically in Figure 1.

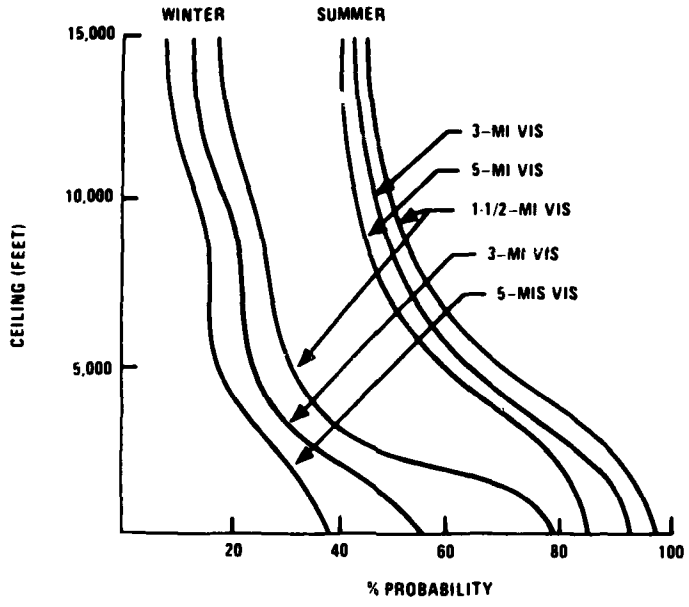

Figure 1. Weather Probability in Central Europe (adapted from Poise Sensor, 1977)

The winter and summer months represent the extremes of the observed seasonal variations. Although spring and fall lie within these extremes, they seem to resemble the worst-case visibility conditions more closely than they do the best-case conditions. This is shown in Figure 2.

Visibility is a function of atmospheric transmittance of the radiation and varies as a function of the gaseous and aerosol particles suspended in the atmosphere. The effect of these particles is two-fold: they both absorb and scatter the radiation being transmitted through the atmosphere. In either case, they reduce target-to-background contrast (Poise Sensor, 1977).

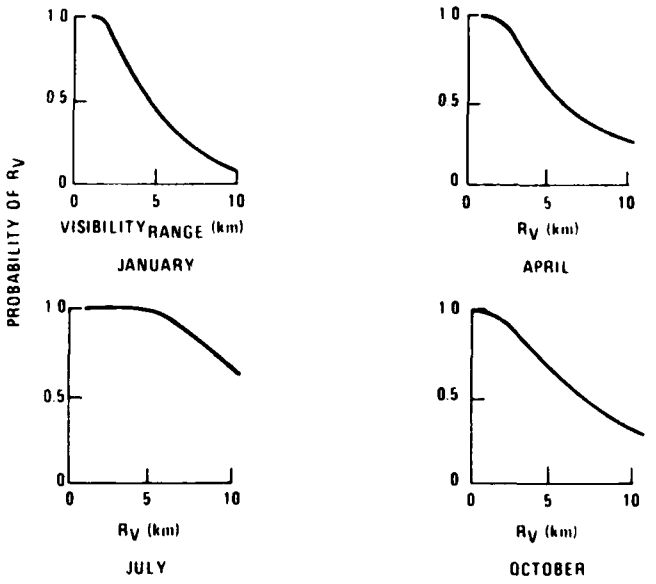

Figure 2. Visibility Variation with Season in Eastern Europe; cloud height = 500 to 1,000 feet (Hanson, et al., 1978, p. 34.)

The principal absorbers of infrared radiation are listed in Table 2 in their order of importance. As each molecule absorbs the radiation in broad bands, the central wavelength of each band is also given.

The first three molecules are the most significant sources of infrared absorption. Such absorption accounts for most of the extinction that occurs, except where there are dense suspensions of smoke, fog, haze, etc.* However, practically speaking, the 6.3 μm water band and the 2.7 and 15 μm carbon dioxide bands limit atmospheric transmission in the 2 to 20 μm range

*In the lower atmosphere, the extinction accounted for by nitrous oxide and carbon monoxide is negligible (Lloyd, 1975b).

TABLE 2. ABSORBERS OF THERMAL RADIATION*

Molecule	Wavelengths around which absorption is centered (μm)
Water	2.7, 3.2, 6.3
Carbon Dioxide	2.7, 4.3, 15
Ozone	4.8, 9.6, 14.2
Nitrous Oxide	4.7, 7.8
Carbon Monoxide	4.8
Methane	3.2, 7.8

*Based on Lloyd, 1975b.

to two atmospheric "windows," the 3.5 to 5 μm and the 8 to 14 μm bandwidths (Lloyd, 1975b).

The 8 to 14 μm bandwidth has the higher sensitivity when no transmission losses are considered. However, given the absorption effects, there are relative advantages and disadvantages for each of the two bands. Carbon dioxide absorbs radiation heavily in the 3.5 to 5 μm range, making it the less preferred band for use in mid-latitude dry air masses. However, where humidity is a factor, the 3.5 to 5 μm band becomes superior to the 8 to 14 μm band, given the degree to which water absorbs 8 to 14 μm radiation (Lloyd, 1975b).

The tradeoffs become even more complex when the effects of scattering are taken into account. Particles suspended in the atmosphere not only absorb radiation, they scatter it. The result for an infrared sensor system is that a signal becomes attenuated for two additional reasons. First, the signal is scattered outside its path and second, background radiation is scattered into its path (Tuer, 1977).

Scattering is caused by air molecules (Rayleigh scattering) and by aerosol particles (Mie scattering). The magnitude of these effects for any particular band of radiation depends upon wavelength-particle size relationships. Because the size of air molecules is so small relative to infrared wavelengths, Rayleigh scattering is not a major consideration for an infrared system (Lloyd, 1975b). However, aerosol scattering is significant. Unfortunately, its effects have often been underestimated in performance evaluations of FLIR systems, and relevant data have been lacking. Nonetheless, Biberman (1976) states that, "[a]erosol effects are more important than gaseous absorption for infrared systems in the 8.5-11 μm radiation band..." (p. 43).*

Aerosol particles that typically affect FLIR system performance are: water droplets, sand, salt, dust, smoke, and soot (Tuer, 1977; Poise Sensor Display Design Evaluation Study, 1977). Because of the size of these aerosols relative to the infrared wavelengths, aerosol scattering attenuates radiation in the 3.5 to 5 μm band more than that in the 8 to 14 μm band (Lloyd, 1975b).

---

*Biberman's analysis does not consider the shorter infrared bandwidth.

The relative effectiveness of these two bands must be evaluated in the context of their intended use. For example, in a European setting both haze and humidity are meteorological factors that must be dealt with (Biberman, 1976; Kruse, 1976). Consequently, the haze penetration ability of an infrared sensor that has a bandwidth in the 8 to 14 μm range might be offset to some measurable extent by the greater energy absorption in this band, which is attributable to water. If, on the other hand, a particular mission requires detection over short ranges, the 3.5 to 5 μm band may be preferred, since attenuation due to scattering will be minimized. Nevertheless, it has been the general practice to choose infrared sensors that operate in the 8 to 14 μm band. Field tests have shown this band to have three advantages over the 3.5 to 5 μm band. These are:

1) A higher signal-to-noise ratio for a given set of system parameters

2) Better atmospheric transmission weighted by frequency of occurrence of various atmospheric conditions

3) Less reflection of solar radiation during daytime operation so that the thermal image remains reflectively undiluted by visible scene components (Lloyd, 1975a)

Recently, however, a shift toward the 3 to 5 μm band has been occurring (Kruse, 1976). Performance evaluations using various seasonal, latitudinal, and aerosol models available in Lowtran III transmission model and Radst path transmission model (Tuer, 1977) have indicated that the shorter infrared wavelengths may be superior to those in the longer band under certain operational conditions (notably, most of those modeled by the Tropical and Midlatitude Summer models for ranges up to 20 km)

and adequate in others (the winter conditions modeled).* The shorter wavelength band also is used when background uniformity requirements have discouraged the development of FLIR systems using the longer wavelengths (Miller, 1973b).

System Factors

The purpose of an infrared system is to respond to the infrared radiation that is transmitted through the atmosphere and is available at the sensor. This radiation must be processed so that it can be displayed to and used by a human operator whose job it is to detect, recognize, and identify targets of actual or potential interest. However, in order to effect this end, a multi-component system is required, one in which each component imposes its own limitations upon the image that is ultimately displayed.

Although FLIR systems differ in their particulars and may utilize various component architectures, they share basic features. These are represented in Figure 3. Performance constraints are imposed by each of the subsystems represented: optical, scanning, detector, image processing, and display. The influence of each of these on system performance will be discussed separately.†

---

*However, the author questions the adequacy of the aerosol model used.

†Except where otherwise noted, this discussion is based largely on two sources: Lloyd (1975b) and Sendall and Rosell (1973).

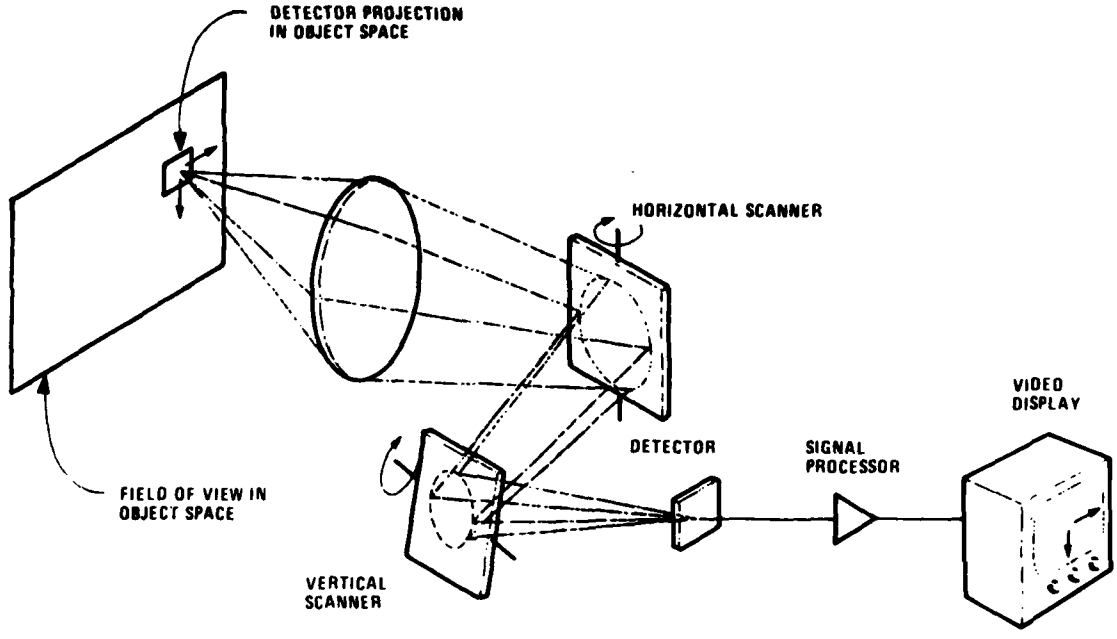

Figure 3. Simplified Single-Detector Dual-Axis Scanner (Lloyd, 1975b, p. 10.)

Optics--The primary purpose of the FLIR system's optics is to collect the available radiant energy and focus it on the image plane composed of detector elements.

Two kinds of optical systems have been developed: reflective and refractive. Lloyd (1975b) describes the relative advantages and disadvantages of each in the following paragraph:

> For a specific lens diameter and focal length, the reflection and absorption losses of a refractor will be greater than the absorption losses of a reflector, but the overall collection efficiency of the reflector may or may not be better depending on the amount of central obscuration. A reflector tends to be lighter in weight and less expensive than an equivalently sized

> refractor but the reflector may not have the same image quality. For example, spherically-surfaced reflectors cannot be corrected for off-axis aberrations without use of a refractive corrector plate, whereas spherically-surfaced refractors facilitate aberration-balanced optical designs. Since spherical surfaces are less expensive to produce than aspherics, this is an important consideration. On the other hand, refractors suffer from chromatic aberrations, while reflectors do not. The prevailing bias in FLIR design is in favor of refractive systems since so many ingenious concepts exist which enable good quality to be achieved in a compact package. However, the cost advantages of reflectors make it necessary to re-evaluate that bias each time a new optical system is conceived (p. 212).

Because most FLIR systems use refractive optics, this review deals exclusively with this type. And since the expense and complexity of fabricating aspheric lenses have led to the use of spherical and flat lens surfaces in most FLIR systems, these optics are stressed.

For simple refractive lens systems, the parameters of primary concern are field of view, the effective clear aperture diameter, and the effective focal length of the lens system. The field of view of an optical system is the amount of a scene that is optically imaged by the system. It is characterized by the shape and angular dimensions of the cone that is projected from the optics onto object space. Emitted or reflected radiation from objects within that cone is imaged by the system.*

---

*It should be noted that the optical field of view need not be the same as the system's field of view. System field of view will also depend on other design considerations such as scan angles and what portion of the video is chosen for display (Lloyd, 1975b).

The effective clear aperture diameter defines the entrance pupil of the FLIR system, unless there is an internal F-stop. If the latter is the case, then this F-stop determines the entrance pupil. In either case, the shape and linear dimensions of the entrance pupil determine the region over which infrared radiation will be accepted by the system.

Finally, the focal length is the distance from the lens at which parallel rays of radiation are brought into focus. When the focal length (f) of the lens is related to the lens' clear aperture diameter (D_o), one obtains an index of the lens' radiation gathering power (the F/No.). The relevant relationship is stated in this equation:

$$F/No. = f/D_o$$

Expressed in this way, the lower the F/No. the more radiation the FLIR system will be able to collect. However, infrared technology deviates from the traditional practice used for electro-optical (TV) devices; it does not make use of F/No. as a basic system parameter. Because detectors of virtually any size are available and because system sensitivity is a function of clear aperture diameter and the system's instantaneous field of view, FLIR system performance is essentially independent of F/No. (Sendall and Rosell, 1973). As Sendall and Rosell (1973) state,

> ... for a photon-limited system, either the instantaneous field of view and optics pupil or the F/No. and photo-receiver diameter can be considered to be the important parameters. The IR [infrared technology] took the first two, the TV took the second two (pp. 89-90).

Regardless of how one describes the radiation-gathering power of a FLIR system, however, that power does represent a potential fundamental limitation of the system's overall performance capabilities. Optics affect FLIR system performance in several other ways as well. These effects can be classified according to their sources:

1) Material effects

2) Optical effects

3) Architecture effects

The effects attributable to each source are listed in Table 3.

TABLE 3. OPTICAL SYSTEM EFFECTS THAT INFLUENCE FLIR SYSTEM PERFORMANCE*

Source	Effects
Material	- Transmission loss (through such things as reflection and absorption)
	- Thermal expansions and contractions: change of lens parameters that are attributable to terrestrial temperature changes
Optical	- Seidel aberrations: spherical aberrations, astigmatism, field curvature, distortion, and coma
	- Chromatic aberrations
	- Focus error, blur, and off-axis degradation
Architecture	- Cold reflections

*Based on Lloyd, 1975b.

Faced with these effects, there are a number of options available to a FLIR system designer. Some of the material effects can be minimized with the proper selection of a lens material.* Others that arise from thermal defocussing can be dealt with using compensation techniques such as focus adjustments (manual or automatic) or a-thermalizing the lens through lens construction or lens mounting design (Lloyd, 1975b).

The optical and architecture effects may be minimized through other system design considerations. For example, to correct for field curvatures Lloyd suggests the following possibilities: "...designing the optical system to have a flat focal surface, fabricating detectors on a continuously curving focal plane assembly, or constructing the array of flat canted segments..." (Lloyd, 1975b, p. 244). To correct for cold reflections he suggests five procedures

1) Reduce the focal plane effective radiating cold area by warm baffling.

2) Reduce lens surface reflections by using high efficiency antireflection coatings.

3) Defocus the cold return by designing the optical system so that no confocal surfaces are present.

4) Cant all flat windows.

---

*A wide range of optical materials is available. The properties of some of these are provided by Lloyd (1975b, Table 6.1, pp. 258-259).

5) When all else fails, null out the cold reflection with a thermal source or by electronic video signal compensation (Lloyd, 1975, p. 281).*

Unfortunately, such design considerations also affect system complexity.

Scanning Mechanisms--The image formed by the optical system constitutes the stimulus for the detector system. While many detector array designs exist, most do not have the detector plane positioned at the image plane. Instead, FLIR systems usually have a scanning mechanism that moves the

---

*Lloyd adds that the first four procedures, in combination, are usually adequate to correct narcissus, an effect that arises when detectors sense their own cold surfaces relative to their warm surrounding. Narcissus occurs when detector surfaces are reflected onto the focal plane via the optics of the FLIR system.

Signal dependent and signal independent shading (broad, slow-varying spurious signals superimposed on a displayed scene) may also arise from poor optical design or from scanner-optics configurations (Lloyd, 1975b).

image formed by the optics across a smaller detector plane in such a way that the detectors completely dissect the image.*

There are two basic kinds of scanning mechanisms, convergent beam scanners and parallel beam scanners. In terms of system design, the primary difference between them is the placement of the scanning mechanism relative to the optical system. A convergent beam scanner is often a moving mirror or other scanning device placed between the inner-most focussing element of the optical system and the detector array. A parallel beam

---

*Non-mechanical scanners have been designed. However, compared to the worst mechanical scanners, the best of the non-mechanical devices have a thermal sensitivity and spatial resolution that is worse by a factor of two. If the comparison is made between the best of each kind of device, the relative performance of non-mechanical scanners compared with their mechanical counterparts is an order of magnitude worse.

Lloyd discusses two reasons for the poor relative performance of non-mechanical scanners:

> First, if detection is achieved by heating of the sensing material by the scene radiation, the necessity for imaging scene motion without smearing requires a short thermal time constant, and the resultant high thermal diffusivity gives poor resolution due to image spreading. Second, if the device is electro-optical, it linearly converts either infrared photons or power into either photons or electrical signal. The resulting image contrasts are unacceptably poor because the large and uninformative thermal background has been converted to the visible along with the much smaller scene variations riding on the background (Lloyd, 1975a, p. 51).

Although Lloyd projects that mechanical devices will dominate into the mid-1980's, he adds that the future of non-scanning mechanisms has not been foreclosed; silicon array technology may yet provide feasible electronically scanned mosaics of detector elements. A discussion of this technology and its future appears later in this review.

scanner, by contrast, is typically an optical angle-changing mechanism positioned in a part of the optical system where rays are parallel or collimated. It, too, may be a mirror or some other kind of device. Simplified diagrams of each kind of scanner are shown in Figure 4.

Each type of scanner has its advantages and disadvantages. For example, while convergent beam scanners typically need fewer optical elements than parallel scanners, they introduce aberrations and distortions that subsequently must be corrected. On the other hand, while parallel beam scanners do require more complex optics, they are less susceptible to image quality loss arising from any non-flatness of the scan mirror (Lloyd, 1975b).

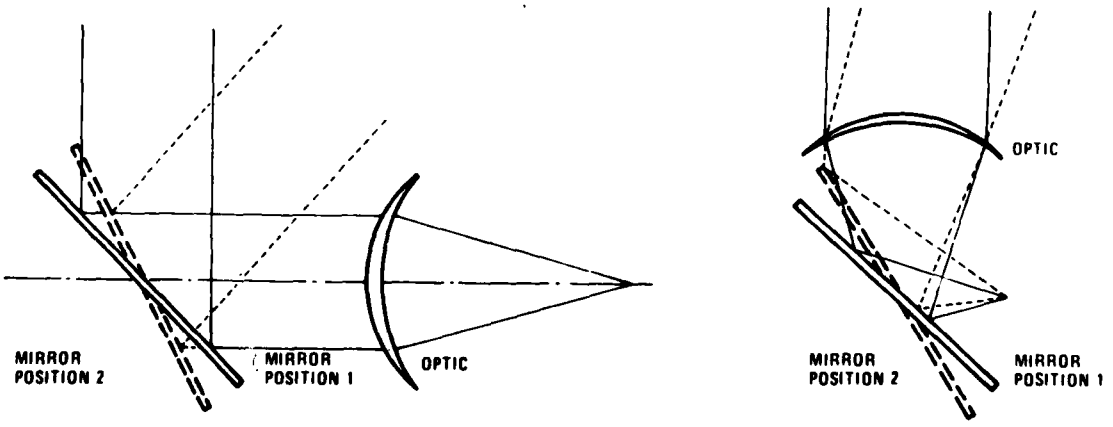

a. Parallel Beam Scanner b. Convergent Beam Scanner

Figure 4. Designs for Two Types of Common Scanners (adapted from Lloyd, 1975b)

There are seven common convergent and parallel beam scanners. They can be organized according to the means by which a scan is effected. This has been done in Table 4. However, taken in various combinations, a wide variety of one- and two-dimensional scanners can be implemented. Which mechanism is used depends upon the tradeoffs that are of concern for a particular application. Some of the major advantages and limitations of several of these systems are summarized in Table 5.

Detector Mechanisms--The purpose of a detector is to transduce the infrared radiation into some kind of observable form, for example, an electric current, an alteration of some physical property of a detector, or a blackening of an infrared film (Hudson and Hudson, 1975).

Detectors--Roughly speaking, detectors can be classified according to the hierarchical scheme shown in Figure 5.

TABLE 4. SCANNING MECHANISMS CLASSIFIED*

MIRROR	REFRACTION	SENSOR
Oscillating mirror	Rotating refractive prism	Rotating sensor
Polygonal mirror	Rotating wedge	
Rotating V-mirror	Revolving lens	

*Based on Lloyd, 1975b.

TABLE 5. ADVANTAGES AND LIMITATIONS OF VARIOUS SCANNING MECHANISMS GROUPED BY MECHANISM TYPE*

I. Oscillating Mirrors:

1. General: not suited for high speed scanning since they become unstable near field edges and demand high amounts of motor drive power.
2. Converging beam versions: wave changing path length/defocus problems that vary as a function of scan angle, but are correctable.
3. Parallel beam versions: (1) require that the scan mirror be located near the exit pupil of the spread of the scanned beams, and, thereby, the detector lens, are to be kept small, and (2) image plane motion, detector angular subtense and scan angle vary as a function of the systems in-focus range since the scanner does not scan a parallel beam unless the object is at infinity.

II. Rotating Reflective Drum Mirrors:

1. Motion is continuous and stable.
2. Scan action resembles oscillating mirror, except that the centers of the mirrors that make up the polygonal drum move in and out. This leads to focal point changes that can cause severe defocusing problems in convergent beam systems.† (Consequently, this design is most often used in parallel beam systems).
3. Interlacing or overscanning is achievable by varying angular relations among the drum's adjacent mirrors, but this may be accompanied by, or at least susceptible to, image rotation and vignetting.
4. Beam shift is not as effectively reduced as it is in oscillating mirrors, due to differences between facet and oscillating mirror motions.
5. Rotation rate is potentially limited in that a polygonal mirror disintegrates if its rotation rate exceeds an analytically derivable maximum; however, before this rate is reached facet deformation imposes a practical limitation on the mirror's usefulness.

TABLE 5. ADVANTAGES AND LIMITATIONS OF VARIOUS SCANNING MECHANISMS GROUPED BY MECHANISM TYPE* (continued)

	6. The drum must have a minimum outer radius if vignetting is not to be a problem.
III.	Rotating Refractive Prisms:
	1. Their motion is continuous and typically stable.
	2. In converging systems this mechanism has the advantage of permitting in-line design that uses small prisms.
	3. Interlacing is easily achieved by canting prism faces.
	4. Prisms are subject to focal length shifts, poor scan efficiency, and optical distortions: aberrations (spherical and chromatic), coma, and astigmatism.
	5. Refractive materials used for prisms tend to have high surface reflection losses. (If anti-reflection coated, efficiency may be reduced for large incidence angles, thereby leading to even higher reflection losses at prism edges.)
	6. Differences between scene and prism temperatures may lead to spurious modulation of the scene image due to prism self-emissions that vary as a function of scan angle.
IV.	Rotating Refractive Wedges:
	1. One of the most flexible scanning systems: Varying the relative rates of rotation of two wedges can result in a variety of different scan patterns.
	2. Must be used in a parallel system since severe aberrations occur in a converging beam system.
	3. Have a disadvantage for line scanning: Sinusoidal scanning leads to lower scan efficiency than is achievable by other scanning designs.
	4. Frame-to-frame and line-to-line registration requires tight control of wedge angular velocities.
	5. Gear mechanisms used to drive wedges are subject to heavy wear. Gear backlash has also been a problem.

TABLE 5. ADVANTAGES AND LIMITATIONS OF VARIOUS SCANNING MECHANISMS GROUPED BY MECHANISM TYPE* (concluded)

V. Other scanners:

1. Revolving lens scanners: impractical for large aperture systems since a lot of glass has to be moved; some versions (for example, the "spin-ball" scanner) have low scan efficiency.

2. Circular scanners unlike most scanners--which generate scans rectilinearly--in that they either rotate a sensor that has a radial detector array or rotate the scene optically.

   a. Rotating sensor scanners: Have the disadvantages of needing to rotate a large sensor mass and to compensate for the associated gyroscopic effects.

   b. Rotating scene scanners: Have the advantage of continuous motion and the optical compensation for image rotation that might occur.

---

*The content of this table is discussed in more detail and treated more analytically in Lloyd, 1975b.

†A design similar to the polygonal mirror scanner that is used to produce stable scans in converging beam systems is known as the "soupbowl." It consists of a circular-segment-raster scanner.

The primary distinction between thermal and photon detectors results from the fact that a solid may be treated as either one of two kinds of thermodynamic systems, a lattice or an electronic system (Hudson and Hudson, 1975). Thermal detectors depend on the heating of the detector's lattice system. This, in turn, influences the detector's electronic system, for example, by altering its resistance. In contrast, photon detectors are designed so that incident radiation interacts directly with the electronic system, effecting an alteration in the detector's electronic state.

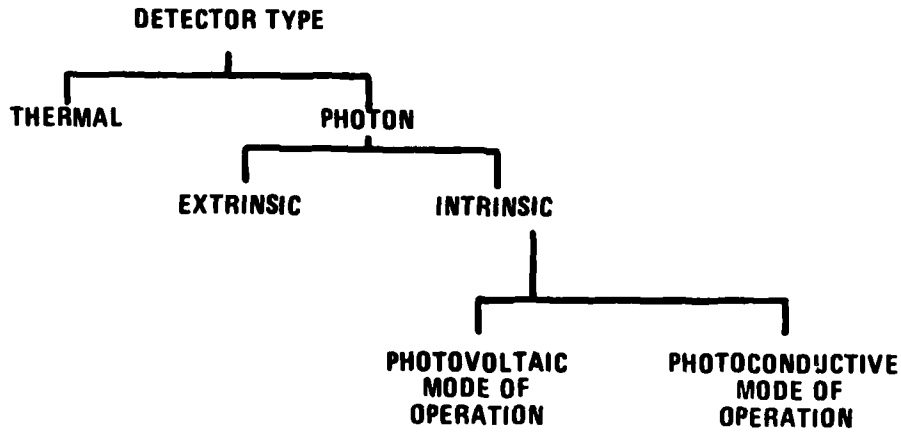

Figure 5. Classification Scheme for Types of Infrared Sensitive Detectors

Depending on how they are produced and the nature of the incident photon interaction, photon detectors may be one of two kinds, extrinsic or intrinsic. Extrinsic detectors are crystalline, but crystals into which impurities have been introduced. Energy from incident photons is used to liberate electrons or excite charge carriers between an impurity state and one of the semiconductor's conduction bands. Intrinsic detectors are also crystalline, but they depend upon photon energy to liberate electrons or excite charge carriers between valence and conductance bands of the semiconductors themselves (Levinstein and Mudar, 1975; Levinstein, 1977).

Infrared detectors are usually operated in either a photoconductive or photovoltaic mode (Levinstein, 1977). In the case of intrinsic photon detectors, most are available in both modes (Levinstein and Mudar, 1975).

The photoconductive mode requires a DC power source which is connected to a load resistance and to the detector. Energy induced variations in the carrier charge concentration alters the detector's conductivity and thereby the voltage across the load resistor. Photovoltaic operation uses p-n junctions separating charge carriers of opposite sign as a built-in battery. Consequently, no external power supply is needed. Either the p or the n region of a junction is made very thin so that photons can pass through it to excite the charge carriers located at the junction (Levinstein and Mudar, 1975; Levinstein, 1977).

Regardless of a detector's design, detector performance is typically characterized in terms of three parameters: spectral response, speed of response, and signal-to-noise ratio per watt of incident power (Corsi, 1975; Levinstein and Mudar, 1975; Levinstein, 1977).* Each of these parameters is in some way influenced by or related to the material composition of the detector.

Detector spectral response is directly related to the material properties of the detector and is the parameter that most clearly distinguishes between thermal and photon detectors (Levinstein and Mudar, 1975). Although thermal detectors are hypothetically wavelength invariant, in practice not all thermal detectors have the same spectral response. This is because "...absorption by the sensing layer is wavelength dependent and since the energy usually

---

*Corsi's list also includes operating temperature. Levinstein and Mudar augment their list by noting the following factors, viz., the noise spectrum, the magnitude of the signal which may be obtained, the saturation and temperature characteristics, as well as the interrelations of these and other properties (Levinstein and Mudar, 1975, p. 6).

passes through a protective 'window' which will have its own characteristic absorption" (Levinstein and Mudar, 1975, p. 6).

The spectral response of photon detectors is limited by a somewhat different set of theoretical and practical considerations. Because energy is inversely related to wavelength, there is a long wavelength cutoff for each kind of detector beyond which photons do not have enough energy to alter the detector's electronic structure (Hudson and Hudson, 1975; Levinstein and Mudar, 1975). This cutoff depends on a variety of material factors, such as element temperature, sample purity, and, in the case of ternary compounds, material composition. Furthermore, in actual operation such things as element thickness and surface preparation affect performance. But, aside from aging, once the detector is constructed the shape of the spectral response at the selected operating temperature usually stays constant (Levinstein and Mudar, 1975). The spectral response characteristics for several detectors are shown in Figure 6.

A detector's speed of response is a measure of its ability to respond to temporal variations in the incident radiation.* In thermal detectors the speed of response depends upon how quickly the detector's heat-sensitive element heats and cools; this, in turn, depends upon the detector's thermal capacity and its contact with the environment.

---

*Because decay is usually not exponential, the speed of response time constants are often measured in terms of the time it takes for a signal to drop from 90% to 10% of its illuminated value (Levinstein, 1977). See Levinstein and Mudar (1975) for a description of this and an alternative measurement technique.

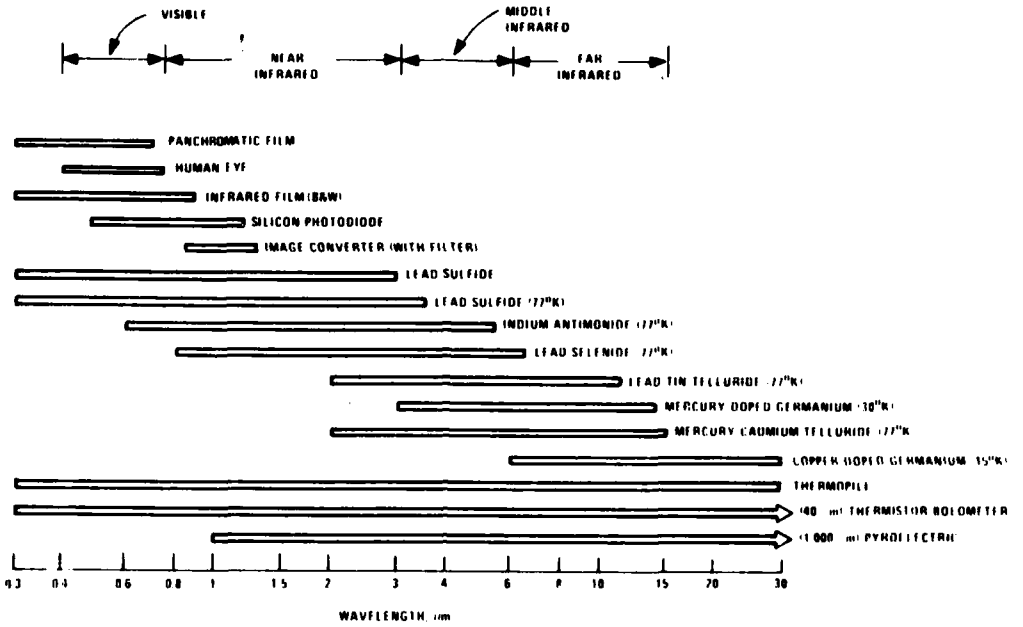

Figure 6. Useful Spectral Ranges for Infrared Detectors (operating temperature of all detectors is 300 K unless noted) (Hudson and Hudson, 1975, p. 107).

The speed of response of a photon detector is determined by the length of time that a charge carrier remains mobile after it has been excited. It is also a function of the number of recombination centers that there are and their capture cross-section (Levinstein and Mudar, 1975; Levinstein, 1977).

Today detectors are capable of achieving speeds of response measurable in nanoseconds. However, for a particular detector, speed of response may depend on detector temperature, amount of incident background radiation, and, for some detectors, the spectral composition of the background radiation. On the other hand, the variability of the response depends on the complexity of the recombination process (Levinstein, 1977).

The detectivity of a detector is the minimum power to which the detector will respond. It is defined by the relation:

$$D = \frac{(S/N)}{EA}$$

where D is detector detectivity, S is the signal voltage, N is the noise voltage, E is the signal root mean square power density (irradiance) at the detector, and A is the detector's area (Levinstein and Mudar, 1975). Because noise is a function of amplifier bandwidth (Δf) and detector area, detector detectivity is usually reported as a normalized quantity:*

$$D^* = \frac{(S/N)\ (\Delta f)^{1/2}}{E(A)^{1/2}}$$

The higher the D^* value, the smaller the amount of radiation that the detector detects. Notice, however, that the normalized D^* involves two assumptions, that detector noise is a function of $A^{1/2}$ and of $(\Delta f)^{1/2}$. Those assumptions are not always correct. Therefore, the significance of particular D^* values must be interpreted cautiously (Levinstein and Mudar, 1975; Levinstein, 1977).†

---

*A detector with 1 cm^2 area and amplifiers of 1 Hz bandwidth is used as the detector to which the other detectors are normalized.

†Levinstein and Mudar (1975) note:

> The first assumption is valid for photon detectors as long as detector areas do not vary by more than an order of magnitude. It may not be valid at all for certain thermal detectors. The second assumption requires that noise is frequency invariant over the amplifier bandwidth or that it is measured over such a narrow band that its variation is insignificant (p. 7).

Once a detector's spectral response and D^* are known, D_λ^*, the detectivity of the detector for a given wavelength, can be evaluated and its theoretical limit calculated (see, for example, Figure 8, discussed below). The best modern detectors achieve within 10%-20% of this limit while the average detector attains within 50% of this figure (Levinstein and Mudar, 1975; Levinstein, 1977). Some typical spectral response curves for detectors operating at near-optimum temperatures are shown in Figures 7a and 7b.

There are several noise sources that can potentially limit a photon detector's responsiveness: Johnson noise (noise attributable to the random motion of charge carriers), 1/f noise (noise whose power varies inversely with wavelength and has a variety of causes), and GR noise (noise arising from generation and recombination of charge carriers). In semiconductors, Johnson noise is negligible compared with the other noise sources, and 1/f noise is controllable, through production, above 100 Hz and often above 20 Hz. Thus the limiting source of noise is GR noise.

GR noise is attributable to thermal generation of the charge carriers due to lattice vibration. To minimize the effects of GR noise, detectors are usually cooled to a point where either the effects of this noise become negligible or

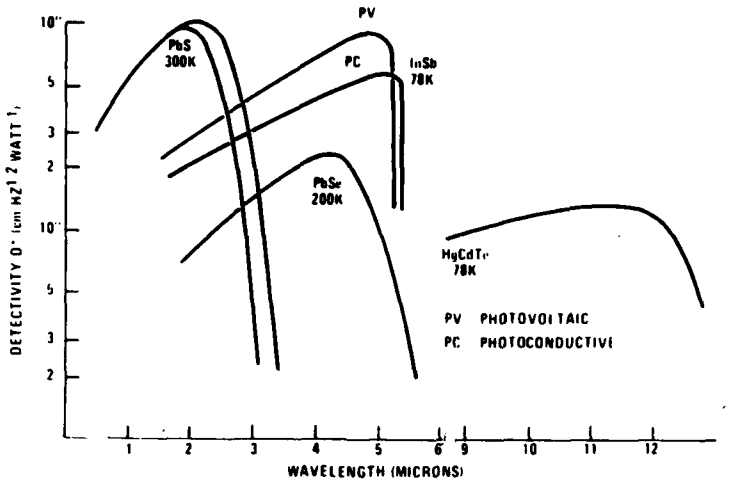

a. Spectral Response of Typical Intrinsic Detectors (for an angular field of view of 180° and temperatures of operation as shown)

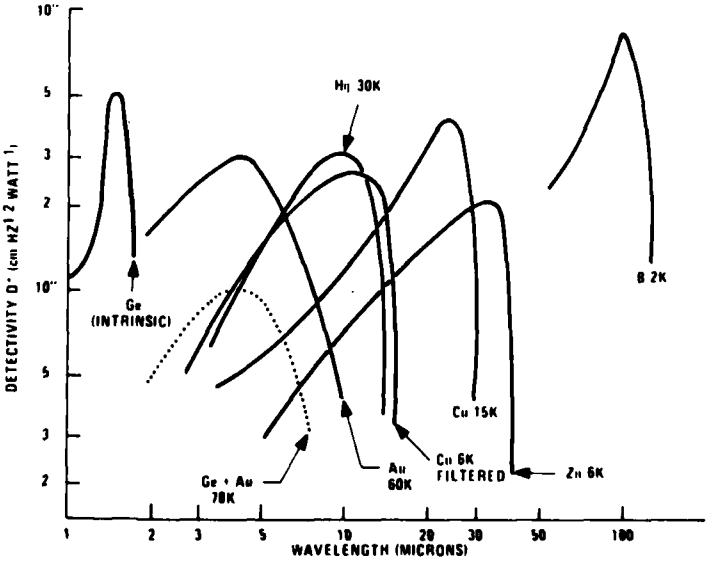

b. Intrinsic and Various Doped G_e Extrinsic Detectors (curves compare spectral response for the materials and temperatures shown)

Figure 7. Spectral D^* for Various Intrinsic and Extrinsic Detectors Operating at Near-Optimum Temperatures (adapted from Levinstein, 1977)

no further improvement is possible.* At this point, the detector is said to be background limited.

An ideal detector, under these conditions, is referred to as a background-limited infrared photoconductor (BLIP) and the operation of the detector is referred to as BLIP operation. For BLIPs, noise from the background is the performance-limiting factor (Corsi, 1975) and spectral detectivity is given by the following expression:

$$D^*_\lambda = \frac{\lambda}{2hc} \left(\frac{\eta}{Q_B}\right)^{1/2}$$

where h is Planck's constant, c is the speed of light, η is the detector's quantum efficiency (assumed constant with λ), and Q_B is the photon flux from the background. For a given locale, such as Central Europe, Q_B

---

*Hudson and Hudson (1975) note that,

> In general, thermal detectors can be operated without cooling, respond over large portions of the spectrum, have lower values of D^* than photon detectors, and exhibit relatively long response times so that they are not well suited for high-information-rate systems. Photon detectors, by comparison, generally require cooling for operation beyond 3 μm, respond over relatively narrow portions of the spectrum, have values of D^* that are one or two orders of magnitude higher than those of thermal detectors, and exhibit very short response times so that they are well suited for use in high-information-rate systems (p. 107).

For those detectors that do require cooling, the longer the wavelength that is to be detected, the more cooling required. Thus, 3 μm detectors with a 180° field of view operating at 300K need no cooling, while 3 μm to 12 μm detectors need to be cooled from dry ice to liquid nitrogen temperatures. Longer wavelength detectors must be cooled to even lower cryogenic temperatures. For example, liquid helium temperatures are necessary for detectors responding to wavelengths exceeding the 20 μm to 30 μm range (Levinstein and Mudar, 1975).

can be determined from knowing the background temperature and the detector's field of view. For analytic purposes, η is assumed to be 1. Thus, for a given detector, with a given field of view, detectivities of a BLIP detector are a function only of the spectral composition of the background and the long wavelength cutoff of the detector.

Figure 8 shows the spectral D^* for a BLIP detector having various fields of view. Actual performance is somewhat lower since not all sources of noise (such as 1/f noise) may be eliminated and because quantum efficiency usually is not 1, since not all incident photons are absorbed (Levinstein and Mudar, 1975).*

Because D_λ^* depends upon the detector's angular field of view and background radiation, it can be increased by using cold apertures to reduce the field of view or by filtering the spectral band passed by the detector. However, there are some fundamental tradeoffs involved. As Levinstein (1977) observes:

> A reduction in background radiation...usually requires additional detector cooling for the number of thermally excited charge carriers to remain negligible. Furthermore, such a reduction in background will lengthen the time constant and, if filtering is improperly done, it may reduce radiation from the source (p. 25).

The performance characteristics of various kinds of detectors are summarized in Table 6.

---

*Also, Levinstein (1977) notes that:

> For photovoltaic detectors D_λ^* is greater by $\sqrt{2}$ than for the equivalent photoconductive detector, because one need consider only noise produced by the generation of charge carriers but not by their recombination (p. 25).

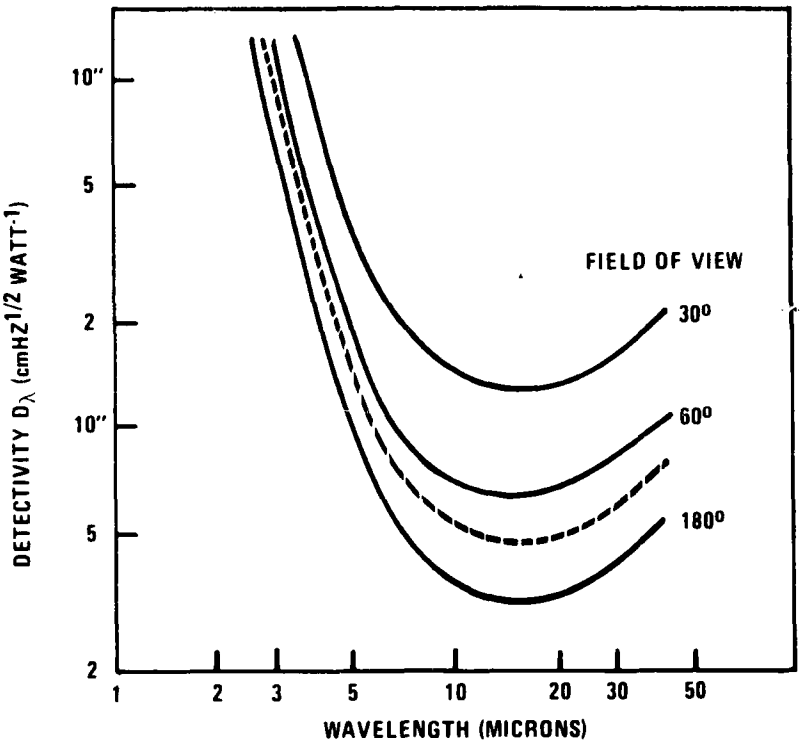

Figure 8. Background-Limited Detectivity at Spectral Peak as a Function of Long-Wavelength Threshold (adapted from Levinstein, 1977, p. 25.)

TABLE 6. CHARACTERISTICS OF TYPICAL PHOTON DETECTORS

Material	Operating Temperature (K)	Peak Wavelength (K)	Peak Detectivity D* (cm Hz$^{\frac{1}{2}}$ watt^{-1})	Time Constant (μs)
PbS (F)	300	2.5	10^{11}	300
PbSe (F)	200	4.8	2×10^{10}	20
InSb (PV)	80	5.0	10^{11}	0.2
Ge:Au	80	5.0	10^{10}	0.001-0.1
Ge:Hg	30	10	10^{10}	0.0002-0.1
Ge:Cu	4	20	2×10^{10}	0.01-0.1
PbSnTe (PV)	80	11	$1\text{-}2 \times 10^{10}$ 1×10^{10}	~ 1 ~ 0.01
HgCdTe (PC)	80	11	$1\text{-}2 \times 10^{10}$	~0.5

Field of view if 180 in each case.
F = Film
PV = Photovoltaic mode
PC = Photoconductive mode

Adapted from Levinstein, 1977.

Detector Arrays--In common practice, FLIR systems do not use single element detectors. Rather, the per frame and the per resolution element signal-to-noise ratios are increased by increasing the number of detectors that are used to dissect the scene. The direct result is the enhancement of the FLIR system's sensitivity (Lloyd, 1975b).

Detector array architectures vary depending on how the scene is dissected. The two common architectures currently in use are parallel and serial arrays.

> In parallel scene dissection, an array of detectors is oriented perpendicular to the primary scan axis, as in a unidimensional detector array used with an azimuth scanner. All of the detector outputs are amplified, processed and displayed simultaneously or in parallel. In serial scene dissection, an array of detectors is oriented parallel to the primary scan axis and each point of the image is scanned by all detectors. The detector outputs are appropriately delayed and summed by an integrating delay line which superimposes the outputs, thereby simulating a single scanning detector, or they may be read out one-for-one on a similar array of scanning display elements (Lloyd, 1975b, p. 330).

When the two modes of scene dissection are compared, each has its relative advantages and disadvantages. These are summarized in Table 7.

In assessing the performance of these alternative designs, Lloyd (1975b) is personally predisposed toward the serial array concept. In support of his bias, he makes the following two points: (1) given current technology and system design considerations, when compared with parallel systems, serial systems attain a given level of performance using a fewer number of

TABLE 7. RELATIVE ADVANTAGES AND DISADVANTAGES OF SERIAL AND PARALLEL SCENE DISSECTION*

PARALLEL DISSECTION	
Advantages	**Disadvantages**
1. Electronic bandwidth requirements per channel are minimized and optical signal processing becomes possible (Sendall and Rosell, 1973).	1. More complex processing is required for response equalization and DC restoration due to the large number of independent detectors.
2. Simpler scanning mechanisms are required.	2. There is greater potential for image nonuniformities attributable to (1) intransic detector detectivity and responsivity differences and (2) AC coupling artifacts arising from different average scene values generated by different detectors (Lloyd, 1975b).
3. Slower scan rates are possible (Sendall and Rosell, 1973).	3. The potential for information loss from malfunctioning or broken detector(s) is greater.
4. Longer dwell times improve sensor sensitivity.	
SERIAL DISSECTION†	
Advantages	**Disadvantages**
1. Integration of several detectors increases the effective sensor performance.‡	1. More complex processing is required for signal integration (for example, time-delay-and-add processing call for the implementation of delay lines).
2. The system is relatively simpler because responsivity equalization and DC restoration are easily accomplished.	2. The system requires more complex optics since dissection requires a parallel beam scanner (Lloyd, 1975b).
3. Image nonuniformities do not occur because the different detectors' outputs are integrated (Lloyd, 1975b).	3. Scanners are more complex.

TABLE 7. RELATIVE ADVANTAGES AND DISADVANTAGES OF SERIAL AND PARALLEL SCENE DISSECTION* (concluded)

SERIAL DISSECTION† (concluded)

Advantages	Disadvantages
4. There is less low-frequency undershoot of hot targets, because of shorter dwell times.	4. Wider bandwidth detectors are needed, due to shorter dwell times.δ

*Unless otherwise noted, material for this table was taken from Mortensen (1978). Aspects of the material will be discussed in more detail below.

†Serial-parallel systems have also been developed. These are essentially serial devices that scan more than one line at a time. The additional lines are time delayed for insertion into the output at the appropriate time. Such a system improves the system's sensitivity by allowing slower scan rates. However, this is at the expense of increased delay and multiplexing electronics. "Staring" arrays, which substitute electronic for mechanical scanning, are also under development (Mortensen, 1979). These staring sensors will be discussed briefly below.

‡If the single detector gains are optimized, the effective signal-to-noise ratio, as given by Lloyd (1975b), is the root sum squared value of the individual detector signal-to-noise ratios. The effective detectivity is then:

$$D_o^* = \sqrt{n}\sqrt{\frac{\Sigma D_i^{*2}}{n}} = \sqrt{n}\ D^*_{rms} = \sqrt{\Sigma D^{*2}_i}$$

where D_o^* is the effective detectivity, n is the number of detectors and D_i^* is a detectivity for a particular detector. Note: This assumes equal detector responsivity.

δSendall and Rosell (1973) state that

> The disadvantages of the system are that the large bandwidth required right out of the detector pushes the present state of the art limiting the number of picture elements per second and precluding effective scan overlap leaving the data sample data limited in one direction. Also the scan speeds required are a mechanical design burden (p. 112).

detectors; (2) serial systems provide an image which is subjectively better than that provided by parallel systems.*

Nevertheless, the development possibilities of serial and parallel are limited. In order to increase sensitivity, larger arrays than are presently used have been sought. But there are practical considerations that restrict the simple enlargement of existing architectures. These have to do with the cooling and image processing complexities which are introduced (Lloyd, 1975b; Levinstein, 1977). However, there have been a number of recent advances in charge-coupled devices (CCDs) and charge-injected devices (CIDs). (See, for example, Barbe, 1976; Bower, 1978; Hirshberg, 1975; Lewis, 1978; Sachs, 1975, 1978; and Savoye, 1978.) These advances have led to interest in the military applicability of charge-coupled and charge-injected devices (Barbe, 1976; Bower, 1978; Hirshberg, 1975), as is shown in Table 8. Most of the interest, however, seems to have focused upon developing CCD technology for the 3 μm to 5 μm infrared range. Therefore, even though most of this technology currently exists only for the visible and near-infrared range (Barbe, 1976; Bower, 1978) it will be discussed briefly below.

Charge-coupled devices are silicon semiconductors that are capable of image sensing, analog signal processing, and digital or analog memory

*Unless an automatic responsivity control is incorporated into a parallel system, image nonuniformities (from detector detectivity and responsivity differences) degrade image quality. On the other hand, if an automatic responsivity control is used, then line-to-line detector noise differences are exaggerated. The nonuniformity problems are not found in a serial system because of the integration processes used (Lloyd, 1975b).

TABLE 8. CCD AND CID MILITARY APPLICATIONS*

Mode of Operation	Application	Important Characteristics
Integrating†	Missile guidance	Sensitivity Ruggedness High frequency Metricity Light weight
	Artillery TV	Ruggedness Small size
	Day/night ground-based surveillance	Sensitivity High resolution
	Satellite surveillance	Sensitivity High resolution Low power Small size Light weight
Time Delay and Integration‡	E-O day/night periscope	Sensitivity High resolution Low voltage Small size
	Remote piloted vehicles	Sensitivity High resolution Low power Small size Light weight

*Barbe, 1976, p. 112.

† Integrating arrays look at a scene for a period of time to integrate a frame of video information. (This note is based on Barbe (1976) but was not part of table.)

‡ Time delay and integration arrays are M x N cell arrays that shift charges along the M columns at the same rate that the scene is being scanned. Because of this, integration time is increased by a factor M and the signal-to-noise ratio improved by a factor of $M^{\frac{1}{2}}$ or M without a loss of resolution. (Because of a tradeoff between signal-to-noise ratio and resolution, signal improvement occurs at the expense of resolution when a linear array is used in a parallel scan mode of operation. Barbe notes that:

> The ability of the CCD to perform TDI is very important for imaging systems applications where mechanical scan is provided in one direction and where the light level is very low. The ability to perform TDI is also useful in infrared imaging applications. (1976, p. 113)

This note is based on Barbe (1976) but was not part of table.

(Bower, 1978). When used as image sensors, CCDs take advantage of the photoelectric and shift register properties of these semiconductors. Their operation is described in the following:

> Absorption of . . . incident radiation [ranging from 400 to 1100 nanometers] in the silicon generates a linearly proportional number of free electrons in the specific area illuminated. If a silicon device structure having a repetitive pattern of small but finite photo-sensing sites is created, the number of free electrons generated in each site (charge-packet) will be directly proportional to the incident radiation on that specific site. If the pattern of incident radiation intensity is a focused light image from an optical system viewing a scene, the charge-packets created in the finite photo-sites array will be a faithful reproduction of the scene projected on its surface.
>
> After an appropriate exposure time, during which the incident light on each site is generating its time and intensity proportional electron charge-packet, the charge-packets are simultaneously transferred by charge-coupling under an adjacent single long gate-electrode to a parallel CCD analog transport shift register. . .
>
> Each charge-packet corresponds to a picture element (pixel) and, when transferred to the adjacent CCD transport shift register, continues to faithfully represent the total sensed radiant energy which was absorbed in the specific photo site. The transfer gate is immediately returned to the non-transfer clock level (LOW) so photo-sites can begin integrating the next line of incident image information. At the same time, the CCD analog transport register now loaded with a parallel-transferred line of picture information in the form of charge-packets from a line of sensor sites, is rapidly clocked to deliver the picture information in serial format, to the device output circuitry. (Bower, 1978, pp. 17, 28)

The general characteristics of CCDs are summarized in Table 9.

TABLE 9. CHARACTERISTICS OF CCDs*

TEMPERATURE

1. Works best at low temperatures (-55°C) but can perform at full capability at +70°C.

2. Cooling is relatively simple.

DYNAMIC RANGE

1. Operation achievable with cooling: 10,000:1.

2. Common operation at room temperature: from 200:1 to 500:1.

SPEED

1. Theoretically, speed limitation is set by electron mobility.

2. Practical speed limits are a result of ". . . edge-dependent charging current associated with delivering the clock voltages to the capacitances of the shift-register gate electrodes (C dv/dt current)," (Bower, 1978, p. 29).

3. Because surface-state trapping slows the overall mobility of surface carriers, buried channel devices are faster than surface channel devices.†

NOISE

1. The basic CCD register is practically noiseless since it does not have p-n junctions.

2. Some noise is introduced by on-chip charge detectors and buffer amplifiers that do have p-n junctions.

RADIATION HARDNESS

1. Basically not "hard". (That is, they can be altered by radiation.)

2. Buried channel devices are reported to be more radiation-tolerant than surface channel devices.

TABLE 9. CHARACTERISTICS OF CCDs* (concluded)

PACKING DENSITY

Storage elements may be packed three to five times more densely in CCDs than in the next most dense MOS large-scale integrated circuits.

OTHER CONSIDERATIONS

1. CCDs require low voltage and consume little power.
2. CCD image sensors do not exhibit lag or memory.
3. Although sensors might oversaturate and "bloom" under intense illumination, they are not damaged by it.

*Based on Bower, 1978.

†The difference between surface-channel and buried-channel devices is described below.

There are two important design considerations for CCDs:

1. The proximity of the carrier "channels" relative to the semiconductor-insulator interface, and
2. The mode of information transfer (Barbe, 1976).

The carrier channels can be buried or on the surface of the interface. If they are buried, the charge packets do not interact with the interface states. Buried-channel and surface-channel CCDs are compared in Table 10. Barbe (1976) concludes that:

> BCCD's are superior to SCCD's in terms of temporal noise, spatial noise, and speed. However SCCD's have the advantage in terms of fabrication simplicity and lower theoretical dark current (p. 113).

TABLE 10. SURFACE CHANNEL BURIED CHANNEL COMPARISONS*

SURFACE CHANNEL		BURIED CHANNEL
Limiting temporal noise	Surface trapping, hundreds of electrons	Bulk trapping, signal level dependent, tens of electrons at low-signal levels
Limiting pattern "noise"	Nonuniform background charge Hundreds of electrons	Nonuniform dark current density, highly dependent on temperature, several electrons at -20°C
Detectivity limit	Hundreds of electrons	Tens of electrons, low-light level solid-state imaging possible
Speed limit[a]	< 10 MHz	25 MHz for shallow buried channels

[a] Assuming standard photolithographic design rules

* Barbe, 1976, p. 110.

Information transfer can be effected through either of two designs: interline transfer (IT) or frame transfer (FT). The tradeoffs involved in each are shown in Table 11, along with a comparable CID area array design.

Barbe (1976) notes that:

> The primary advantages of the FT CCD area array organization are 1) versatility and 2) high sensitivity in the backside illuminated mode. The primary advantage of the IT CCD area array organization is its response to high-spatial frequencies. The primary advantage of the epi-CID area array organization is its excellent anti-blooming control (p. 113).

TABLE 11. TRADEOFFS BETWEEN FRAME TRANSFER CCD, INTERLINE TRANSFER CCD AND CID AREA ARRAYS

	Frame Transfer CCD	Interline Transfer CCD	CID
Versatility	Frontside or backside illumination possible, can be used for TDI	Frontside illumination only, separate sensors make video signal processing possible	Frontside illumination only with epi-CID, different design required for backside illumination, random readout possible
Sensitivity	Large fraction of theoretical silicon response in backside illuminated mode	Less than theoretical silicon response by a factor between 2 and 4 due to frontside layers and shielded vertical registers	Large fraction of theoretical silicon response in backside illuminated mode
Anti-blooming control	Accumulation around cells can be used in surface channel arrays	Drain diodes between columns can be designed into the array to provide column anti-blooming	Accumulation around cells and the epi-substrate junction provide excellent anti-blooming control
Integration MTF at limiting resolution:			
Vertical[a]	0	0.6	0.6-0.9
Horizontal	0.6	0.9	0.6-0.9
Problems	High-speed vertical transfer	Complex cell	Pattern "noise"

[a]With 2:1 vertical interlacing

Barbe, 1976, p. 110.

Signal Processing--Detectors respond to radiation emitted or reflected from two sources: targets of interest and the background. Signal processing is used to enhance the prominence of target-produced signals relative to those that have the background as their source.

A basic processing approach has been to isolate the target signals by removing the background-produced signals. This is commonly achieved by means of amplifying electronics that use AC coupling (as implemented, for example, in a RC high-pass circuit). Such circuitry approximates background subtraction and thereby improves the relative target-to-background contrast. It also achieves two other desirable ends, removing whatever DC biasing potential exists on a detector and minimizing the effects of a detector's 1/f noise (Lloyd, 1975b).

Unfortunately, however, AC coupling has undesirable effects on image quality; most of these stem from the fact that AC coupling entails that the average output value of the circuit be zero.* This means that if a detector outputs a positive signal in response to a very hot target, then given the response characteristics of the system, that signal will be followed by a lower amplitude negative signal of longer duration. In this way the average output of zero is attained; however, it is at the risk of what is referred to as "DC droop" (Lloyd, 1975b), the effect of which is shown in Figure 9. As Lloyd notes, "Clearly any low frequency elements of the scene will suffer from DC droop and cause undershoot whenever this circuit is used" (1975b, p. 341).

*Zero represents the value of the background, once it is subtracted. The fluctuations around it, therefore, represent the potential targets of interest.

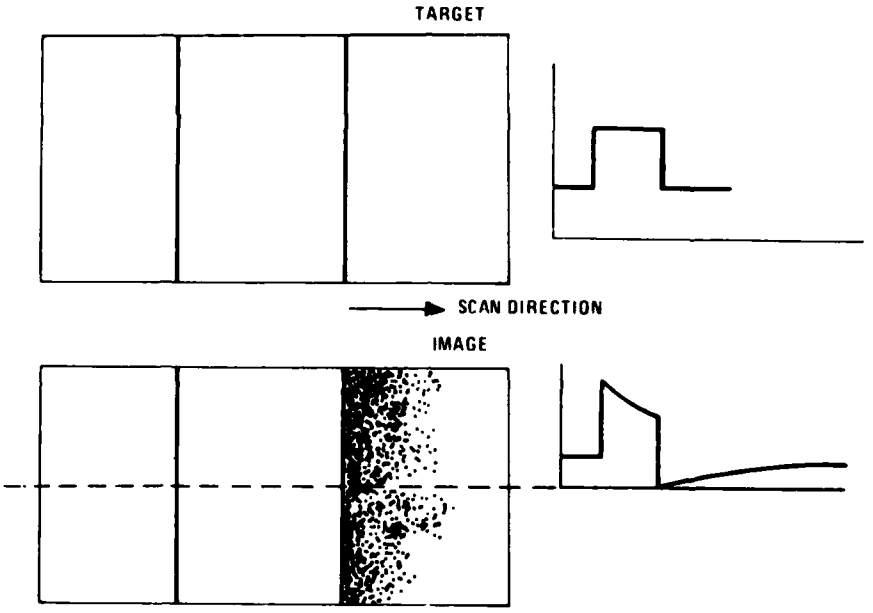

Figure 9. Appearance of Extreme DC Droop (Lloyd, 1975b, p. 342)

When the effects of unidirectional or bidirectional scan are taken into account, the image degradation becomes even more pronounced, as is shown in Figure 10. Moreover, it becomes a particularly bad problem in multiple-channel systems where different channels may have different response histories. In such cases, channels that view the same target against different backgrounds may produce different outputs in response to it (Lloyd, 1975b). This further distorts the target's appearance when it is ultimately displayed.

Because of the tradeoffs involved there is no single solution for these problems. Lloyd (1975b) puts the problem this way:

> DC droop can be eliminated by reducing the time constant, but this increases the duration of the undershoot. Undershoot can be

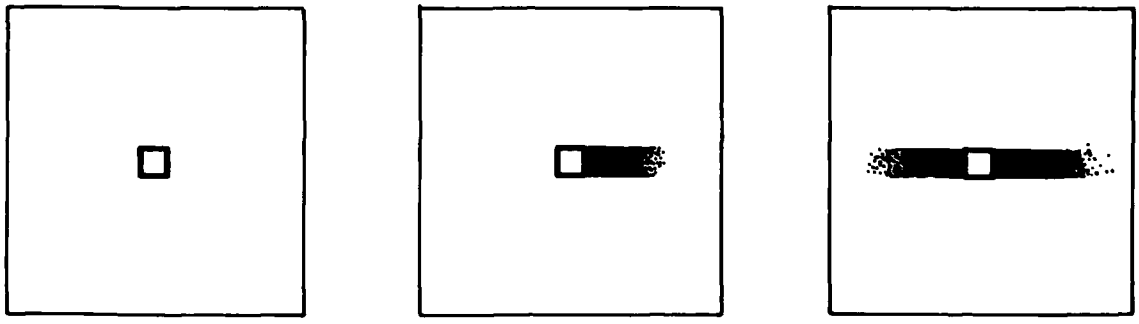

Figure 10. Effects of DC Droop with a Small Hot Source in Unidirectionally and Bidirectionally Scanned Systems (Lloyd, 1975b, p. 343)

> cured by increasing the time constant, but this increases droop. Channel responses can be made more uniform by DC coupling, but this complicates detector biasing and reduces contrasts for small delta-T targets. Droop and undershoot may be reduced by greatly increasing the signal frequency passband relative to the low frequency cut [sic], as in serial scanning, but this does not eliminate the third defect [that arising from the output differences of different channels] (p. 345).

An acceptable solution has been developed, however, through what is referred to as "DC restoration" (Narendra, Tack, and Joseph, 1978; Lloyd, 1975b). It works as follows: During the inactive portion of a scan, a detector is exposed to a thermal reference source which allows the detector signal coupling capacitor to charge to a DC value that is characteristic of

the detector's output for that source. Consequently, when the detector starts the active part of its scan, only the signals varying around the reference capacitor voltage are passed through to the system (Lloyd, 1975b). The benefits of DC restoration are apparent in Figure 11.

Currently under development are a number of other image enhancement techniques. (See, for example, Mengers, 1978; Narendra, Tack, and Joseph, 1978; and Real Time FLIR Image Enhancement, 1977). The techniques are intended to improve various aspects of the FLIR system, including detector responsivity equalization, image contrast, system sensitivity, and system resolution. Some of these developments are intended for use in extant systems. For example, Narendra, Tack, and Joseph (1978) have developed a synthetic DC restoration algorithm for systems that do not have a built-in thermal reference. It uses a line-to-line comparison

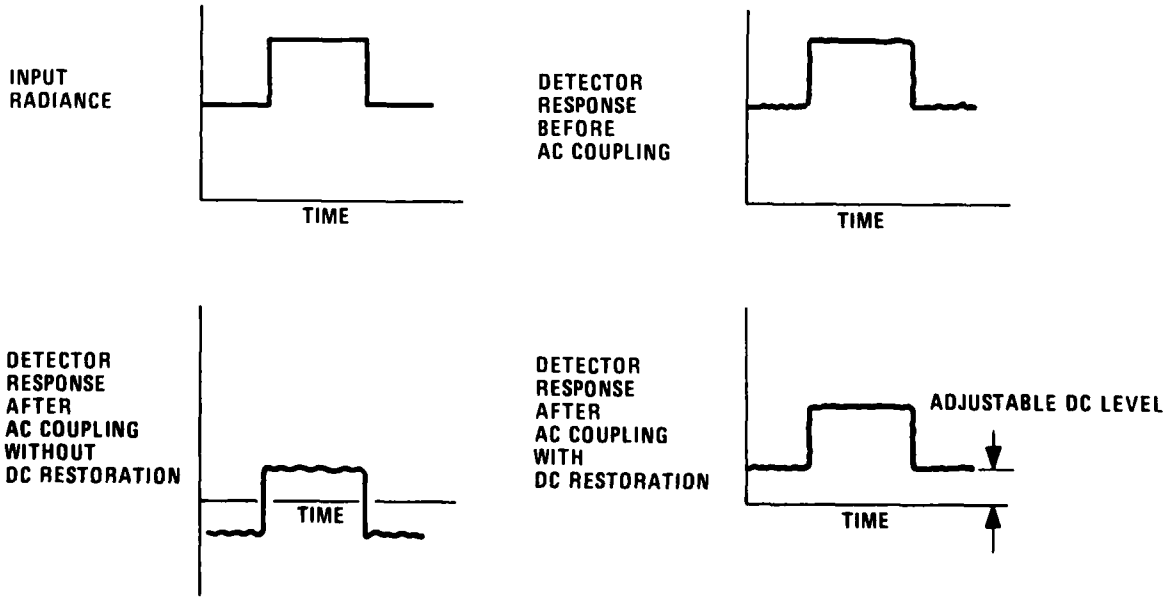

Figure 11. Non-Restored and DC-Restored Signals (Lloyd, 1975b, p. 346)

technique to restore the line-to-line correlation that exists in most scenes and to eliminate the streaking that occurs in parallel systems in the presence of hot targets.

Other techniques, however, are being developed with a view toward implementation in second-generation FLIR systems. Narendra, Tack, and Joseph have evaluated the image enhancement requirements for the large photovoltaic array/CCD processor systems that are currently under development. They have concluded that for these focal plane arrays, DC coupling, background subtraction, and two-dimensional contrast enhancement schemes may prove to be superior to traditional AC coupling/DC restoration techniques.

In order to achieve high temperature resolution in these multidetector systems, Narendra and his colleagues have begun to address a number of important problems. For example, they are exploring new methods that would equalize detector responsivity in these arrays. One method involves the use of a two-temperature reference near the focal plane. It would provide gain and offset equalization. A stochastic approach has also been developed which circumvents the need for the reference source to be uniform. Given the availability of these two methods, Narendra and his associates conclude that the responsivity equalization problem is "tractable" (Narendra, Tack, and Joseph, 1978).

Narendra, Tack, and Joseph (1978) have also been working on a variety of other image enhancement algorithms that would be implemented in real-time or near-real-time in second-generation FLIR systems. Particular algorithms are intended to enhance contrast, signal-to-noise ratios (as measured by the

system's minimum resolvable temperature), or resolution. They are described in Table 12. While they can be implemented individually, Narendra and his associates have also shown that there is nothing to prevent their incorporation into enhancements that use sophisticated versions of cascade processing (Narendra, Tack, and Joseph, 1978).

The Display--If the detector signals are to be of some immediate use to a FLIR operator, they must be made visible once they have been processed. This is the purpose of the display; it makes an infrared image available to the human operator. Two aspects of this display process are discussed below: first, the general nature of the designs used to convert a detector signal into a video signal, and, second, the parameters that characterize the most commonly used display, the single element cathode ray tube (CRT).*

Detector-to-video signal conversion can be characterized in terms of two FLIR system design parameters: the scan pattern (parallel or serial) and the manner in which the preamplified detector signals are video processed. Lloyd (1975b) describes the three kinds of video processing that are most commonly used:

> Video processing typically takes one of three forms: multichannel serial or parallel processing, standard television format processing, or pseudo-TV processing. In multichannel processing there is a one-to-one throughput of detector elements to display elements. In standard video the final electronic output of the system is a single video signal whose characteristics conform to one of the commercial standards and which is suitable for use with standard composite video equipment. In pseudo-standard video, a TV-like video format and monitor are used (p. 348).

*Multichannel systems are also in operation.

TABLE 12. IMAGE ENHANCEMENT ALGORITHMS*

ENHANCEMENT LOCUS	ALGORITHM	PURPOSE	EVALUATION/COMMENTS
Contrast Signal-to-Noise Ratio (minimum resolvable temperature)	High Frequency Emphasis: Recursive Non-recursive	To enhance edges and detail by attenuating low frequency scene components and emphasizing high frequency components	Recursive and non-recursive versions perform comparably well. Seems to improve target resolution (by removing MTF-induced blur).
	Local Area Gain and Brightness Control: Recursive Non-recursive	To compress the overall dynamic range of scene into display limits by varying local average brightness while at the same time enhancing local contrasts	Found to be the most effective target and edge enhancement technique; *because it is automatic, it is also very promising.* Recursive and non-recursive implementations are both efficient but the former might be easier to implement in real time. Found to be supersets of the high-frequency emphasis algorithms.
	Histogram Modification: Full frame (equalization, hyperbolization) Local area	To redistribute frequent and less often used grey levels of a scene within the available dynamic range of the system with a view toward separating out details in the frequently occurring grey levels	Despite their ease of implementation, these algorithms were ineffectual for FLIR contrast enhancement in a noninteractive environment. --Details could be masked as well as enhanced by the comparison techniques. --Undesirable texture can become amplified and local area versions can remove the relative contrast between areas as well as accentuate banding and clutter in the FLIR image. --Of the two full frame algorithms, hyperbolization seems to give the better results. In an interactive mode these schemes may be best suited for non-real-time analysis of FLIR imagery.
	Intraframe Smoothing:	To spatially smooth the noise within each frame without sacrificing or blurring detail or edges	Overall, the best smoothing algorithms were the 5x5 median filters and the curvature directed adaptive filters. They gave roughly comparable signal-to-noise improvements. Which is *used will depend upon the implementation tradeoffs.* (Note, though, that the adaptive filters will permit field programming to yield different tradeoffs between noise smoothing and resolution in different scenarios.)
	Median filtering: 3x3, 5x5 Separable 5x5	To smooth noise without blurring edges or destroying target-to-background or within-target contrast	Most useful for spiky noise (as a prefilter for edge operators and post-filter after edge emphasis filtering); does not blur step edges and corners are insignificantly affected. The 3x3 filter is too small to provide substantial noise smoothing. The separable 5x5 filter is easier to implement in real-time than full 5x5 filter, but they give equivalent (although not identical results). They can lead to a "blockiness" in the smoothed images which may be objectionable when the images have a large amount of noise present.

TABLE 12. IMAGE ENHANCEMENT ALGORITHMS* (continued)

ENHANCEMENT LOCUS	ALGORITHM	PURPOSE	EVALUATION/COMMENTS
Signal-to-Noise Ratio (cont'd)	Hysteresis filtering (2 dimensional)	To smooth local fluctuations while preserving extrema of the signal waveform	Shown to be ineffective for smoothing image's uncorrelated noise.
	Adaptive variable width filtering (directed by either local contrast or local curvature of the image's intensity function): Recursive Non-recursive (Gaussian)	To vary the amount of smoothing that is done contingent upon the amount of target and edge detail that is detected within each local area of the image	Recursive and non-recursive versions were equally effective, but the former are easier to implement. The curvature-directed filter performed better than the gradient (contrast)-directed filter.
	Interframe Smoothing: Frame-to-frame registration and averaging correlation tracker algorithm	To smooth out uncorrelated noise by averaging across several FLIR frames that have been registered and stacked	The signal-to-noise ratio is improved but it does not reach its theoretical limit to the extent that registration does not correct for all motion-induced changes (for example, skew and rotation) that occur from one frame to another; it only corrects for translations. Two correlation criteria have been used and may be adequate for real-time stacking of FLIR images at reduced data rates. These are the squared canonical product correlator and the minimum absolute difference correlator. The former has been the more robust in the presence of noise. The feasibility of this algorithm has been demonstrated for registering and stacking up to nine frames that are 0.20 seconds apart and contain moving and stationary targets. The principle limitation is that registration must be done against a hot spot or target, which must already be acquired. (The development of automatic target screeners, however, means this acquisition process may be automated and prioritized.)
Resolution	Inverse Filtering (Weiner filter)	To restore attenuated high spatial frequencies near to the system cutoff and thereby equalize resolution out to the optical Rayleigh diffraction limit	It can be performed in real-time. Linear inverse filtering works about as well if (1) one assumes an average space invariant blur and uses one analog filter as if (2) one assumes spatially variant blur and adaptively filters using four analog filters. The shape of an inverse Weiner filter approximates that of a high-frequency emphasis filter. Therefore, high-frequency emphasis might be able to replace adaptive resolution enhancement in simple image enhancement designs. The best implementation may be in a CCD analog spatial filter configuration (similar to the non-recursive high-frequency emphasis filter mentioned earlier in this table).

TABLE 12. IMAGE ENHANCEMENT ALGORITHMS* (concluded)

ENHANCEMENT LOCUS	ALGORITHM	PURPOSE	EVALUATION/COMMENTS
	Superresolution Gradiant projection Stochastic approximation	To restore resolution by recovering information that is available in the sidelobes of the diffraction pattern and using it to extrapolate beyond the Rayleigh limit.	Where sampling rate exceeded the Nyquist rate, both of these algorithms were effective. In undersampled images, however, the results were less conclusive. Not implementable in real-time, but computationally efficient. Usable in an off-line mode and on a sub-image frame (for example, one containing an object of interest that is cued by the operator). The two versions are roughly equivalent in their effectiveness when applied to already magnified and interpolated sub-images, but the stochastic approximation technique may be slightly better. It definitely is easier to implement in a CCD processor. (So implemented it would operate in near-real-time, requiring a delay of about one-third of a second.)

Based on Real-Time FLIR Image Enhancement (1977) and Narendra, Tack, and Joseph (1978).

There is a tradeoff that exists between the realization of recursive and non-recursive versions of an algorithm: recursive implementations require fewer line delays and filter weights (which lends them to real-time applications) while non-recursive implementations can be symmetric (zero phase) and isotropic (but are generally used for non-real-time image enhancements). (See Narendra, Tack, and Joseph (1978) for more details.)

Theoretically, with uncorrelated noise, noise variance will be reduced by a factor of N (the number of frames) when several frames are registered and time averaged.

A second registration approach is being developed at Honeywell Radiation Center. It will compensate for both translational and rotational between-frame changes. It uses algorithms which will be implementable in real-time for full-frame video processing. Product correlation techniques are unable to achieve this.

This means that it can stack more frames at longer time constants then the eye. Therefore, in noisy environments it is a viable way to improve the signal-to-noise ratio.

Resolution enhancement attempts to correct an entire field of view for resolution losses that are attributable to diffraction-limited optics and to detector blur. The enhancement algorithms discussed here assume full-frame focus (either manually or automatically achieved) and minimal range effects (that is, optimal focus of all areas of the image). Furthermore, the image to be enhanced must be sampled adequately. If it is not, then the aliasing of any high frequencies will become accentuated. Narendra, Tack, and Joseph (1978) state,

> We cannot over-emphasize the importance of adequate sampling in thermal imagers if resolution enhancement is to have any impact on the design of second-generation FLIRs. If FLIR designers insist on sampling once per detector dwell and future imagers continue to be detector limited as in the current generation, there is no hope for resolution enhancement. The only application we can see under these circumstances is when a very small aperture is dictated by size constraints. This could result in a system which is optics limited. In such a system, sampling once per detector dwell would hopefully be better than the Nyquist rate (p. 138).

Systems based on the TV-like format have not proven to be cost effective (Lloyd, 1975b). The most widely used systems, therefore, tend to be classified in terms of parallel or serial video used in conjunction with either a serial or parallel scanner. This leads to four common generic systems: parallel scan/parallel video, parallel scan/serial video, serial scan/parallel video, and serial scan/serial video. Each combination has its own advantages and disadvantages. For example, the parallel scan/parallel video system design is fairly straightforward,* requires no scan synchronizer, uses little power for its scanner, and allows for a cost effective, compact display. However, these advantages may be offset (depending, of course, on the system's intended use) by a number of potential limitations: the small display size permits only one person to view it at a time; all channels must be controlled simultaneously but separately balanced and waveform-shaped; loss of one input channel means the loss of one line of video; and the channels may require DC restoration.

Where scanner-to-video format changes are called for, video processing may become more complex. In the case of parallel scan/serial video, for example, some kind of multiplexing is required (a process whereby the system's parallel channels are reduced to a single video channel.)† In light

*Lloyd (1975b) points out that "This system requires only a collecting converging optic, a two-sided scanner, a detector array, amplifying electronics, display drivers, and an eyepiece" (p. 349).

†Two approaches to multiplexing are available: the electronic approach and the electro-optical approach. Each approach has its own set of pluses and minuses. Thus, while the electronic approach is complex and may introduce noise and transients, it does not affect the bandpass characteristics of the system. In contrast, electro-optical designs are relatively easy to implement, noiseless and transient-free, but the optics that it introduces into the system necessarily affect the system's bandpass characteristics. Both approaches also exhibit sampling defects (see Lloyd (1975b) for a more detailed discussion of these factors).

of such design considerations, the serial scan/serial video is the most direct design for obtaining a standard video display format. It does not require scan conversion or multiplexing, and it offers (1) the advantages of serial scanning that were described above and (2) the availability of standard video display and peripherals (Lloyd, 1975b).

Regardless of the system architecture chosen, however, one design constraint must be satisifed and one operational problem must be recognized. The first of these is the perfect synchronization between scene and display scanning, when they occur[*] (Lloyd, 1975b). This condition is commonly met. Unfortunately, the complication that arises from a FLIR system's operation is harder to resolve.

The problem is one of sampling a continously varying scene with a discretely operating system. Two kinds of sampling are possible: window sampling and averaging sampling (Lloyd, 1975b). As described by Lloyd, window sampling is the result of transmission of an object distribution through a periodic window function (as occurs in electronic multiplexing which samples each of a parallel system's multiple channels in order to reduce it to one channel). Averaging sampling is due to the periodic structure of an aperture array. It results in the sampling of the average value of the incoming object distribution within each aperture of the array (and occurs, for example, in the direction that is perpendicular to the scan of discrete scene dissection systems like televisions, scan converters, etc.). The result of either kind of sampling is descriptively the same, however.[†] Both lead to a sampling

---

[*] This is not required, for example, in a parallel scan/parallel video system (Lloyd, 1975b).

[†] See Lloyd (1975b) for their analytic differences.

of object distribution and to the production of sidebands that replicate the object spectrum and in which aliasing occurs.*

Sampling effects directly influence image quality. The most notable effects are due to (1) time sampling of target motion in the direction perpendicular to the direction of scan and (2) spatial sampling that occurs as the result of the raster scanning process (Lloyd, 1975b).

With these general issues of detector-to-video signal processing in mind, some of the more important parameters used to characterize CRT displays are reviewed below. These include the following: field of view, aspect ratio, number of scan lines per picture height, frame rate, interlace ratio, field rate, modulation transfer function (MTF), bandwidth, and dynamic

---

*Aliasing refers to the fact that sideband frequencies, which are not part of the original object spectrum, interfere with object frequencies, even to the point that frequencies along one dimension (the one which is sampled) interfere with frequencies along the perpendicular non-sampled dimension. The aliasing frequencies are hard to filter out. Furthermore, depending on the source of the sampling (for example, a one versus a two-dimensional detector array), the aliasing may occur in one or two dimensions (Lloyd, 1975b).

As Sendall and Rosell (1973) point out, however, in the case of multiplexing, aliasing need not be a problem if the bandwidth of each channel is chosen appropriately, as follows:

> Since the multiplexer is a time sequential sampling switch (nonlinear) it is necessary that the per channel bandwidth be limited to less than twice the per channel sampling frequency (p. 110).

range, (Biberman, 1971; Farrell and Booth, 1975; Jones, Freitag, and Collyer, 1974; Nash, 1978; Sendall and Rosell, 1973).*

A number of these parameters have to do with the format of the video display. Field of view, for example, refers to the area (in angular dimensions) of the object space that will be imaged on the display. It need not be the same as the field of view of the FLIR system's optics. Aspect ratio refers to the relationship that exists between the display's horizontal and vertical dimensions, independent of their linear extent. In CRT displays, typical format calls for a horizontal-to-vertical ratio of 4:3.

The number of scan lines per picture height, in electro-optical terminology, has two possible meanings. It may refer to the number of scan lines that make up the display's raster or it may refer to the time that has been allocated for scanning each image frame that is presented. If the latter definition is the one being used (and it is the more common one) then one must distinguish between the number of lines that are actually scanned (active lines) and the system's scan-line-per-picture-height value, which depends not only on the time it takes to scan these lines but also incorporates the time that it takes to reset the spot scanner vertically (that is, the time

---

*The parameters are described in terms of a line raster display, one which provides a continuous representation of the object scene in one dimension (typically the horizontal) and a sampled representation in the other (usually the vertical). Its raster consists of a series of vertically arrayed lines, each with a continuous scan. However, the parameters pertain to, and could be described in terms of, systems that sample in both the horizontal and vertical dimensions. In such a case, one speaks of a point raster system, the raster consisting of a matrix of discrete picture elements (pixels) that are horizontally and vertically arrayed.

allocated for vertical retrace). For clarification, consider the following example from Farrell and Booth (1975):

> By this last definition, commercial broadcast TV in the U.S. is a 525-line system. This means that the time taken to complete one scan of the image is equal to 525 individual line-scan periods. However, fewer than 525 actual scans are possible because approximately 35 of the periods are used for the vertical retrace. The actual number used for vertical retrace varies from 35 to 42, depending upon the design of the transmitter. Thus the number of actual or active TV lines, is between 483 and 490, with 490 being the most common figure (p. 4.1-10).

Some FLIR systems use this kind of 525-line display, but displays with a greater number of scan lines (for example, 875 or 1025) are also available. The number of scan lines and, more particularly, the number of active scan lines per picture height, is an important display parameter since it reflects the resolution capabilities of the display (Dyall, 1978).*

Other parameters specify the rate and manner of information transfer. For example, frame rate refers to the number of times per second the object scene is completely scanned and displayed. A typical value is 30 frames per second. However, it is common for each frame to be made up of separate, non-overlapping fields that are interlaced.

Interlacing refers to the fact that each field is presented on alternate lines of the display's raster. For example, if three fields are used, raster lines

*However, it is also important to keep in mind that the number of active scan lines does not correspond to the number of cycles of a periodic target that can be displayed. Each active line can only represent a light or dark bar, so that two scan lines are required to represent a cycle of periodic spatial information (Farrell and Booth, 1975). Also, it should be noted that the number of active scan lines represents the vertical resolution only, as modified by the Kell factor which is defined in Table 13.

1, 4, 7 . . . will display the first field: lines 2, 5, 8 . . . will display the second field: and lines 3, 6, 9 . . . will display the third field. This is an interlacing of three fields to one frame, (or an interlace ratio of 3:1). In common practice, though, only two fields are used so that the interlace ratio is 2:1.*

Since an entire frame is presented at a rate of 30 frames per second, the fields that compose it must be presented at a faster rate if the image is not to flicker. A field rate of 60 fields per second is usually used.

A last set of parameters concern the information that is displayed and the characteristics of the display. The display is intended to depict the spectral content of the object scene that has been transmitted through the FLIR system. However, not all spatial frequencies are transferred equally well. The display's bandpass characteristic is measured by its modulation transfer function (MTF). This is a plot of the normalized video output as a function of sine wave modulated inputs. The high and low frequency inputs that produce the minimum acceptable outputs determine the bandwidth of the display. However, display bandwidth is influenced by the interrelation of interlacing and frame rate, and, in turn, influences the resolution of the display, as follows:

1) In terms of display bandwidth there is a tradeoff that exists between interlacing and frame rate. The faster

---

*Higher-order sequential interlacing (interlace ratios of 4:1 or 5:1, for example) introduces artifacts into the image that can impair operator performance. Thus, if the 60-field-per second field rate (defined in the text below) is used with these higher-order interlace schemes, line crawl becomes pronounced (Farrell and Booth, 1975). (Line crawl refers to the appearance of brightness differences across the CRT screen that appear to move in a direction perpendicular to the scan lines.)

the frame rate the larger the display's bandwidth must be. Given this, interlacing is a way to decrease frame rate (Farrell and Booth, 1975) and to restrict the required bandwidth (Dyall, 1978; Farrell and Booth, 1975). Nevertheless, there are practical limits to the usefulness of interlacing. For example, as was footnoted above, higher-order interlacing may introduce artifacts that can degrade the display's overall image quality.

2) The display's horizontal resolution is affected by bandwidth in the manner described in Table 13.

TABLE 13. TELEVISION SYSTEM RESOLUTION VS BANDWIDTH SCAN LINES*

Frequency generated by pickup tube beam scanning a bar pattern =

$$\frac{\text{cycles}}{\text{active time}} \times \frac{\text{width}}{\text{height}} = \frac{\text{TV lines/height}}{2} \times \frac{W}{H} \times \frac{1}{t_{line} - t_{blank}}$$

Thus, for given bandwidth Δf,

$$\text{horizontal resolution (TV lines/height)} = \Delta f \times \frac{2H}{W} \times (t_{line} - t_{blank}).$$

vertical resolution = number of active scan lines x Kell factor

$$= \text{lines per raster} \times \frac{\text{frame time - blank time}}{\text{frame time}}$$

$$\times \text{ Kell factor}$$

where the Kell factor is the fraction of the total number of scan lines which actually can be resolved (about 70%, depending upon the test conditions).

*Dyall, 1978, p. 29.

W = Picture width
H = Picture height
t_{line} = Line time
t_{blank} = Blank time

The remaining parameters relate to the dynamic range of the display. Within the object scene, there may be a 100° temperature difference between the cold sky and a hot engine. If a detector can detect differences of 0.1 , then 1000 different temperature levels are resolvable. This leads to an object scene dynamic range of 1000:1. Ideally, this range will fit within the more limited luminance range of the video display. Typically, displays have dynamic ranges on the order of 15:1 or 30:1 (Narendra, Tack, and Joseph, 1978).[1] Because of this, other parameters such as gamma (Jones, Freitag, and Collyer, 1974), display/surround luminance (Lloyd, 1975b), display square-wave (contrast) transfer function (Dyall, 1978), and display signal-to-noise ratio (Farrell and Booth, 1975; Jones, Freitag, and Collyer, 1974; Lloyd, 1975b) are also important. These will not be discussed separately in this review.

Before ending this portion of the review, however, it is important to note that human operators can use about ten different levels of luminance (Lloyd, 1975a; Jones, Freitag, and Collyer, 1974), at best. This may necessitate the development of FLIR systems that are manually or automatically adaptable to different regions of the dynamic range.

System Limitations/System Performance--Now that the components of the system have been described and the parameters that influence their performance defined (and where possible evaluated), some representative parameter values can be provided. Many of these numbers are classified information

---

[1] It is in order to maximize the more limited range of the display that these authors try, in part, to enhance contrast through background subtraction and other methods.

but those that are available for two FLIR systems are presented in Table 14. The F-18 FLIR system is a scanning system; the other is a CID system. Table 15 provides similar and more complete information for a second-generation CCD FLIR system design.

Ultimately, however, the total system must be considered. Two things are of concern: (1) the evaluation of overall system performance and (2) the

TABLE 14. PARAMETER VALUES FOR TWO FLIR SYSTEMS

PARAMETER	System	
	CONTRACT SPECIFICATIONS FOR F-18*	BASELINE CID SYSTEM (used in a background suppression technique evaluation; detector, optical and system parameters as noted)†
Aperture	5.4" x 6"	10" (optical system diameter)
Field of view (FOV)	12° x 12° (wide FOV)	
	3° x 3° (narrow FOV)	5.7° x 5.7° (system FOV)
f number	f/2.41	f/1 (optical system f number)
Resolution	---	---
MRT† or NETD‡	MRT: ---	NETD: ---
Detector type	---	InSb (detector material)
Spectral region	---	1.5 μm - 5.5 μm (detector spectral region)

*Nash (1978); Note: these are not measured performance values.

†Baldwin (1974).

‡Defined in the text below.

---Classified information.

TABLE 15. SECOND-GENERATION FLIR SYSTEM PARAMETERS*

PARAMETER	VALUE
Aperture (mm)	152.4
f/#	3.3
Spectral wavelength (μm)	9-12
Optical spot size for 84% encircled energy (mils)	---
Transmission (%)	55
IFOV (μrad)	---
Field of view (deg)	$<3° \times 3°$
Frame rate (per sec)	30
Number of detectors in parallel	---
Number of detectors in series	2
Detector size (mils)	near state of the art

---Classified information.

*Adapted from Narendra, Tack, and Joseph, 1978.

design considerations that impose performance limitations on the state-of-the-art (and, when known, future) FLIR systems.

There are a number of ways to assess the overall performance of a FLIR system (see, for example, Lloyd, 1975b). However, if one considers the purpose of a FLIR mission and what distinguishes a FLIR system from other electro-optical systems, then there are two aspects of a FLIR system's performance that one wants to optimize: its thermal sensitivity and its spatial resolution.

Recall that what distinguishes a FLIR system from electro-optical systems, in general, is its ability to respond to the thermal characteristics of the object scene it is scanning. This permits it to penetrate atmospheric conditions that leave most electro-optical devices "blind." Remember, too, that FLIR systems have to detect signals that vary independently of their thermal background. Thus, a typical minimum temperature difference of interest is 0.5°K or 1°K, and it may occur within a scene that has an overall temperature difference of 20°K to 100°K. Thus, the thermal sensitivity of a FLIR system is of critical concern. Accepted tools to evaluate this sensitivity are the system's minimum resolvable temperature (MRT) (Decker, 1976; Lloyd, 1975b; Sendall, 1971) and its noise equivalent temperature difference (NETD). (See, for example, Lloyd, 1975b.)*

MRT is operationally defined as the lowest blackbody temperature difference that is required for an observer to resolve (with a probability of 50%) a four-bar, square-wave pattern (with a bar aspect ratio of 7:1 and a spatial frequency of f_t) when it is displayed on a uniform background by an infrared system limited by white noise. The MRT of a proposed Chaparrel FLIR system is shown in Figure 12.

NETD is usually defined as the ". . . blackbody target-to-background temperature difference in a standard test pattern which produces a peak signal-to-rms-noise [root-mean-square noise] ratio (SNR) of one at the

*The systems MRT and NETD, in turn, have been used by the Army's Night Vision Laboratory (NVL) to predict operator performance for various FLIR systems (Ratches, Lawson, Obert, Bergemann, Cassidy, and Swenson, 1975). Because the NVL model that makes these predictions is evaluated empirically below, discussion of this model will be deferred until the experiment is introduced.

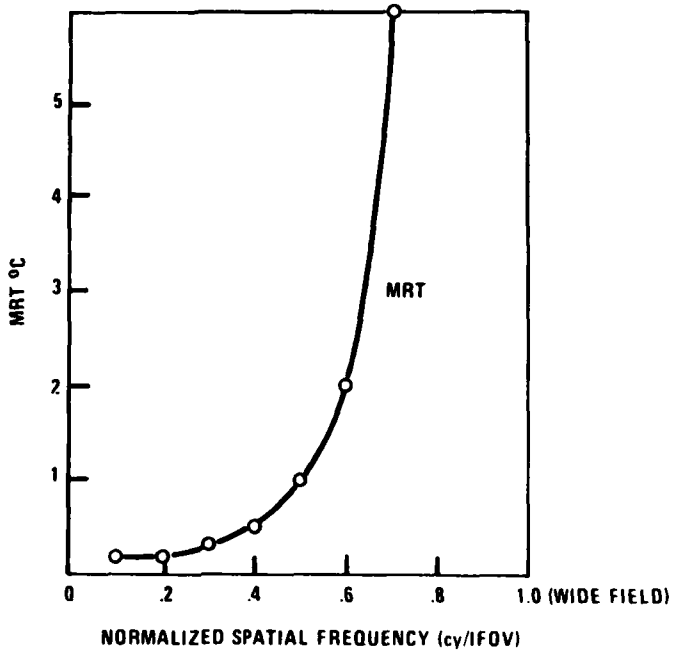

Figure 12. Proposed Chaparrel MRT (Adapted from Pratt, 1975)

output of a reference electronic filter when the system views the test pattern" (Lloyd, 1975b). Many systems in use today have an NETD that is less than 1°C.

MRT and NETD are important measures because they are related to the system's signal-to-noise ratio (see, for example, Lloyd, 1975a, 1975b). This is a system parameter, optimized in a FLIR system, that, in practice, cannot always be optimized in devices used for visible spectrum imagery.

As Lloyd (1975a) notes,

> The theoretical performance limits of thermal imaging differ somewhat from those of visible imaging because of the differences between thermal and visible scenes. With visible imagery,

> increasing the image signal-to-noise ratio (SNR) indefinitely does not always produce better imagery because scene contrasts can be so poor that increasing SNR does not improve image interpretability. With thermal imaging systems which necessarily subtract background from the scene signals, attention can be focused on as small a thermal slice as is desired. Then by improving SNR and appropriately adjusting displayed dynamic range, the information in the image can be increased until no more thermal differentials exist to be distinguished.
>
> Aided-vision devices are designed to amplify light to levels at which natural scene contrasts are discriminable by the eye, beyond which point improving SNR indefinitely produces diminishing returns. On the other hand, thermal imagers are designed to produce the highest practicable image SNRs. Therefore, in FLIR the fundamental limit of interest is the achievable SNR, and we desire to know this limit as a function of system size and complexity (pp. 51-52).

By determining the system's achievable signal-to-noise ratio, then, one can also determine the achievable minimum resolvable temperature and noise equivalent temperature difference (for example, see Lloyd, 1975a, 1975b).

Turning now to system resolution, the reasons for optimizing it are apparent. The greater the amount of detail that can be imaged on the display of a FLIR system, the greater the chances are that the human operator will be able to detect, recognize, and identify targets of interest.

The accepted measure of system resolution is the system modulation transfer function.[1] The transfer function of the display was described above. One

---

[1] It should be noted that the modulation transfer function is the modulus of a more complex optical transfer function, a function which also incorporates a system's phase transfer characteristic (Lloyd, 1975b).

can obtain a similar function independently for each of the components of the FLIR system. The system modulation transfer function is the multiplicative product of these component functions (see, for example, Mortensen, 1978, or Lloyd, 1975a). The relationships among these various functions for a proposed Chaparrel FLIR system are shown in Figure 13.

In order to see how the MTF and MRT functions characterize one system's performance, both functions for the proposed Chaparrel system are shown in Figure 14.

Given these basic considerations, there are a number of ways in which a FLIR system's performance may ultimately be limited. Its optics may be diffraction limiting; its detectors may be background or noise limiting; its display may be resolution or contrast limiting. However, in current state-

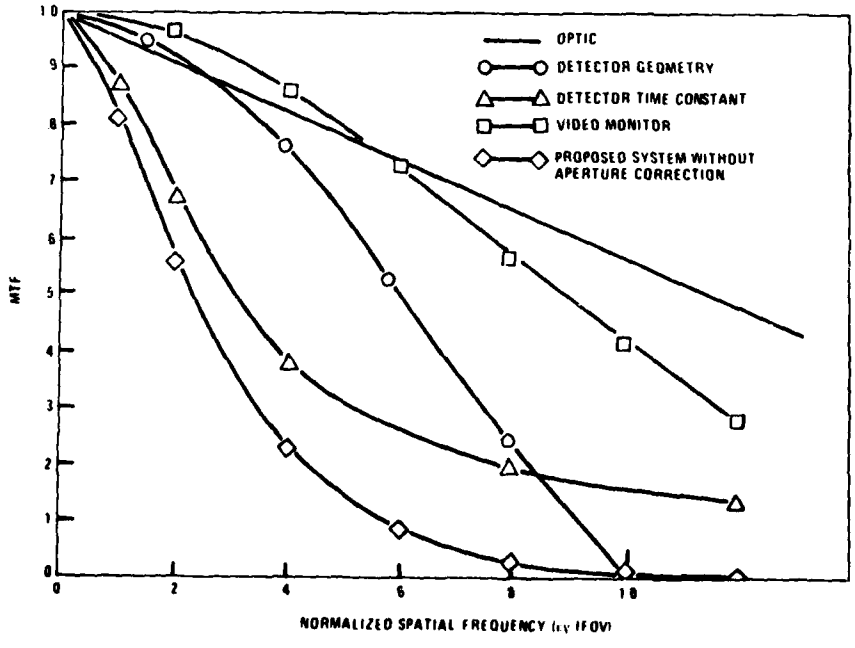

Figure 13. FLIR System and Component MTFs for a Proposed Chaparrel FLIR System (Pratt, 1975)

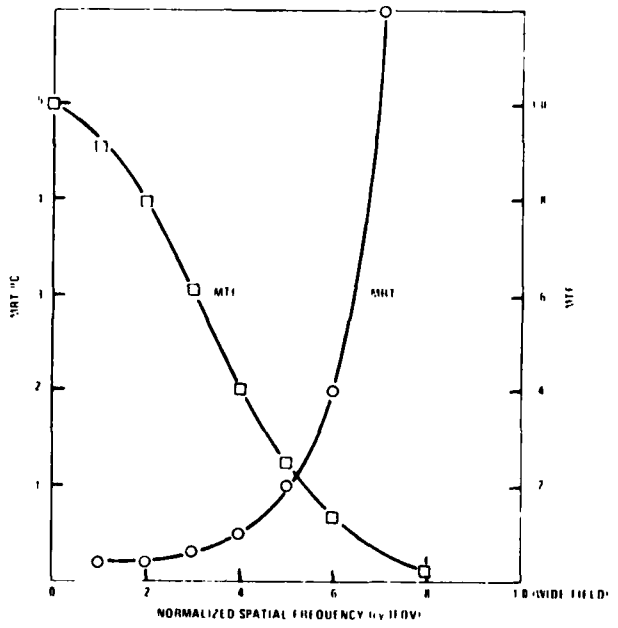

Figure 14. Proposed Chaparrel MRT and MTF (Pratt, 1975)

of-the- FLIR systems, one speaks more often in terms of the two performance specifications described above: the system's ultimate thermal sensitivity and the system's spatial resolution capabilities.

The theoretical limit of a FLIR system's thermal sensitivity is usefully thought of in terms of the signal (a temperature difference relative to a specified background) that is indistinguishable from the system's noise. That is, the system's thermal sensitivity will be limited by the signal that produces a signal-to-noise ratio of 1. However, the system's thermal sensitivity typically is not expressed as a signal-to-noise ratio. Rather the inverse of this ratio, the NETD mentioned above, is used (Lloyd, 1975a).*

*See Lloyd (1975a) for a more analytic treatment of this topic.

To put this parameter into some kind of perspective, Lloyd, writing in 1975, stated that the best available FLIR systems could be expected to have a thermal sensitivity of at least .21°K.*

In projected FLIR systems, large non-scanned photon detector arrays will be used instead of single scanning detectors. These are the so called "staring" sensors (Lloyd, 1975a). If the NETD of these arrays is calculated using parameter values that are comparable to those used for the single detector system, one can expect an improvement of approximately two orders of magnitude on a per element basis.† Yet, if these arrays are not sensitivity-limited, as single detector systems tend to be, they may prove to be response-limited. As Lloyd (1975a) notes, "Since detection or energy conversion in an incoherent device necessarily occurs before background subtraction, the responsivities of the individual non-scanning detecting elements must be extremely uniform to prevent spurious image modulation"

---

*Lloyd notes, however, that NETD is, at best, a crude performance measure. It leaves out the temporal integration and spatial filtering effects of the human observer's visual system. These come into play when the viewer looks at the FLIR image. If some of these effects are taken into account, the typical maximum acceptable NETD for a single detector scanning system is about .25°K (corresponding to a signal-to-noise ratio of 10). Nearly perfect imagery is produced by such a system when its NETD is approximately .12°K (corresponding to an effective signal-to-noise ratio of 20; Lloyd, 1975a).

†Lloyd points out that staring sensors also operate with a bandwidth that is orders of magnitude narrower than the bandwidth of a system that has only a single scanning detector (maybe 30 Hz). This is achieved (1) at the price of needing orders of magnitude more detectors but (2) despite the fact that these detectors may not be operating very efficiently (Lloyd, 1975a). That is, because these large detector arrays are difficult to cold-shield, the detectors are not likely to be background-limited.

(p. 54). Any nonuniformities that do exist constitute a source of relatively fixed-pattern noise that can interfere with performance.*

As thermal sensitivity is theoretically and practically limited in FLIR systems, so is spatial resolution. In present state-of-the-art systems there are a number of limiting sources. The primary limit to angular spatial resolution is the diffraction limit of the optical system. But it is not the limiting factor of the overall FLIR system. Lloyd (1975a) states that,

> . . . the detector angular subtense, the detector temporal frequency response, the signal processing response, the video monitor spot size, and manufacturing tolerances all contribute to reducing resolving power. In current FLIR designs the detector angular subtense α is the limiting factor, and determines the system cut-off at a frequency of $1/\alpha$. Once the system field of view and the detector angular subtense are determined, the diameter of the optic is usually set by the thermal sensitivity requirements and not by the desired resolution.
>
> The result is that the spatial frequency limit set by the optic is typically at best double the limit set by the detector subtense. Consequently, the diffraction limit on resolution does not determine current FLIR performance (p. 55).

Nevertheless, Lloyd adds that the practical limit to FLIR resolution may, in fact, have nothing to do with the system itself. Rather, in his words,

> The practical limit to FLIR resolution is likely to be the MTF of the atmosphere due to turbulence. At present, this limit as a function of atmospheric conditions is not well understood (Lloyd, 1975a, p. 55).

---

*The cooling requirements of these large sensor arrays also present a potential limitation. Recent advances have decreased the total power consumption of a high performance FLIR system to below a kilowatt. But because staring arrays require that a lot of circuitry be put on the cold head of the detector dewar, in their case some of these gains are likely to be negated (Lloyd, 1975a).

One can express the resolution capabilities of a FLIR system in terms of a system MTF. This will tend to have a gaussian shape described by

$$MTF(f) = \exp(-2\pi^2 \sigma^2 f^2)$$

where σ is the standard deviation of the system line spread function (in mrad) and f is a spatial frequency (in cycles/mrad). For a good system σ will be in the region of $0.5\alpha \leq \sigma \leq 0.6\alpha$ (Lloyd, 1975a) and represents the detector's angular subtence (in mrad).

In light of the described limits to thermal sensitivity and spatial resolution, Lloyd (1975a) summarizes the existing state-of-the-art of FLIR systems and the prospects for the future in this way:

> The state-of-the-art in thermal imaging systems is that in the best instruments, thermal sensitivity is a factor of two worse than the theoretical limit. This is due to the achievable efficiency factors of the optics, the scanner, the cold shield, and the detector. Theoretical limits of resolution are not approached because apertures are determined by the required thermal sensitivity, so that the diffraction limit exceeds the resolution set by the detector size.
>
> Development efforts over the past decade have been directed toward achieving the theoretical limit using scanning systems with the fewest possible detectors. Since the prospects for significantly improving efficiency are not good, future efforts will be directed toward improving thermal sensitivity by greatly increasing the number of detectors. During the next decade, it is likely that mechanical scanning will continue to be the preferred method for thermal imaging, with self-scanned arrays being far in the future.
>
> FLIR systems are evolving sufficiently so that their weight, power consumption, performance, and most importantly their cost, will permit widespread civilian and military use. In terms of overall image quality, FLIR has attained the reproduction standards of broadcast television (p. 56).

Human Operator Performance Factors

In his 1975 book on thermal imaging systems, Lloyd lists no less than 44 variables that can influence human operator performance, noting that, even at that, the list is not exhaustive. Some of these variables are specific to the FLIR system; among them are frame rate, dynamic range, and measures of resolution. Other variables have to do with states of the observer (including training, prebriefing, workload, and peripheral visual acuity), characteristics of the scene (such as background luminance or amount of clutter), or the operator's own situation (for example, required search area, ambient illumination, permitted search time, and vehicle vibration). A final set of variables has to do with the properties of the displayed targets. These include critical angular subtense, contrast ratio, contour complexity, and location on the display; however, these sets of variables will not be surveyed here. Similarly, models of the human operator (for example, Schnitzler, 1973) and aspects of the FLIR system design† that rest upon human physiological and perceptual processes will not be emphasized. Instead, the present review focuses upon two parameters: system resolution

---

Many of these variables (or variables like them) have been comprehensively reviewed elsewhere. (The reader is encouraged to see, for example, Farrell and Booth, 1975; Jones, Freitag, and Collyer, 1974; and Lloyd, 1975b.)

† Consider as examples three aspects of design that are now taken for granted: First, that the FLIR system converts thermal radiation into visible light, and not some other form of energy; second, that the standard 4:3 aspect ratio of the display corresponds to the proportions of the eye's "moderate quality field of view" (Lloyd, 1975b, p. 117)--the field of view that is used for most visual tasks; and third, that the field and effective frame rate of the FLIR system are selected, in part, to be above the eye's critical flicker-fusion frequency (Lloyd, 1975b). The critical flicker-fusion frequency is the frequency at which the perception of image frame fluctuations gives way to the appearance of a uniform and persistent image, when the observer is standing far enough away from the display so that the raster lines are not resolvable.

and system sensitivity. Because these parameters are of central concern to the optimization of FLIR systems, particular attention will be paid to the tradeoff and asymptotic relationships that exist between system resolution and system sensitivity and their effects upon operator performance, as well as to the dependence of these effects on the limiting factors of the system being used. In the research reported below the influence of these parameters on operator performance will be assessed empirically for first- and second-generation FLIR systems.

Resolution--There are two aspects to system resolution and its effects upon operator performance. The first concerns the effects of a display's raster structure upon an operator's ability to accomplish different tasks; the second pertains to the spatial resolution of the system in the direction of the raster's scan. Each aspect will be discussed in turn.

The effects of raster structure have commonly been studied in terms of the resolution required for particular operator tasks. J. Johnson (Johnson, 1958) showed that the resolution needed to satisfy different target acquisition criteria--detection, orientation, recognition, and identification--could be specified independently of particular targets or the camera-to-target distance. He did this by developing the concept of the equivalent bar pattern.

Equivalent bar patterns are square wave patterns that completely fill the projected minimum dimension of a target and are as long, projectively, as the target in the direction perpendicular to that minimum dimension. Table 16 shows that the resolution requirements for a particular target acquisition task can be specified fairly precisely and that more exacting decisions require better resolution.

TABLE 16. JOHNSON's TARGET ACQUISITION CRITERIA AND DATA*

A. LEVELS OF DISCRIMINATION DEFINED

Classification of Discrimination Level	Definition
Detection	An object is present.
Orientation	The object is approximately symmetric or asymmetric and its orientation may be discerned.
Recognition	The class to which the object belongs may be discerned (for example, gun, truck, man, etc.)
Identification	The target can be described to the limit of the observer's knowledge (for example, 105 mm howitzer, jeep, soldier, etc.)

B. JOHNSON'S CRITERIA FOR REQUIRED RESOLUTION

Target	Resolution (in TV lines) per Minimum Dimension			
Broadside View	Detection	Orientation	Recognition	Identification
Truck	1.8	2.5	9.0	16.0
M-48 Tank	1.5	2.4	7.0	14.0
Stalin Tank	1.5	2.4	6.6	12.0
Centurion Tank	1.5	2.4	7.0	12.0
Half-Track	2.0	3.0	8.0	10.0
Jeep	2.4	3.0	9.0	11.0
Command Car	2.4	3.0	8.6	11.0
Solder (Standing)	3.0	3.6	7.6	16.0
105 Howitzer	2.0	3.0	9.6	12.0
Average	2.0 ± .5	2.8 ± .7	8.0 ± 1.6	12.6 ± 3.0

*Jones, Freitag, and Collyer, 1974, p. 4-8.

The resolution requirements for Johnson's decision criteria have been corroborated in a number of experimental situations. For example, several studies have examined how resolution (measured in scan lines) influences operator performance at a given level of decision). In many of these studies raster size is held constant while target image size is varied in order to change the number of scan lines lying across a target.* These studies, by and large, validate Johnson's findings. Thus, Scott, Hollanda, and Harabedian (1970), using high contrast, noiseless photographic imagery, found that any more than 13.5 scan lines per target produced little change in identification performance for most of the targets used.† Similarly, Erickson (1978) has reviewed a number of target acquisition experiments that use electro-optical raster scan systems. Although they differ in their particulars, several are formally comparable to Scott's experiment. The data from these experiments were fairly consistent for recognition performance. Most targets required 10 to 12 scan lines for recognition. The detection data were less consistent; three to nine scan lines were required, depending on the target. Still, these figures are in fairly close accord with Johnson's data.

Other studies (such as Baker and Nicholson, 1967; Erickson and Hemingway, 1970, cited in Erickson, 1978; and Humes and Bauerschmidt, 1968) have varied target size and raster structure independently.‡ It is found again

---

* In these studies, then, it is important to note that the effects of target size and number of scan lines per target height are inextricably related.

† Note, however, that when these experiments took into account the variability among the subjects, they concluded that 20 scan lines per vehicle would result in a more homogeneous level of performance across observers.

‡ Also see Scanlan, 1976.

that operator performance varies as a function of raster structure (measured either in terms of the lines per image--Baker and Nicholson, 1967; Erickson and Hemingway, 1970--or lines per picture height--Humes and Bauerschmidt, 1968) and is optimized by having a certain number of lines per image height (see Baker and Nicholson, 1967, and Erickson, 1978). What is also of note in these studies is that asymptotic levels of performance that are less than 100% are attained. As an example, consider one of the studies that Erickson (1978) reviews. In this study target size, target background, and the number of scan lines across the target are independently varied. The results of this study are shown in Figure 15. Note that although background and target size each influence identification performance, they do not alter the scan line requirement. Regardless of the level of performance that is attained, it does not improve substantially after there are 10 scan lines across the target. This suggests that raster composition can limit target acquisition performance, but also that a point is reached after which other variables dominate as limiting factors.†

Humes and Bauerschmidt (1968) did not perform a comparable analysis. What they find, however, is that the optimal number of scan lines depends on viewing angle and target size.

†There are other reasons not to overinterpret the results that have been presented thus far: The line criteria that are summarized in Table 15 may be limited to the particular angle from which the targets were viewed (Johnson and Lawson, 1974; Jones, Freitag, and Collyer, 1974); they assume the targets are of uniform luminance (Jones, Freitag, and Collyer, 1974), and they assume that the bar equivalents are always of the same contrast as the targets themselves. Lloyd (1975b) points out that, for infrared imagery, this means that the equivalent bar patterns have to have the same apparent delta-T as the target and be viewed under the same conditions.) However, while Johnson and the other experimenters mentioned above always used levels of contrast that were sufficient to accomplish their required tasks, FLIR imagery is often low-contrast. Thus, the line criteria that have been summarized may not be applicable to FLIR systems without taking into account the functional interrelations that exist among sensor/observer resolution, image contrast, and image signal-to-noise ratio (Jones, Freitag, and Collyer, 1974; Rosell and Willson, 1973).

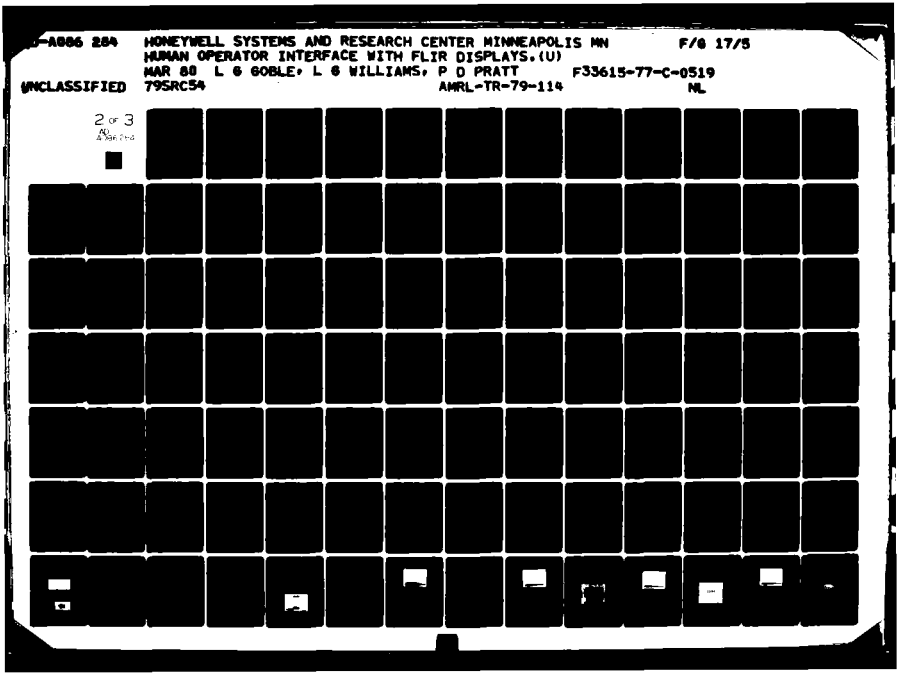
-A086 284
HONEYWELL SYSTEMS AND RESEARCH CENTER MINNEAPOLIS MN
F/G 17/5
HUMAN OPERATOR INTERFACE WITH FLIR DISPLAYS.(U)
MAR 80 L G GOBLE, L G WILLIAMS, P O PRATT
F33615-77-C-0519
UNCLASSIFIED
79SRC54
AMRL-TR-79-114
NL
2 OF 3

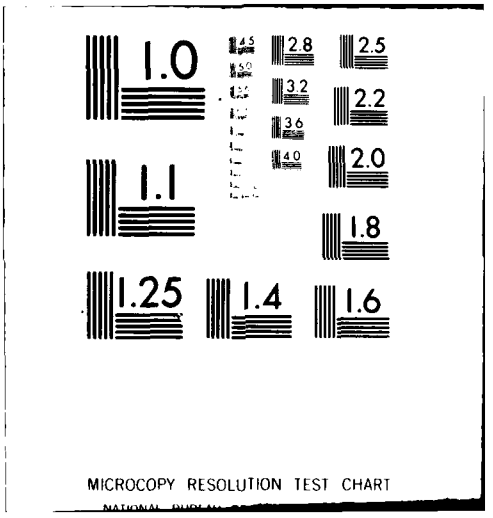
1.0
1.1
1.25
1.4
1.6
1.8
2.0
2.2
2.5
2.8
3.2
3.6
4.0
MICROCOPY RESOLUTION TEST CHART

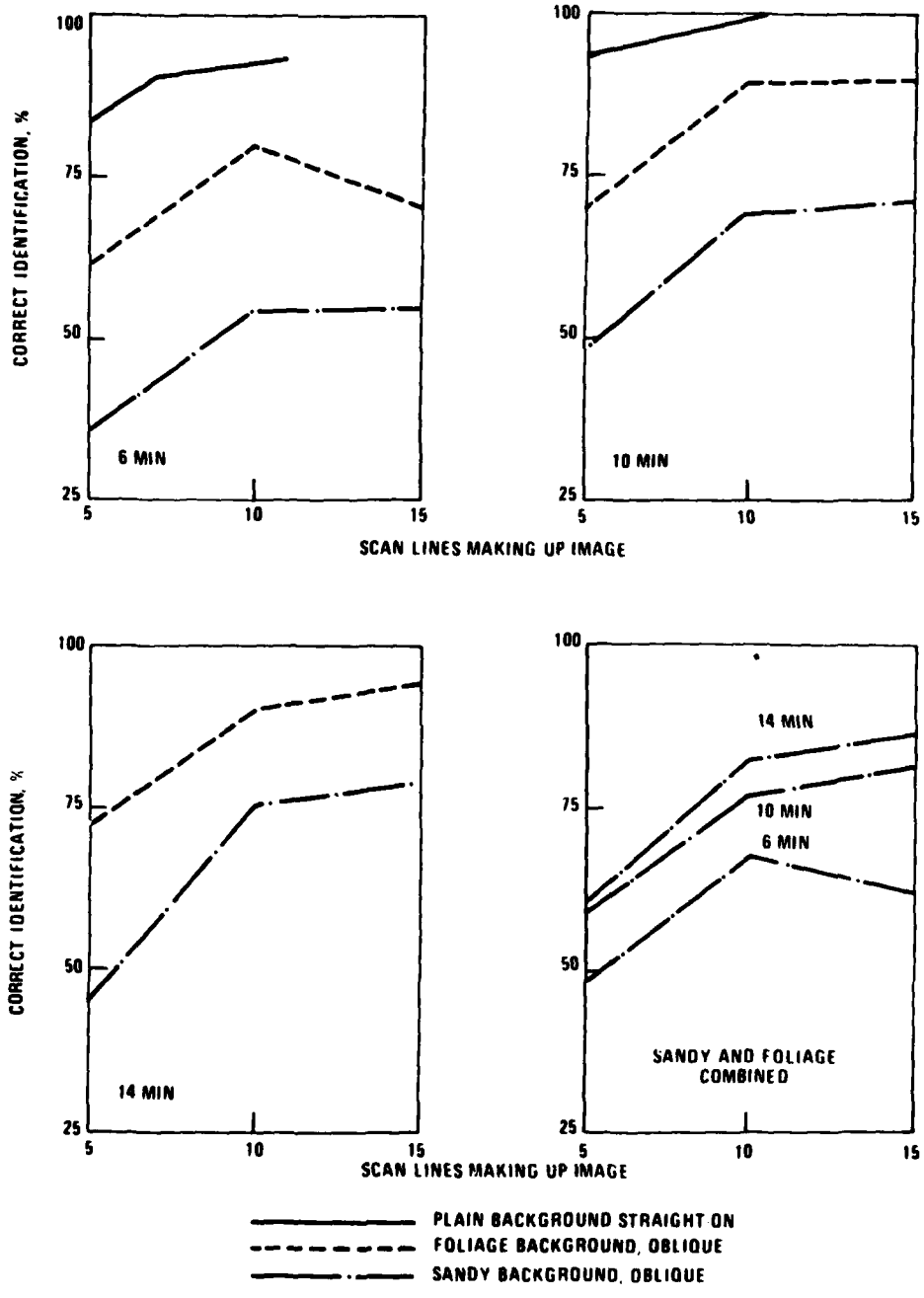

Figure 15. Vehicle Identification on Television (Target size, in Minutes of Arc, is Given for Each Set of Curves) (Erickson, 1978, p. 578)

Several variables are suggested by the literature; among these are spatial resolution in the direction of the raster scan and signal-to-noise ratio.* Spatial resolution in the direction of the scan is the next topic discussed; signal-to-noise ratio is dealt with in the following section of the report.

Resolution in the direction of the raster scan is typically measured by the system's modulation transfer function. A look at Figure 14 shows that the modulation transfer function representing a system's spatial resolution capabilities can be characterized by its bandwidth of spatial frequency transmission, its shape, and the area that lies below the envelope of the curve. Each of these parameters of the curve has been evaluated in terms of its effect on an operator's target acquisition performance.

There are some indications that wider bandwidths lead to relatively better target identification performance (Shanahan, 1964; Task, 1979) and that the effects of bandwidth interact with target contrast (Shanahan, 1964). However, the results from another study (Humes and Bauerschmidt, 1968) are less conclusive. There is also accumulating evidence that operator performance is relatable to other bandpass characteristics of an imagery system. Schade (1964; also see Lloyd, 1975b) has written that the overall shape of the modulation transfer function can influence how an image is perceived. He has stated that systems that have a Gaussian sine-wave response curve are judged to have good image quality insofar as it approaches the form of the visual system's own response curve. Significant departures from this general form are judged to be inferior (or, in Schade's words, "unnatural or defective," p. 20).

---

*Other variables include target contrasts and target size; they are not discussed, per se, in this paper.

Regardless of the shape of an imagery system's modulation transfer function, the area underneath it (the MFTA) also appears to be an important system parameter. Conceptually, this area function indexes the "amount" of spatial information that is transmitted by the system. Several measures based upon this area have been proposed (see Sendall, 1971). Several of these measures, in turn, take into account the operator's threshold requirements for performance tasks (see, for example, Charman and Olin, 1965; Snyder, 1973, 1974, 1976; Snyder, Keesee, Beamon, and Aschensach, 1974; Task, 1979; Task, Pinkus, and Hornseth, 1978; Task and Verona, 1976). The latter measurement approach, which can be thought of as indexing the spatial information that is usable by an operator, is demonstrated in Figure 16.

By and large, the area measures of spatial information transmission are related to subjective impressions of image quality (Schade, 1964), to the resolving power of the imaging system (Charman and Olin, 1965), and to overall target recognition performance (Snyder, 1973; Snyder, Keesee, Beamon and Aschenbach, 1974).* It should be noted that those measures which adjust for operator requirements are more highly related to overall performance than those that do not (Task, 1979; also see Snyder, Keesee, Beamon and Aschenbach, 1974). Also, the relationship between the area measure of spatial resolution and performance appears to be fairly robust;

---

*These measures have been less successful in relating operator performance to the recognition of particular individual targets (see, for example, Snyder, 1973; but also see Snyder, Keesee, Beamon, and Aschenbach, 1974, for more promising results).

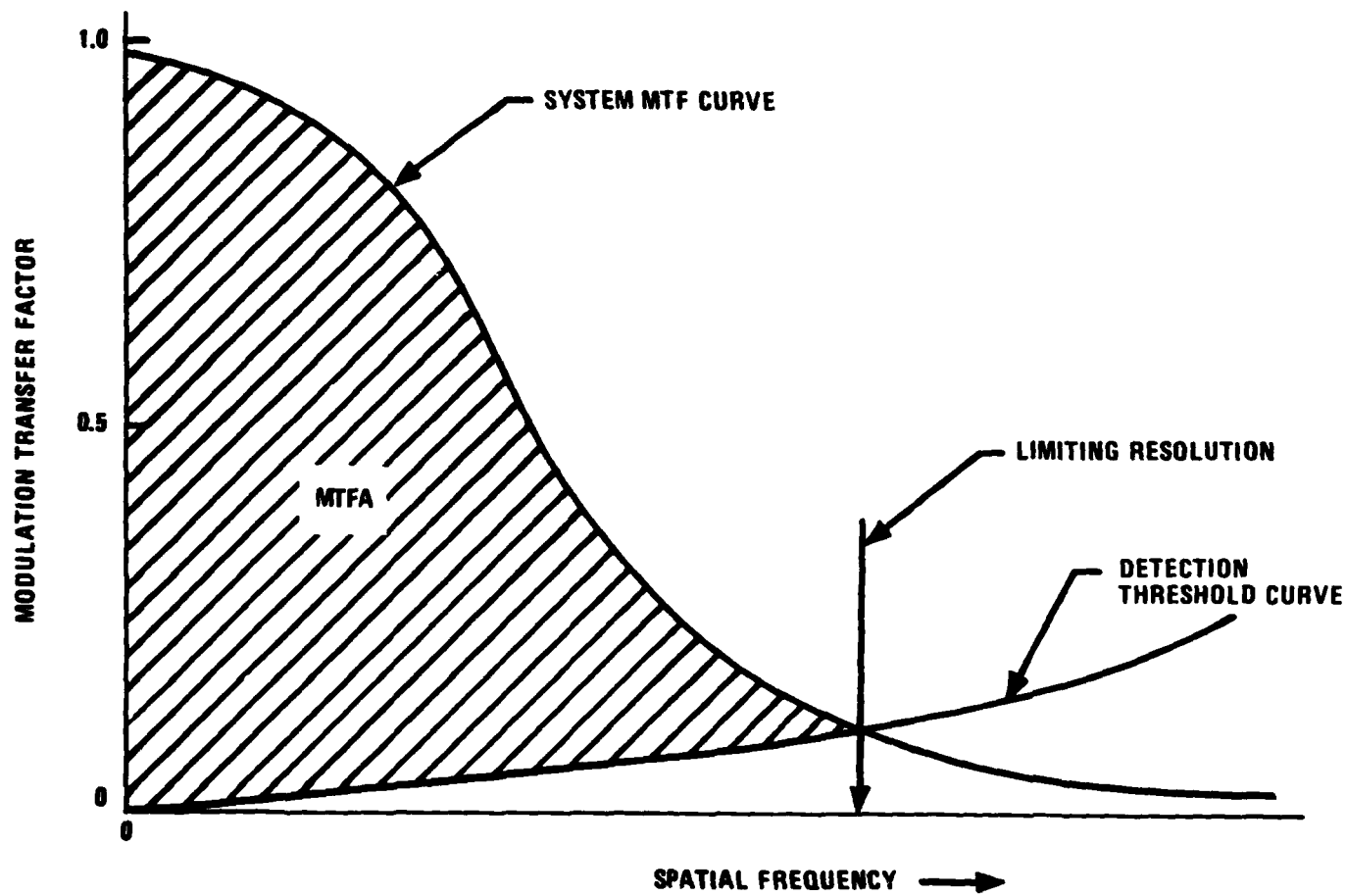

Figure 16. Modulation Transfer Function Area (MTFA)
(Snyder, 1976, p. 8)

that is, experiments that manipulate the area function in different ways* arrive at similar findings. This suggests that it is not spatial resolution (as represented by the system's modulation transfer function) per se that influences operator performance. Rather, it is spatial information that is usable by the operator that is of principal importance and may ultimately determine a system's usefulness.†

Sensitivity: Signal-to-Noise Ratio--The performance limitations that are attributable to a display's raster structure or to its spatial resolution in the direction of the raster scan are important, but they certainly are not the only system parameters that affect operator performance. In fact, the actual importance of the observed resolution effects may be related to the extent to which the imaging system is aperture-, as opposed to noise-, limited (Rosell, 1975) or the extent to which the effects themselves are not a function of other sampling or signal-to-noise ratio considerations

---

*For example, Snyder (1973, 1974) and Snyder, Keesee, Beamon, and Aschenbach (1974) vary signal-to-noise level--and thereby the observer's threshold requirements--with respect to a fixed modulation transfer function, while Task (1979) and Task, Pinkus, and Hornseth (1978) vary bandwidth and contrast ratio of the display.

†The limiting resolution of the system also depends upon the operator's threshold demand characteristics as shown in Figure 16. However, it is not as highly correlated with operator performance as are other system parameters (Task 1979; Task, Pinkus, and Hornseth, 1978; also see Coluccio, Macleod, and Maier, 1969). This suggests that effective system bandwidth may not have as important an influence on the performance on target acquisition tasks as the effective information that is passed through the system.

(Biberman, 1974).* Nevertheless, even though signal-to-noise and resolution are integrally related to one another (Biberman, 1974; Rosell, 1975; Snyder, Keesee, Beamon, and Aschenbach, 1974) the effects of the former have most often been studied independently of the latter.

In general, one finds that increases in a system's signal-to-noise ratio enable an operator to improve his performance. For example, Levine, Jauer, and Kozlowski (cited in Erickson, 1978) had subjects look at a TV monitor that was viewing photographs. The subjects had to make detection, recognition, and identification responses as the signal-to-noise ratio (measured as the square root of the video-root-mean-square voltage to the noise-root-mean-square voltage) was incremented in steps from 4 to 100. The number of scan lines per target was also manipulated; 6 TV lines, 8.67 TV lines, and 11.16 TV lines per target were used. In keeping with the results described in the last section, the number of correct responses decreased as the decision level became harder and there was a large improvement in performance going from 6 lines per target to 8.67 lines per target, but little after that. Considering signal-to-noise ratio alone, as the signal-to-noise ratio was increased, performance improved without asymptoting.

Other studies, however, have not shown this continued improvement with increasing signal-to-noise ratio. Rather, they have shown that larger

---

*For example, as was noted above, Snyder manipulated the signal-to-noise ratio of the system he was using in order to alter the operator's demand requirements for the tasks that he was studying. The usable spatial information represented by the area below his system's modulation transfer function was thereby altered and operator performance was affected accordingly (Snyder, 1973, 1974; Snyder, Keesee, Beamon, and Aschenbach, 1974).

signal-to-noise ratios do improve operator performance, but only up to some limit. Thus, in the data from the Humes and Bauerschmidt experiment (Humes and Bauerschmidt, 1968), one observes an improvement in both target recognition accuracy and latency as one goes from signal-to-noise ratios of 1 dB to 16 dB. The still higher signal-to-noise ratio of 37.6 dB did not markedly better performance on either of these response measures, although some further improvement did occur.*

Hollanda, Scott, and Harabedian (1970) obtained data comparable to this using photographs as their imagery base. Stimuli varied both in terms of the number of scan lines across the vehicle and in terms of the signal-to-noise ratio (computed as square root of the ratio of signal variance to noise variance).† They found that target identification varied as a function of both the number of scan lines per vehicle and the signal-to-noise ratio used.

Of particular note are the following results from Hollanda's experiment: In the presence of noise, 30 or 40 lines per vehicle (compared with 20 lines per object reported by Scott, Hollanda, and Harabedian, 1970, for noiseless, high contrast imagery) were required to produce an identification accuracy of 80%-90%, depending on the vehicle and the level of noise present in the

---

*The same general effects were observed for 10 small and 10 large targets and 12 high and 12 low-contrast targets. However, size and contrast did influence the level of performance attained. When compared with the large targets, the small targets appeared to be responded to more slowly (especially at the lower signal-to-noise ratios) and less accurately (by about 10% at the highest signal-to-noise ratios). The same effects are observed when performance on the low-contrast targets is compared with performance on the high-contrast targets.

†Target size and number of scan lines per target are again experimentally confounded in this study.

image. In fact, resolution proved to be the limiting factor in the experiment, since even with an infinite signal-to-noise ratio, not every target was identified every time. Given the signal-to-noise ratios that were used (3, 5, 10, 20, 30, infinity), performance improved only slightly (about 5%) beyond the ratio of 20 and only 20% beyond the ratio of 10.* What is significant about their data is that they reflect a tradeoff between resolution and signal-to-noise. Within limits a reduction in one could be compensated for by an increase in the other.† This is shown in the equal-identification accuracy curves shown in Figures 17a and 17b.

---

*This finding seems to support the view of some systems analysts that one does not need the 40 dB signal-to-noise ratios that have been sought for military applications, at least for target acquisition applications. For example, one analyst suggests that to detect the 2% thermal contrasts that are of interest, a 9 dB signal-to-noise ratio may be adequate. He adds that, at this level of noise, the FLIR system will be noise-limited so that MTF measurements will not be very useful, (Miller, 1979). Other data also may be of limited applicability. There are two reasons for this: First, for the most part, the data involve the use of high-contrast imagery. Second, they depend upon the perception of static scenes. Temporal factors, such as frame rate ($\dot{F}$) and temporal integration period of the eye (T_e) also influence operator performance. They enable one to establish a perceptual signal-to-noise ratio that depends upon, but is effectively better than, the measured ratio of any given frame by a factor of $\sqrt{T_e \dot{F}}$ (Lloyd, 1975b). Its effect is apparent in the Williams and Erickson study that is discussed below (Williams and Erickson, 1976).

†Related effects have been observed by Snyder, Keesee, Beamon, and Aschenbach (1974). Other tradeoffs have been reported between target/background contrast and display resolution measured in TV lines (Scanlan, 1976); and between image contrast and limiting resolution (Coluccio, MacLeod, and Maier, 1969).

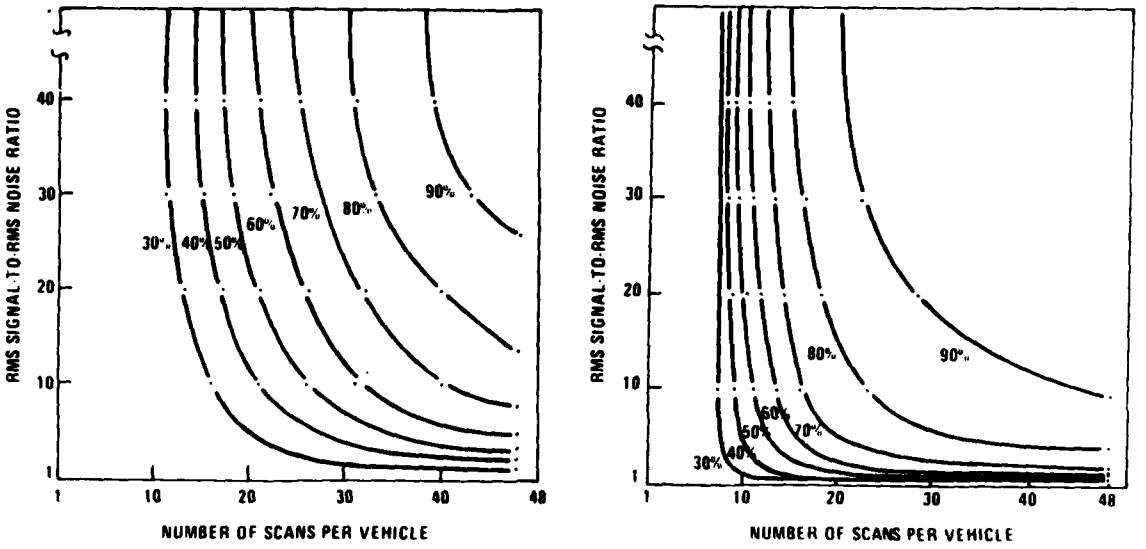

a. Equal-Identification Accuracy Curves for Tanks

b. Equal-Identification Accuracy Curves for Miscellaneous Vehicles

Figure 17. Equal-Identification Accuracy Curves for Two Classes of Vehicles (Hollanda, Scott, and Harabedian, 1970, pp. 411, 412)

This demonstrated tradeoff between resolution and signal-to-noise is important. One of the implications of this relationship is brought out by two studies reviewed by Rosell (1975). Each study found that when a sensor is noise-limited the resolution required to perform a critical task is higher than when the sensor is aperture-limited. This finding forces one to re-evaluate the Johnson criteria presented in the preceding section of this review. In light of the data that Rosell presents, the line criteria given in Table 15 for Johnson's decision levels should not be considered invariant. As Rosell concludes, ". . . it was found that a single resolution requirement is not sufficient; more resolution will be needed when the sensor's resolution is noise-limited as opposed to aperture-limited" (Rosell, 1975, p. 334).

This statement suggests the general conclusion that could be drawn from the data presented in this and the preceding section of this review, namely, that operator performance may be limited, ultimately, by the limiting factors of the system itself.

Resolution and Signal-to-Noise as They Pertain to FLIR System Design-- From the previous two sections it is clear that resolution (both across and along the raster) and sensitivity (as reflected in a system's signal-to-noise ratio) are important determinants of operator performance. However, most of the data presented came from research that used photographic and/or television imagery. Only recently has FLIR imagery been used in this kind of study. Consider as an example the experiments of Williams and Erickson (1976).

Williams and Erickson carried out three experiments that used relatively high-contrast, simulated, FLIR imagery. The first examined the effects of number of scan lines, horizontal modulation transfer function, noise, and magnification on FLIR target recognition.

Recognition time and accuracy performance were most influenced by the number of scan lines (and therefore average lines per target, since target areas remained constant under this manipulation) and noise.* System resolution (as measured by three-bar test patterns) was the best predictor of this performance. This, in turn, was most influenced by the number of scan lines and the level of magnification.

---

*Root mean square noise was a better predictor of performance than other signal-to-noise measures that took target intensity into account.

In their second experiment, Williams and Erickson studied the effects of number of scan lines, scan aperture size, noise, and magnification on FLIR target recognition performance. A number of interesting results were obtained. First, recognition accuracy varied directly as a function of the signal-to-noise ratio. Second, the optimum scan aperture varied directly with the level of noise. When more noise was present, a larger aperture acted as a smoothing filter. Third, for an aperture of a given size, performance was improved as a function of the number of scan lines present (that is, overscanning). Fourth, the effect of magnification interacted with the other variables. With a typical low-resolution, noisy image a point was reached where magnification no longer bettered recognition performance. In fact, in images where resolution was very coarse, magnification was detrimental to performance. Only the performance on noiseless, high-resolution pictures was aided by magnification. Finally, the best predictor of performance was the displayed maximum dimension of a target divided by system resolution (as measured by resolvable cycles on a checkerboard pattern).*

---

*Three points must be made here. First, the fact that the target's maximum dimension correlated more highly with performance than did the minimum dimension argues against the use of the Johnson criteria in this instance. So do other aspects of Williams and Erickson's data. Second, the use of a checkerboard pattern to measure resolution is a unique aspect of this experiment; compared with resolution measured by standard three-bar patterns, resolution measured by the checkerboard patterns was more closely related to the obtained recognition performance. Third, when resolution is measured with the checkerboard patterns, it is more sensitive to the effects of noise than when it is measured with three-bar patterns. Consequently, the last result mentioned suggests that noise was an important determinant of the observer's recognition performance.

Williams and Erickson's last experiment used dynamic imagery, but manipulated the same variables used in the second experiment. There was, however, a critical difference: The noise manipulation was defined in terms of dynamic, non-fixed-pattern noise; that is, although the noise level on each image frame was the same, its pattern differed.

The results of this experiment were highly consistent with those of the second experiment, with this notable exception: Compared with the recognition accuracy of the second experiment, mean recognition accuracy improved 8% on the average, at each level of noise when the noise was dynamic.* Furthermore, when no noise was present in the imagery, there was virtually no difference in overall recognition accuracy for the static and dynamic imagery. Thus, Williams and Erickson conclude that, "The results indicate a degree of equivalence and provide a basis for extending experimental results from static imagery to systems of dynamic imagery" (p. 116). With respect to signal-to-noise data collected on static imagery, they might have added that this data may lead to an underestimation of what is achievable operator performance.

Aside from the behavioral effects of static versus dynamic noise, what is of note here is that many of the important results discussed in the previous sections are also represented in Williams and Erickson's data: target recognition performance depended upon the raster density and the level of noise, performance was relatable to the system's modulation transfer function in the direction of the scan, and the effects of noise could be compensated for by increased resolution (overscanning).

---

*This approximates the effect of doubling the signal-to-noise ratio (Williams and Erickson, 1976).

SECTION II

THE EMPIRICAL EVALUATION OF A FIRST- AND SECOND-GENERATION FLIR IMAGING SYSTEM

INTRODUCTION

The review of the operator performance literature reveals that system resolution (defined in terms of raster structure and spatial frequency modulation in the direction of the raster scan), system sensitivity (here discussed in terms of the system's signal-to-noise ratio), and their interaction influence operator performance on detection, recognition, and identification tasks. It has been shown as well that, with respect to one or the other of these parameters, a point can be reached beyond which further improvements in system resolution and system sensitivity no longer lead to improved operator performance. In light of the asymptotic and tradeoff relationships inherent in these system resolution and system sensitivity parameters, it is important to determine what improvements in operator performance might result from projected FLIR system designs and to compare them with operator performance measures obtained from current FLIR systems.

In the research reported below, a first-generation FLIR system and a second-generation FLIR system are simulated and evaluated. One question of interest is whether or not the increased resolution and sensitivity of the second-generation FLIR system will significantly better the target detection and target recognition performance of human operators. In

order to answer this question, target detection and target recognition data were collected. These data were used to plot the minimum resolvable temperature (MRT) functions for each system under each decision criterion.

The specific experimental procedure for obtaining MRTs is that the target temperature generating and sensing equipment is calibrated to measure T to an accuracy of at least 0.05°C. The room-ambient illumination is approximately 30 fc and back reflection of the laboratory seen by the collimator is minimized. Four or five observers with good visual acuity (corrected if necessary) and normal color vision are used. The target must have a signal-to-noise ratio large enough so the noise is negligible. An oscilloscope is connected to the amplified output of the channel that is scanning the target. The optical focus of the infrared sensor is adjusted for peak signal on the oscilloscope. Display controls are adjusted to establish an operating point by selecting a brightness and contrast setting that corresponds to a point on a linear portion of the system's intensity transfer characteristic and for which noise is just discernible on the display. This setting and focus setting remain fixed throughout the test. The T of the target is set low enough so that no observer can resolve the target and increases at a rate low enough to insure thermal uniformity. Each observer notes the temperature difference at which he can reliably resolve the target. The MRT is defined as that temperature at which a majority of observers can resolve the target with certainty.

Typically, MRT functions are obtained using the psychological techniques known as the method of limits (Biberman, 1971; Decker, 1976). In this procedure, an observer is presented with a known series of stimuli in which the signal strength of successive stimuli is either increasing or

decreasing (depending whether the stimuli constitute an ascending or descending series, respectively).* During the presentation of a stimulus the observer indicates whether or not he/she can detect it. From the data obtained, the signal strength required to attain a particular level of performance (typically 50%) is determined.

Decker (1976) has disputed the validity of MRT data collected using the method of limits. He argues that they are subject to the effects of observer bias and to differences in interpretation of the required task. Furthermore, when Decker compares recognition data he collected using the method of limits with comparable data he collected using a more objective forced-choice methodology,† he finds that ". . . relative to the thresholds produced by the forced-choice method, the method of limits yields lower thresholds when image quality is good and higher thresholds when image quality is poor" (Decker, 1976, p. 14). In light of these results, Decker advocates use of the more objective technique (in this case, the forced-choice procedure). This is significant for the research reported below insofar as a modified forced-choice methodology was used. As modified, the procedure permits one to collect detection, as well as recognition, data.

Aside from the empirical evaluation of operator performance for first- and second-generation FLIR systems, there is a second purpose for the present

---

*MRT measurements typically use only ascending series.

†In Decker's forced-choice situation stimuli are presented in a random, rather than a serial, order and the observer is forced to make one of a fixed number of responses to each. Since Decker (1976) was obtaining recognition data, subjects had to indicate whether the bar pattern stimuli he presented were oriented horizontally or vertically.

research. The research was designed to evaluate the Night Vision Laboratory's (NVL) recognition and detection model. This model, formulated by Ratches and his associates (Ratches, Lawson, Obert, Bergemann, Cassidy, and Swenson, 1975), has been widely accepted for evaluating FLIR imaging systems and has proved to have predictive value for target detection and recognition performance that other suggested figures of merit have yet to achieve (Johnson and Lawson, 1974; Ratches, Lawson, Obert, Bergemann, Cassidy, and Swenson, 1975).* It also has the advantage of being based upon parameters that are specific to FLIR imaging systems, notably the MRT function (which reflects aspects of system resolution and system sensitivity that have been shown to influence operator performance).†

---

*In this regard it may prove to be less limited in predicting performance for individual targets than modulation-transfer-function-based measures.

A second kind of measure has also been developed (Rosell and Willson, 1973; Sendall and Rosell, 1973). Referred to as the SNR_D (the signal-to-noise ratio of the display), it is based upon the video's signal-to-noise ratio, but is adjusted in order to take into account the video bandwidth and the spatial and temporal integration effects of the human operator's eye. As Jones, Freitag, and Collyer (1974) point out, it has already proved useful for characterizing the Johnson criteria in terms of the physical parameters of the system, the target, and the environment; therefore, it is readily adapted to a FLIR system. So far, however, in comparison to the NVL model, a signal-to-noise-based metric has been shown to make less successful predictions (Johnson and Lawson, 1974).

†Through the use of delta-T at the sensor, the NVL model also takes into account the atmospheric conditions that can limit an infrared system's performance. This makes the model particularly relevant to a FLIR system's use in Europe.

Beyond the intrinsic usefulness of validating the NVL model, the evaluation of its predictiveness for the FLIR systems simulated in this experiment seems justified in light of the validation results obtained by Decker (1976). Decker used his recognition data to assess the validity of five target acquisition models, among which was the NVL model. He found that no model's predictions agreed very well with either the recognition data he obtained or with one another.* He also found that in all cases the amount of disagreement between the data and a model's predictions varied as a function of the image quality. Given the image quality differences that are likely to result from the improved capabilities of a second-generation FLIR system relative to those of a first-generation system, the validation of the NVL model for the simulations undertaken here is warranted.†

---

*However, by using linear regression techniques, Decker (1976) did find that ". . . the MRT's spatial frequency dependence was most accurately predicted by the SNRD-based equations [which he takes the NVL model to be] for the noisy image quality conditions and by the "exponential" equation [of Moser--see Decker, 1976
images" (p. 21).

†Along these lines, Decker (1976) notes,

> There is significant variability among MRT models, primarily in a linear scale factor. Therefore, one should not only be careful in the selection of the best model, according to the MTF/noise characteristics of the system under consideration, but should also validate the model as well as can be done and provide, in this way, the best scale factor for the particular system (p. 22).

SIMULATION OF FLIR SENSORS

Introduction: Scaling the International Imaging System (I^2S) Model 70/E to Simulate Two FLIR Systems

The traditional FLIR display study by laboratory simulation typically uses prepared target slides, a light box, a high-quality TV camera and CRT monitor, a Guassian noise generator, and a variable bandpass filter to generate displayed imagery which simulates many different FLIR sensor and scene conditions. However, this analog approach to FLIR simulation no longer provides the precision and control required to make the necessary fine evaluations; therefore, the digital I^2S Model 70/E imaging system was used for this simulation. The I^2S Model 70/E image system is a flexible image array processor based on the LSI-11 microprocessor in which N-bit 512 x 512 images can be manipulated and displayed at video frame rates. The number of bits per pixel (N) may be field configured to any value from 1 to 8 bits. This system has the capability to simulate any FLIR imaging system and provides the user with enough flexibility and control to define precisely such parameters as the MTF function, noise characteristics and distribution, rastering, and target size and position. Another advantage of the I^2S simulation over other FLIR performance prediction models and/or techniques is that the observer's eye/brain temporal integration, spatial filtering, and brightness sensitivity need not be modeled, avoiding the requirement to model a mechanism that is not clearly understood. The I^2S simulation substitutes the human observer for equations that model the human response, such as those used by the Night Vision Laboratory s FLIR performance model. This introduction presents the calculations used to scale the I^2S imaging system to the currently operational and second-generation FLIR systems being simulated.

The I^2S system simulates (1) the image degradation induced in the line bar pattern by the system transfer function and (2) the noise. The I^2S modeling assumes that:

1. The FLIR sensor is operating in the linear portion of its response so that the target can be described by the MTF of the system.
2. The electronic processing and the monitor are noiseless.
3. The system is relatively simple with a well-behaved MTF and a well-behaved noise power spectrum.
4. The image formation is spatially invariant in the scanned direction.

The system transfer function of the various system components, which include optics, spatial detector response, electronic detector response, amplifier response, and the response of the display, meets the above requirements for the FLIR sensor. The transfer function of the system is the product of the component transfer functions.

It is assumed that the FLIR detector output is biased and AC-coupled such that a signal proportional to the difference in temperature between the hot and cold test bars is passed linearly through the system. The I^2S simulation then models this signal transfer through the system. The first function performed on the I^2S is the generation of the degraded line stimulus. This imagery is generated by taking the convolution of the line spread function of the system with the square wave line bar pattern at various spatial frequencies. The line spread function is computed outside of the I^2S simulation by the fast Fourier transform of the system MTF. The line

spread function is entered into the I^2S storage as an amplitude function vs the number of pixels and is scaled from the line spread function in object space to image space. The unit of the line spread pixel spacing is the fractional amount of the sensor picture width (in image space). This frequency is translatable into the spatial frequency in object space in units of cycles per mrad. The parameters that are varied in the I^2S simulation are the amplitude of the line bar pattern and its spacing in image space, which represents a spatial frequency in object space as well.

The second function performed in the I^2S simulation is the reduction of the noise-equivalent temperature by the transfer function of the display. The noise-equivalent temperature difference (NEΔT) is defined as that input temperature difference for a large target (a large target being one whose size is large relative to the system response function) which is required to generate a signal (voltage amplitude) just prior to display (or after the detector preamplifier). This is just equal to the RMS noise (voltage) at that point, assuming that the filtering action of the electronics prior to the measurement point corresponds to that of a standard filter. There is some ambiguity in this definition of NEΔT. The NEΔT is not directly related to signal-to-noise ratio, which is fundamental for perception of targets on a display. It is also not a display noise. It is a point noise figure rather than a noise averaged over the target. However, the NEΔT is a useful indication of system sensitivity and is used to simplify MRT and MDT performance predictions in a number of models such as this simulation. The I^2S simulation accepts the NEΔT or white noise, that is, noise which is flat with respect to the spatial frequency. The display transfer function filters this noise before it is imaged on the display. Consequently, the I^2S simulation performs the convolution of the display line spread function with the RMS noise-equivalent

temperature difference and presents this noise on the display. This noise remains constant throughout the I^2S simulation tests for various amplitudes of the bar pattern temperature difference and variance in spatial frequencies.

The performance of the I^2S simulation is compared with the Night Vision Laboratory (NVL) static performance model for thermal viewing systems. This computer model predicts the static detection and recognition performance of electro-optical imaging systems sensitive to the 3 to 5 and 8 to 14 μm waveband. This model was developed at NVL to aid in the evaluation of designs for IR systems for Army missions encompassing surveillance and target acquisition systems and missile, tank, airborne, and air defense applications. The model mathematically simulates the real-world target, atmosphere, device, and observer. It also calculates the subjective detectability or recognizability of a target. A relatively simple method is used to represent the target atmosphere and MTF, NEΔT, MRT, and MDT equations for the device. The subjective decision-making behavior of the human is derived empirically from the existing field of laboratory perception data. The device and eyeball are represented in the MTF, NEΔT, MRT, and MDT calculations and are straightforward, although extensive. The I^2S simulation results are expressed in terms of the MRT response and compared with the MRT values derived by the NVL model.

Target Bar Temperature and Noise Scaling to I^2S Pixel Storage

The 512 x 512 pixel I^2S system will simulate bar imagery within a 1.0 in. x 1.0 in. central portion of a 6 in. x 8 in. FLIR display. The 512 pixels of the I^2S system will in turn drive an 8 in. by 8 in. portion of a 13 in. 10 in. monitor viewed at a distance of 120 in. to simulate viewing of the 1.0 in. x 1.0 in. central portion of a FLIR display at a 15 in. distance.

Our approach to scaling the I^2S display to a FLIR system was to equate the 8-in. wide FLIR display to the horizontal FOV of the FLIRs to be simulated. Therefore the 1.0 in. x 1.0 in. FLIR display viewed at 15 in. (or, equivalently, 8 in. x 8 in. display at 120 in.) will represent 1/8 of the horizontal angular FOV of the sensor or 1/8 of the picture width (PW) of the FLIR display.

An 8-in. FLIR display at a distance of 15 in. subtends an angle θ, where

$$\theta = 2\ \mathrm{Tan}^{-1}(4\ \text{in.}/15\ \text{in.}) = 29.863\ \text{deg} = 1791.8\ \text{arc-min}$$

The spatial frequency (fx) across the horizontal picture width (PW) is:

$$fx = \frac{\text{angular subtend of display, } \theta}{\text{angular subtend of two bar widths (that is, one cycle)}}$$

$$fx = \frac{1791.8\ (\text{arc-min/picture width})}{2 \times \text{bar width (arc-min/cycle)}}$$

$$fx = \frac{895.9}{\text{bar width}} \qquad \left(\frac{\text{cycle}}{\text{PW}}\right)$$

The spatial frequencies of the one- and four-bar patterns for targets 1 to 6 are listed in Table 17. These bar patterns are the basis for the I^2S MRT simulation, along with an rms noise level. The rms noise levels for FLIRs 1 and 2 are 0.182K and 0.053K and are used to scale the simulation of the MRT measurements. The MRT is the minimum resolvable temperature difference between the bar and background as viewed on the display. Figures 18a and 18b show the MRT function versus spatial frequency for FLIRs 1 and 2, respectively. Our FLIR simulation used values close to the MRT value listed in Table 17 since this value is the temperature at the

TABLE 17. TARGET BAR SPATIAL FREQUENCY AND MRT FOR FLIR 1 and FLIR 2

Target Number	Four-Bar Pattern Width (min of arc)	One-Bar Pattern Width (min of arc)	Spatial Frequency $(fx) = \frac{c}{PW} = \frac{895.9}{\text{Bar Width}}$	Bar Pattern Temperature			
				FLIR 1		FLIR 2	
				MRT	ΔT/Noise	MRT	ΔT/Noise
1	9.38	1.34	668.582	--	--	--	--
2	15.61	2.23	401.749	$> 10^4$	--	.74	13.96
3	24.99	3.57	250.952	2.70	14.835	.11	2.08
4	37.59	5.37	166.834	0.30	1.648	.046	.87
5	56.35	8.05	111.292	.11	.604	.024	.45
6	93.80	13.40	66.858	.04	.220	.011	.21

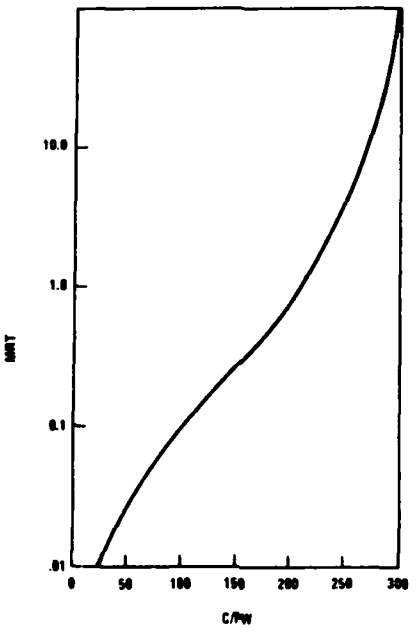

Figure 18a. Predicted MRT Function for FLIR 1

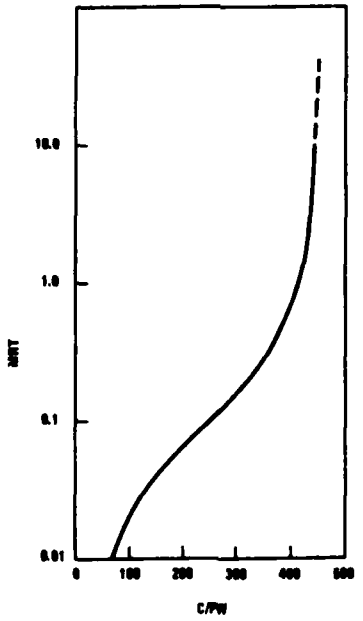

Figure 18b. Predicted MRT for FLIR 2

threshold of detection, that is, at the point "where one of two observers sees a discernable pattern."*

It should be noted that the spatial frequencies for target 1 for both FLIR 1 and FLIR 2 are too high for consideration. Consequently, the corresponding MRT values are too high to be of interest and cannot be easily measured for most sensor applications.

The amplitude of the noise stored in the I^2S system and the display gain was adjusted such that the noise was just discernable on the display.†

Number of I^2S Pixels vs Target Bar Width

The I^2S system was scaled to simulate a 1.0-in. wide display with 512 pixels at a viewing distance of 15 in. The angle θ subtended by 1.0 in. at 15 in. is:

$$\theta = 2 \text{ Tan}^{-1} \frac{1.0 \text{ in.}/2}{15 \text{ in.}}$$

$$= 229.1 \text{ arc-min}$$

---

*Honeywell RPV FLIR Sensor Proposal, pp 12-16.

†Biberman, 1971, p. 35.

The number of pixels per angle bar width η is:

$$\eta = 512 \left(\frac{\text{pixels}}{\text{display}}\right) \quad \frac{\text{bar width (arc-min/bar width)}}{229.1 \text{ (arc-min/display)}}$$

$$= \frac{512 \times \text{bar width}}{229.1} \qquad \left(\frac{\text{pixels}}{\text{bar width}}\right)$$

The number of pixels and bar width for each of the six targets are shown in Table 18.

TABLE 18. NUMBER OF I^2S PIXELS PER BAR WIDTH

Target Number	Number of 512 Pixels	Bar Width (arc min)
1	3	1.34
2	5	2.23
3	8	3.574
4	12	5.37
5	18	8.05
6	30	13.40

FLIR 1: Line Spread Function

The fast fourier transform (FFT) was performed on the I^2S system modulation transfer function (MTF) for the two FLIRS to permit convolution of the system line spread function with the simulated target bar pattern amplitudes. The FFT of the MTF for FLIR 1 (Figure 19) was taken over N = 128 points. The spatial frequency increment was F = 0.5c/mrad. The relationship of the FFT spatial frequency increment FFT input (Table 19) to the distance increment FFT output of the line spread function is given by:

$$X = \frac{1}{NF} = \frac{1}{128 \times 0.5 \text{ cycle/mrad}}$$

$$X = 0.01563 \text{ mrad/increment}$$

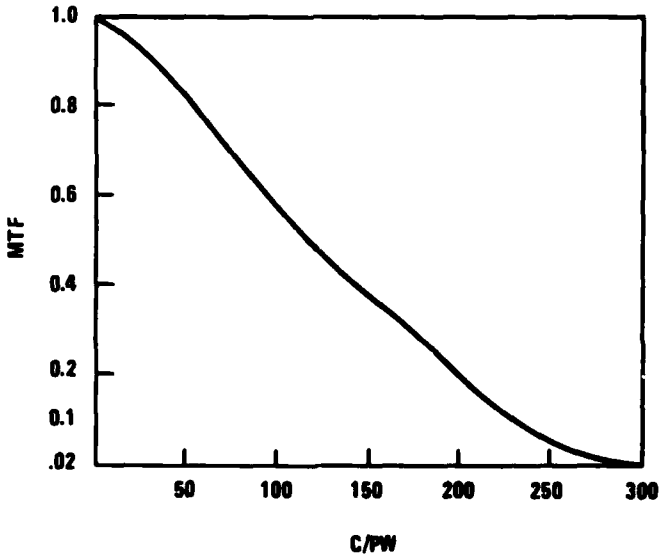

Figure 19. System MTF for FLIR 1

TABLE 19. FLIR 1: MTF DATA FOR THE FFT

$$\text{FFT} \begin{cases} F = 0.5c/\text{mrad} \\ N = 128 \text{ points} \end{cases}$$

Spatial Frequency c/PW	Spatial Frequency (c/mrad)	MTF
0	0.00	1.000
30	0.50	0.903
60	1.00	0.754
90	1.50	0.606
120	2.00	0.481
150	2.50	0.373
180	3.00	0.266
210	3.50	0.154
240	4.0	0.063
270	4.5	0.017
300	5.0	0.000

The units of the line spread function should be in fractions of the picture width (PW). The PW is 3.5 deg x 17.45 or 61.08 mrad/PW. The line spread function increment expressed as a fraction of PW is then:

$$X = \frac{\text{increment}}{\text{PW}} \left(\frac{\text{mrad/increment}}{\text{mrad/PW}} \right)$$

$$= \frac{0.01563 \text{ mrad/increment}}{61.08 \text{ mrad/PW}}$$

$$= 0.0002558 \text{ PW/increment (total increment across display: 3,909.3)}$$

The line spread function of FLIR 1 is shown in Table 20.

TABLE 20. FLIR 1: LINE SPREAD FUNCTION FOR 40 POINTS FROM THE FFT

Unit Increment (X) = 2.558×10^{-4} PW/cycle

8.234
8.117
7.774
7.230
6.524
5.704
4.824
3.938
3.095
2.336
1.689
1.172
0.787
0.526
0.374
0.306
0.298
0.325
0.365
0.401
0.422
0.423
0.402
0.364
0.314
0.258
0.203
0.154
0.114
0.084
0.064
0.053
0.048
0.047
0.049
0.051
0.053
0.054
0.055
0.055
0.054

FLIR 1: Conversion of Line Spread Increments

The line spread function increment in fraction of PW is 2.558×10^{-4} PW. Equivalently, there are 3909.12 increments per picture width. The I^2S system uses 512 pixels to simulate 1.0 in. of the FLIR display (that is, 1/8 of the 8-in. picture width). The FFT increment represents:

$$\frac{1}{8} \times 3909.12 \quad \frac{\text{increments}}{\text{PW}}$$

$$= 488.64 \text{ increments over } 1/8 \text{ of simulated display}$$

across the simulated 1.0-in. FLIR display. Since the I^2S system requires 512 pixels or amplitude points across the 1.0-in. FLIR display, instead of the 488.64 FFT points, 28 FFT increments (in other words, 29 FFT points) were used to represent one half of the line spread function. This scales to:

$$\frac{512}{488.64} \times 28 = 29.34 \text{ increments}$$

A program was used to linearly interpolate 30 points scaled to the I^2S simulation, representing a 1.0-in. portion of an 8-in. wide display by using 29 points from the line spread function. The ratio for increment interpolation is 488.64/512 = 0.9544. This data is presented in Table 21. A linear interpolation is accurate in this case since the line spread function for FLIR 1 is linear from increment 2 through increment 13 and the amplitude is low beyond increment 14 (see Figure 3).

TABLE 21. FLIR 1: INTERPOLATED FFT POINTS SCALED TO I^2S SYSTEM

29 FFT Points		30 Interpolated Points	
1	8.234	1	8.234
2	8.117	2	8.122
3	7.774	3	7.805
4	7.280	4	7.804
5	6.524	5	6.653
6	5.704	6	5.891
7	4.824	7	5.065
8	3.923	8	4.221
9	3.095	9	8.403
10	2.336	10	2.647
11	1.689	11	1.934
12	1.172	12	1.431
13	0.787	13	0.993
14	0.526	14	0.681
15	0.374	15	0.471
16	0.306	16	0.353
17	0.293	17	0.304
18	0.325	18	0.304
19	0.365	19	0.332
20	0.401	20	0.370
21	0.422	21	0.403
22	0.423	22	0.422
23	0.402	23	0.423
24	0.364	24	0.403
25	0.314	25	0.368
26	0.258	26	0.321
27	0.203	27	0.263
28	0.154	28	0.216
29	0.114	29	0.163
		30	0.127

If the 525-TV-line FLIR 1 system has approximately 384 active raster lines* across the vertical display height of 6 in. (3/4 aspect ratio), then a 1.0-in. simulated vertical portion of the display will have:

$$\frac{1.0 \text{ in.}}{6.0 \text{ in.}} \times 384 \text{ raster lines}$$

$$= 64 \text{ raster lines}$$

Consequently, the I^2S system will use eight pixels to simulate the energy distribution of a CRT spot; that is, 8 x 64 = 512 pixels.

FLIR 2: Line Spread Function

The distance increment X of the line spread function for FLIR 2 was calculated in the same manner as for FLIR 1. However, different values for N and F were used. The FFT of the MTF for FLIR 2 was taken over N = 256 points. The spatial frequency increment was F= 1.0 cycle/mrad. The increment of line spread function is X = 0.0039063 mrad/c. The PW for FLIR 2 is 1.7 deg x 17.45 = 29.66 mrad. Consequently, the increment of line spread function in fractions of picture width is 1.3168×10^{-4} PW (in image space).

---

*A standard TV line scan system has 480 to 490 active scan lines; however, FLIR 1 has approximately 384 active scan lines. Consequently, the vertical CRT picture height is expanded to preserve the 3:4 aspect ratio, thus creating some distortion in the displayed image (see pg. 116).

FLIR 2: Conversion of Line Spread Increments

The PW increment for FLIR 2 is 1.3168×10^{-4} PW, which is equivalent to 7594.24 increments across the simulated 8-in. width of the FLIR display (or 949.28 points across 1.0 inch). The I^2S requires 512 points and 32 FFT increments were used to represent half of the line spread function (see Table 22). Therefore, the required scale for the I^2S simulation is:

$$\frac{512}{949.28} \times 32 = 17.2594 \text{ increments}$$

The ratio of large increment (I^2S) to small increment (FFT output) is 1.8541. Therefore, to get 17 increments for I^2S, 33 FFT increments are needed. Table 23 presents the FFT printout over 34 points and the interpolated 18 points of the line spread function scaled to the 512 point I^2S system.

FLIR 2 is an 875-TV-line system with an estimated 768 active raster lines across the vertical display height of 6.0 in. (3/4 aspect ratio). This yields 128 raster lines across the 1.0-in. simulated vertical portion of the display. Therefore, four vertical lines of the 512-pixel I^2S system were used to simulate the CRT spot energy distribution; that is, $4 \times 128 = 512$ pixels.

TABLE 22. FLIR 2: LINE SPREAD FUNCTION FOR 40 POINTS FROM THE FFT

Unit Increment X = 1.32×10^{-4} PW/c

19.350
19.032
18.101
16.621
14.694
12.449
10.033
7.595
5.276
3.198
1.455
0.107
-0.822
-1.342
-1.494
-1.342
-0.965
-0.450
0.120
0.671
1.143
1.496
1.709
1.778
1.716
1.546
1.299
1.010
0.709
0.425
0.177
-0.022
-0.165
-0.254
-0.294
-0.295
-0.266
-0.219
-0.161
-0.101
-0.044

TABLE 23. FLIR 2: INTERPOLATED FFT POINTS SCALED TO I^2S SYSTEM

34 FFT Points		18 Interpolated Points	
1	19.350	1	19.350
2	19.032	2	18.237
3	18.101	3	15.256
4	16.621	4	11.090
5	14.694	5	6.629
6	12.449	6	2.727
7	10.033	7	-0.009
8	7.595	8	-1.331
9	5.276	9	-1.367
10	3.193	10	-0.611
11	1.455	11	0.413
12	0.107	12	1.232
13	-0.322	13	1.726
14	-1.342	14	1.693
15	-1.494	15	1.310
16	-1.342	16	0.766
17	-0.965	17	0.260
18	-0.450	18	-0.096
19	0.120		
20	0.671		
21	1.143		
22	1.496		
23	1.709		
24	1.778		
25	1.716		
26	1.546		
27	1.299		
28	1.010		
29	0.709		
30	0.425		
31	0.177		
32	-0.022		
33	-0.165		
34	-0.254		

Noise and Spot Size Simulation

The 512-x-512 I^2S pixel noise storage represents the display noise before it is filtered by the system MTF (convolved with system line spread function). Therefore, to determine how the noise should be simulated, it is necessary to evaluate the noise generation characteristics of the viewed FLIR display.

FLIR 1 has a vertical overscan (OVERSC) of 1.98. OVERSC is defined as:

$$\text{OVERSC} = \frac{\text{IFOV}_{\text{vert}}}{\text{raster spacing}}$$

Solving for the space between detector scan lines,

$$\text{raster spacing} = \frac{\text{IFOV}_{\text{vert}}}{\text{OVERSC}}$$

$$= \frac{0.236 \text{ mrad}}{1.98}$$

$$= 0.1192 \text{ mrad}$$

Therefore, the number of active scan lines is:

$$\text{active scan lines} = \frac{\text{VFOV}}{\text{raster spacing}}$$

$$= \frac{2.6 \text{ deg} \times 17.45 \text{ mrad/deg}}{0.1192}$$

= 384 active scan lines across the vertical display height of:

$$\frac{2.6 \text{ deg}}{3.5 \text{ deg}} \times 8 \text{ in.} = 6.0 \text{ in.}$$

The noise was generated over 384 lines per frame with a 4:1 interlace and a 1.98 vertical scan overlap. The overlap refers to the detector IFOV in object space. Notice that the overlap is greater than the raster spacing. This means that the detector sees the target twice during a frame. However, if it is assumed that the display CRT spot diameter is set equal to the raster spacing, then the target signal in object space is integrated twice but noise downstream from the detector is not integrated. The noise originates at the output of the detector, not in object space. Therefore, the noise is only correlated from pixel to pixel of the I^2S in the horizontal direction over the width of the line spread function and is not correlated from raster line to raster line.

With the I^2S system scaled to FLIR 1, there are 64 raster lines across the vertical display height. Therefore, the noise stored on the I^2S should be correlated over 512/64 = 8.0 vertical lines. These eight lines correspond to the width of the CRT spot. The intensity/amplitude of the noise was varied across the spot width to simulate spot intensity.

Gaussian CRT Spot Distribution

A Gaussian spot distribution was assumed for the CRT display spot intensity. Spot cutoff was defined as the shrinking raster with e^{-1} amplitude at a distance W from the spot center (Figure 20).

The normalized amplitudes for a four-line and an eight-line display spot simulation are presented in Table 24.

Figure 21 presents the display spot amplitude distribution that was simulated by the I^2S pixel amplitude storage with an e^{-1} amplitude cutoff point. Figure 22a.

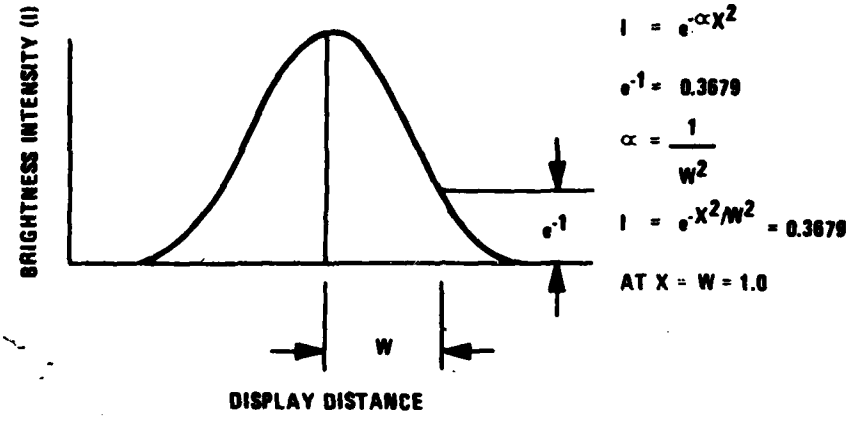

Figure 20. Gaussian CRT Spot Distribution

TABLE 24. NORMALIZED INTENSITY AMPLITUDE DISTRIBUTION

Four-Point CRT Spot/FLIR 2		Eight-Point CRT Spot/FLIR 1	
X/W	I	X/W	I
±.3333	.895	± .1429	.980
1.0000	.368	± .4286	.8322
		± .7143	.600
		1.0000	.368

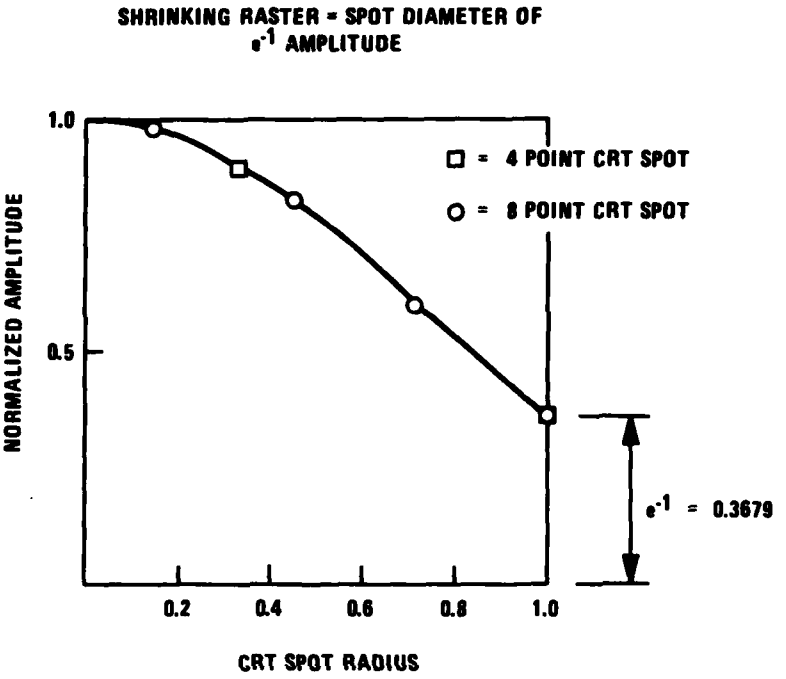

Figure 21. CRT Spot Simulation: Amplitude vs No. of Points

shows that the four-line spot simulation (for FLIR 2) represents a display raster scan that has a nearly zero intensity amplitude between scans. The eight-line spot simulation represents a raster that has a 0.369 amplitude between scans (see Figure 22b).

Line Spread Function for Noise Convolution

Figure 23 shows the extrapolation of known MTF data from the FLIR 1 display (for a spatial frequency of five where the system MTF cuts off). The tabulation of the line spread function of the display is shown in Table 25 for both the FFT output and interpolated points for the 512 I^2S digital display. These points represent one side of the display line spread function for convolution with the rms detector noise.

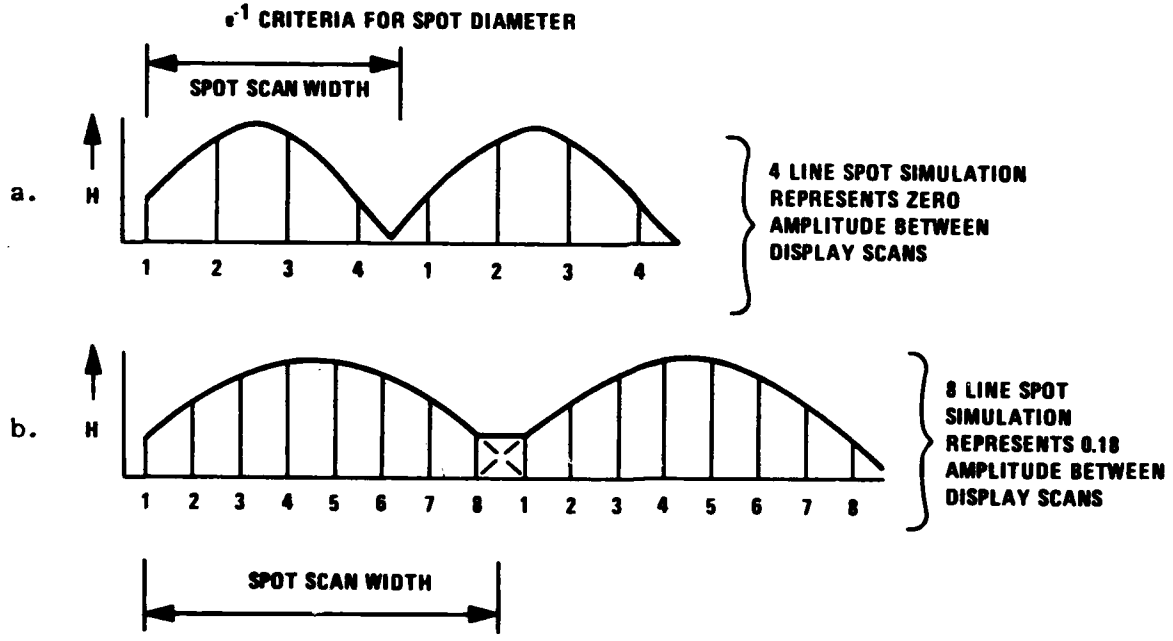

Figure 22. Line Spot Simulation

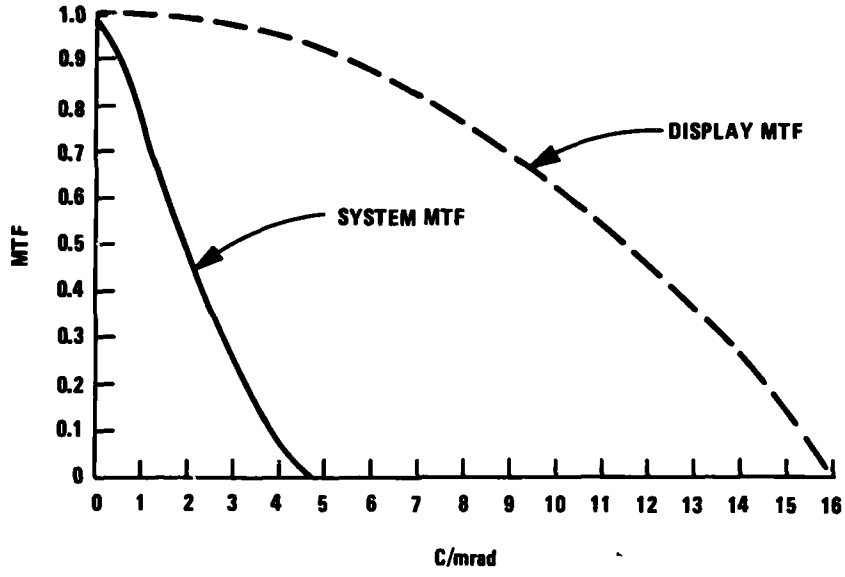

Figure 23. FLIR 1: Display and System MTF

Table 26 shows the line spread function tabulations for FLIR 2. Both display line spread functions are much narrower than the FLIR sensor system line spreads since the display MTF's are much better (extend over higher spatial frequencies). However, the two display lines' spreads have about the same width, which indicates that both FLIRs use similar displays (Conrac with 2000 TV line resolution).

TABLE 25. FLIR 1: COMPUTER OUTPUT FOR FFT OF DISPLAY MTF

The 29 Data Points are:

1	43.554	
2	33.516	
3	12.776	
4	-1.593	
5	-3.288	
6	0.394	
7	1.342	
8	-0.406	
9	-0.977	
10	0.121	
11	0.586	
12	-0.109	
13	-0.434	
14	0.094	
15	0.366	LINE SPREAD FUNCTION
16	-0.021	OF DISPLAY MTF (FFT
17	-0.265	OVER 128 POINTS)
18	0.011	
19	0.188	
20	-0.044	
21	-0.184	
22	0.035	
23	0.181	
24	-0.003	
25	-0.154	
26	-0.019	
27	0.114	
28	0.016	
29	-0.082	

Increment size = 0.9544

The 30 Interpolated Points are:

1	43.554	
2	33.974	
3	14.667	
4	0.373	
5	-2.979	
6	-0.445	
7	1.083	
8	0.152	
9	-0.769	
10	-0.330	
11	0.374	
12	0.240	
13	-0.256	
14	-0.221	
15	0.191	INTERPOLATED FFT POINTS
16	0.245	SCALED TO t^2S SYSTEM FOR
17	-0.087	NOISE CONVOLUTION
18	-0.203	
19	0.043	
20	0.157	
21	-0.056	
22	-0.175	
23	0.034	
24	0.174	
25	0.014	
26	-0.133	
27	-0.044	
28	0.083	
29	0.043	
30	-0.050	

TABLE 26. LINE SPREAD FUNCTION OF DISPLAY MTF (FFT OVER 256 POINTS)

The 34 Data Points are:

1	39.374
2	37.133
3	31.154
4	22.635
5	13.649
6	5.825
7	0.421
8	-2.187
9	-2.417
10	-1.218
11	0.339
12	1.424
13	1.662
14	1.147
15	0.278
16	-0.485
17	-0.830
18	-0.700
19	-0.264
20	0.203
21	0.465
22	0.432
23	0.171
24	-0.146
25	-0.348
26	-0.342
27	-0.153
28	0.103
29	0.293
30	0.325
31	0.199
32	-0.011
33	-0.195
34	-0.267

Increment Size = 1.8541

The 18 Interpolated Points are:

1	39.374	
2	32.034	
3	16.286	
4	2.786	
5	-2.283	
6	-0.797	
7	1.454	
8	1.158	
9	-0.357	INTERPOLATED FFT POINTS
10	-0.741	SCALED TO I^2S SYSTEM
11	-0.011	FOR NOISE CONVOLUTION
12	0.452	
13	0.092	
14	-0.347	
15	-0.161	
16	0.257	
17	0.241	
18	-0.107	

METHODOLOGY

Stimuli

Equal numbers of two target shapes--four-bar and solid square--were used in the experiment. Bar width was 1/7 of bar height. Initially, there were six different target sizes. Five levels of target contrast * were selected for each target size and viewing condition. The levels were chosen in pilot studies which bracketed the target recognition threshold of a normal observer. The pilot studies indicated that the smallest target could not be recognized regardless of contrast. Consequently, it was excluded from the main experiment.

The stimuli were convolved with a line spread function. Noise was then added to simulate viewing each of the two FLIRs operating at three noise levels. The resulting images appeared as blurred versions of the original target, seen against a background of dynamic noise.

Apparatus

Stimuli were computer-generated with the I^2S Model 70/E image analysis computer interfaced to a Honeywell level 6/43 (digital) computer. The images were displayed on-line with a Tectronix Model 632 television picture monitor using standard 2:1 interlaced composite video signals.

---

* Contrast defined as $\frac{\text{Target Luminance - Background Luminance}}{\text{Target Luminance + Background Luminance}}$

Operators viewed the display from a distance of 10 ft. The central 8 in. x 8 in. portion of the monitor represented a 1.0 in. x 1.0 in. area of a FLIR display viewed from 15 in.

Gain and brightness levels were reset prior to each experimental session. A five-step gray wedge was displayed on the screen and the levels adjusted to yield five equally spaced luminance steps from 0.2 to 25 ft-L. Luminances were checked with a Gamma Scientific telephotometer.

Two separate video channels simulated FLIR MTF and noise. The test target was generated on one channel; then the system MTF for either FLIR 1 or FLIR 2 and an intensity transform were applied, producing a degraded image at the desired contrast. With the second channel, noise was created line by line; then the display MTF and intensity transform were applied. The contents of the two channels were added together and written on the monitor at the rate of 30 fps.

The noise level had a Gaussian distribution and was made to appear dynamic by randomly selecting an (x, y) offset 30 times each second to define the noise field on channel two.

Design

A repeated-measures factorial design was used. All possible combinations of shape, size, contrast, MTF, and noise levels yielded 300 different stimuli. Five replications of each target yielded a total of 1500 trials. The targets were grouped into 30 blocks of 50 stimuli. Each block maintained

constant size, MTF, and noise levels, simulating an observer being tested on a particular FLIR for one size target. Subjects were run in groups of either three, four, or five.

Trials within a block were randomly ordered. Order of block presentation was randomized across subjects, except that all targets representing FLIR 1 were presented first.

Subjects

Observers were males between the ages of 19 and 45. All were required to have normal, uncorrected vision: 20/20 near and far binocular acuity, normal stereopsis, and color vision. Assessments were made with a Titmus Optical Vision Tester.

Procedure

Observers viewed the display binocularly. Ambient illumination was maintained at 0.5 ft-L. A 20-minute period of dark adaptation preceded testing.

The target appeared in one of the positions on the display--80 pixels (10.3 mrad) left or right from the center of the screen. Trials lasted five seconds and were followed by a one-second inter-trial interval during which the screen appeared homogeneous at the background luminance level.

Subjects were instructed to watch the display for the entire five-second trial interval and then record the shape and position of the stimulus on their answer sheets. They were instructed to give their best guess when uncertain. See Appendix A for a transcript of the instructions given to the subjects.

Two hundred practice trials, with feedback, familiarized observers with the stimuli and procedures. The 30 test blocks followed. A five-minute break was allowed after every nine blocks. The experiment required about four hours to complete.

RESULTS

Twelve subjects completed the experiment. Responses were counted as correct detection if the observer indicated the correct location (left or right) of the target. Responses were counted as correct recognition if both location and target identification (four-bar or square) were accurate. A third category of correct four-bar recognition was based on correct identification of four-bar patterns conditioned on their detection. Trials on which a detection error occurred were not included in the tabulation of four-bar recognition responses.

The proportion of correct responses was determined for each of the above categories under all 30 viewing conditions. The raw data from which these proportions were calculated are included in the tables in Appendix C. The proportions were then averaged across subjects.

Figures 24 through 33 show the percentage of correct detection responses as a function of target contrast for each viewing condition. SIGNAL TOP is the digital pixel value of either the four-bar or square target which corresponds to the peak signal. SIGNAL BASE for all conditions was 200 (digital pixel value). All noise levels used for a given combination of FLIR MTF and target size are represented in the same graphs. Noise Levels 40, 80, and 160 digital pixel values correspond to 0.033V, 0.065V, and 0.130V rms. Figures 34 through 43 and 44 through 53 show the same information for recognition and four-bar recognition responses, respectively.

The 75 percent correct point was interpolated by eye for each four-bar recognition and detection graph and considered the contrast threshold. For FLIR 1, target size three (250.9 cycles/PW), the threshold was approximated by extrapolation from the lowest noise condition. The same was achieved for FLIR 2, target size two (401.7 cycles/PW). These approximations are indicated on the graph by asterisks.

The contrast thresholds for four-bar recognition are summarized in Figures 54 and 55. These graphs also show the results at each of the three noise levels for each FLIR.

As indicated in Figure 55, the thresholds for FLIR 1 monotonically decreased with increasing target size. The noise parameter interacted with target size, but, in general, higher noise levels led to increased thresholds. The results for FLIR 2 (Figure 54) were less straightforward. The recognition threshold did not monotonically decrease with increased target size nor increase with increased noise levels. A comparison of the two figures does indicate that performance was superior using the FLIR 2 simulation.

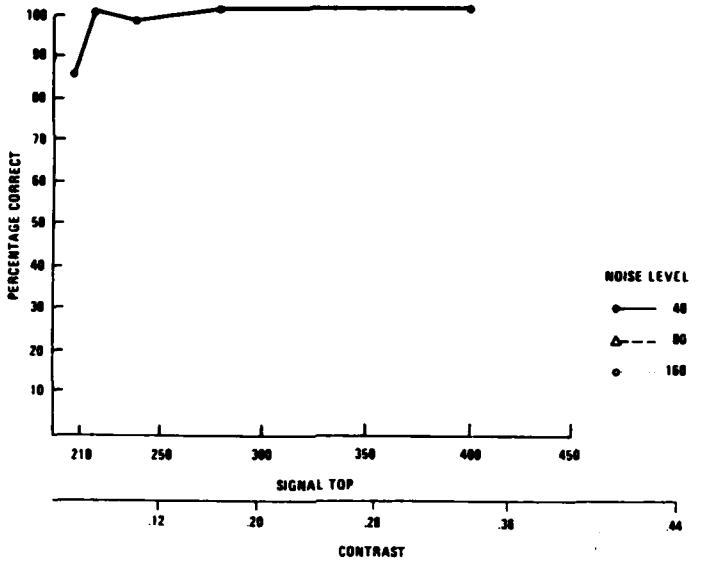

Figure 24. Percentage Correct Detection Rate for FLIR 1, Target 2 as a Function of Target Contrast

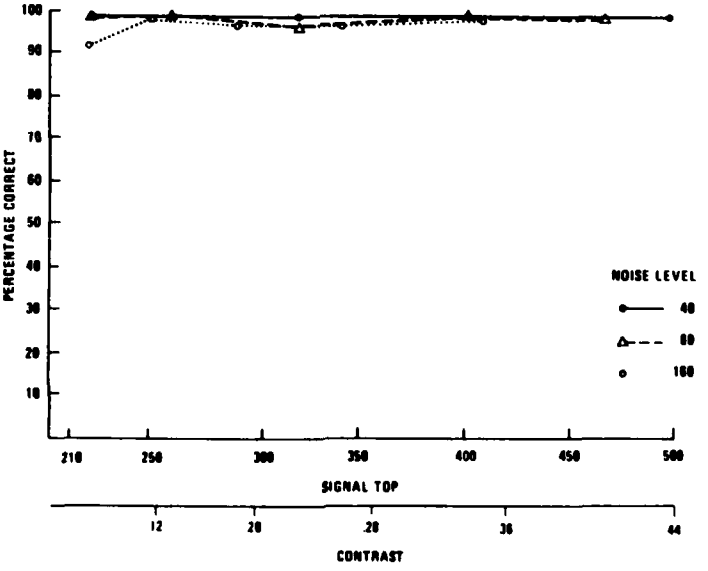

Figure 25. Percentage Correct Detection Rate for FLIR 1, Target 3 as a Function of Target Contrast

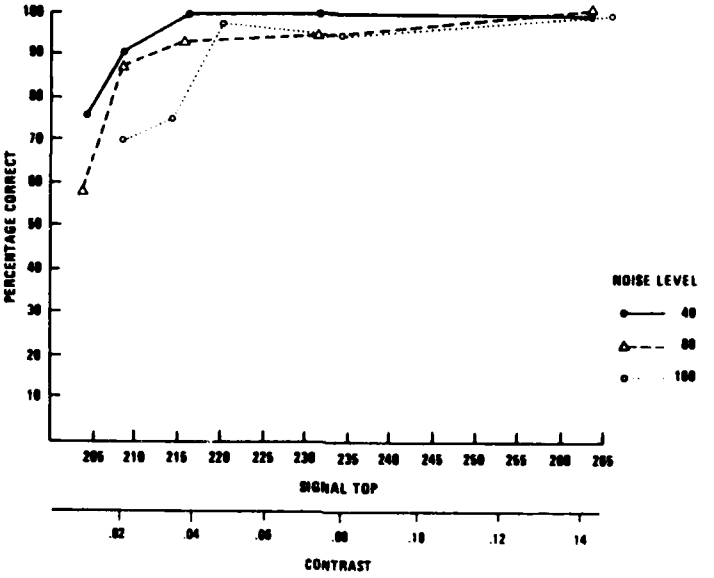

Figure 26. Percentage Correct Detection Rate for FLIR 1, Target 4 as a Function of Target Contrast

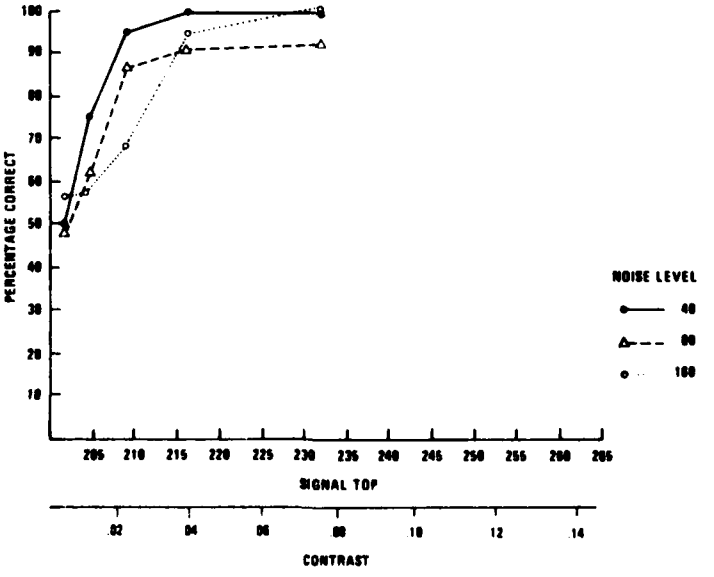

Figure 27. Percentage Correct Detection Rate for FLIR 1, Target 5 as a Function of Target Contrast

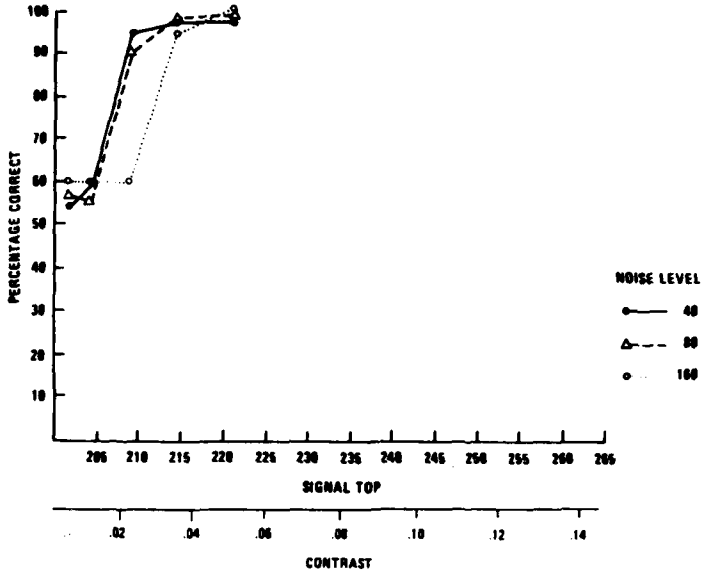

Figure 28. Percentage Correct Detection Rate for FLIR 1, Target 6 as a Function of Target Contrast

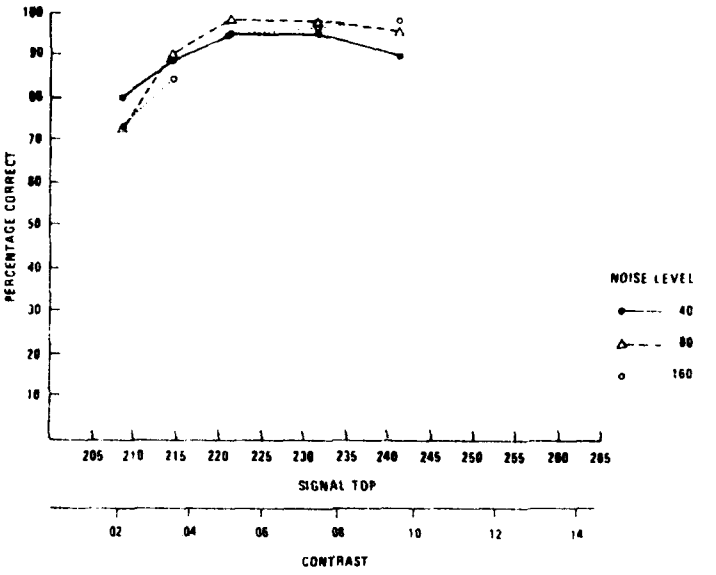

Figure 29. Percentage Correct Detection Rate for FLIR 2, Target 2 as a Function of Target Contrast

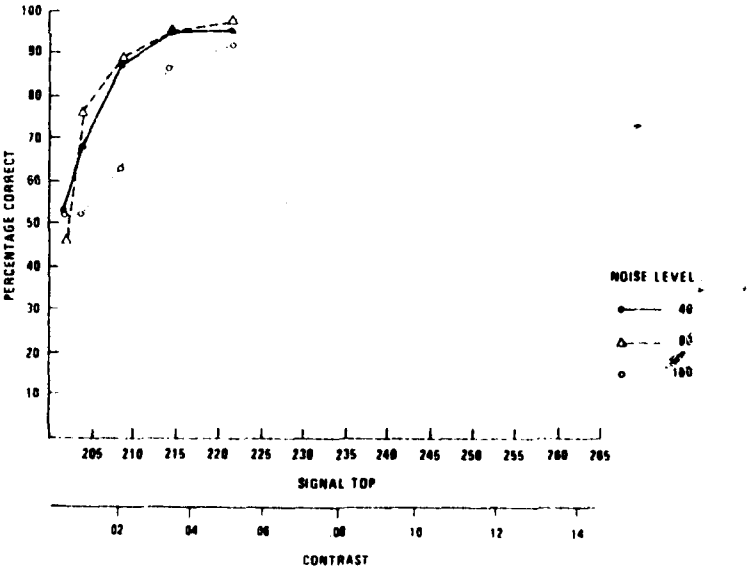

Figure 30. Percentage Correct Detection Rate for FLIR 2, Target 3 as a Function of Target Contrast

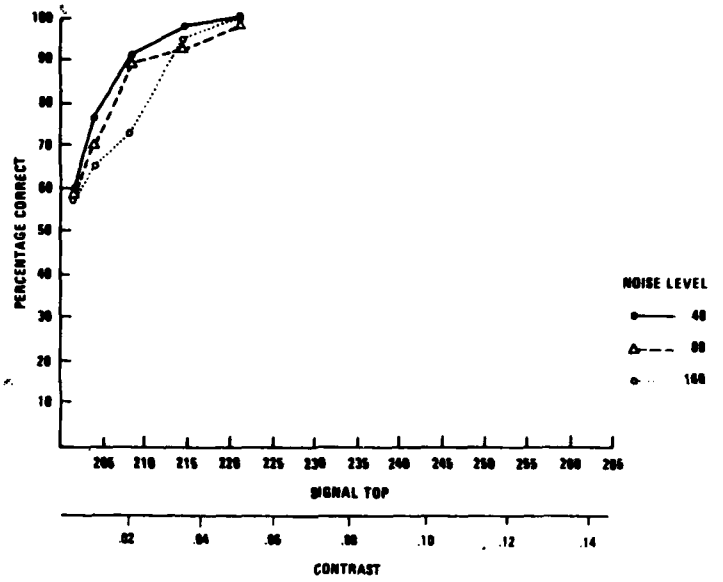

Figure 31. Percentage Correct Detection Rate for FLIR 2, Target 4 as a Function of Target Contrast

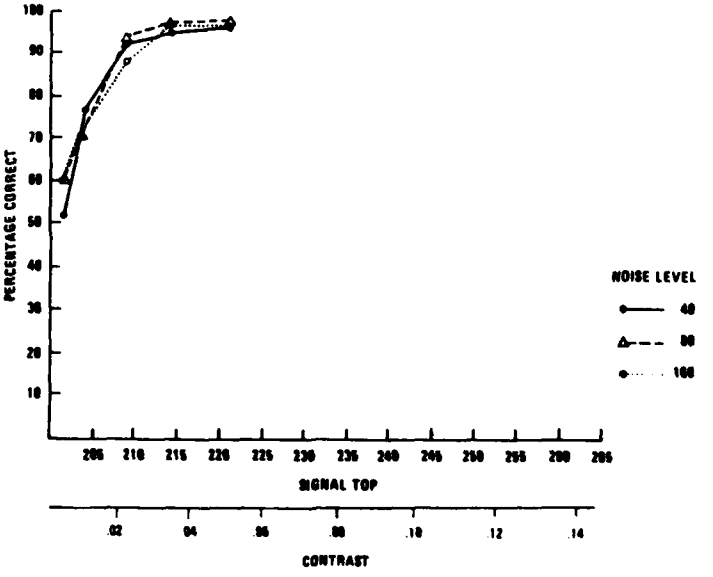

Figure 32. Percentage Correct Detection Rate for FLIR 2, Target 5 as a Function of Target Contrast

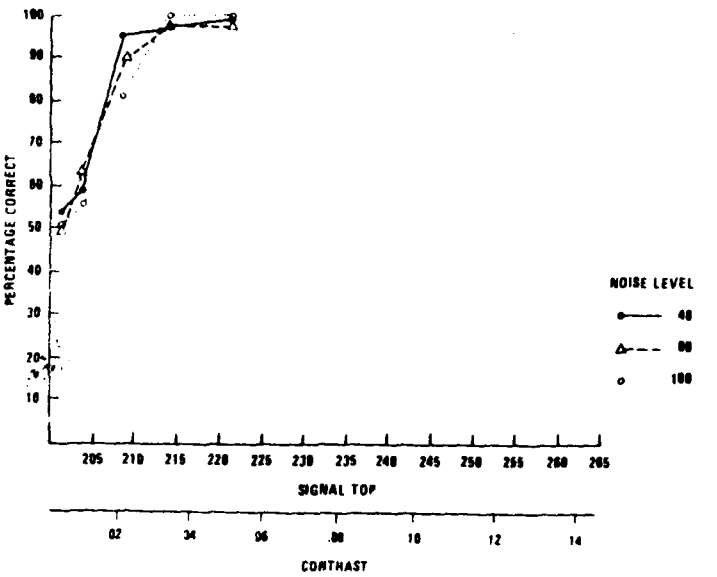

Figure 33. Percentage Correct Detection Rate for FLIR 2, Target 6 as a Function of Target Contrast

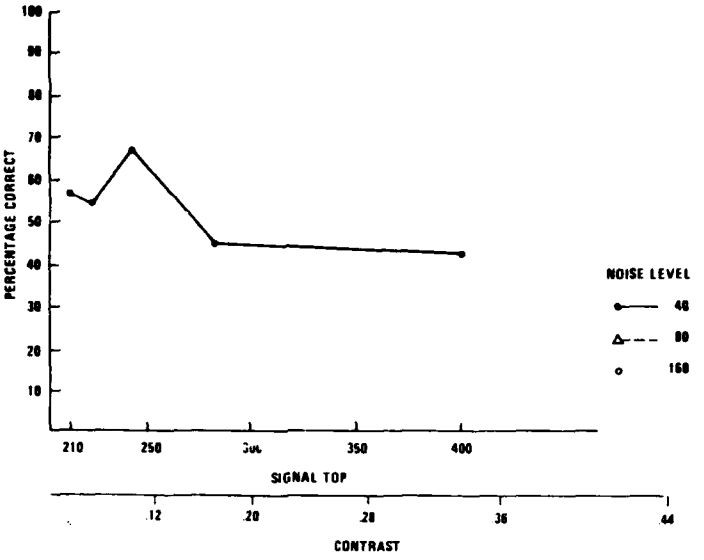

Figure 34. Percentage Correct Recognition Rate for FLIR 1, Target 2 as a Function of Target Contrast

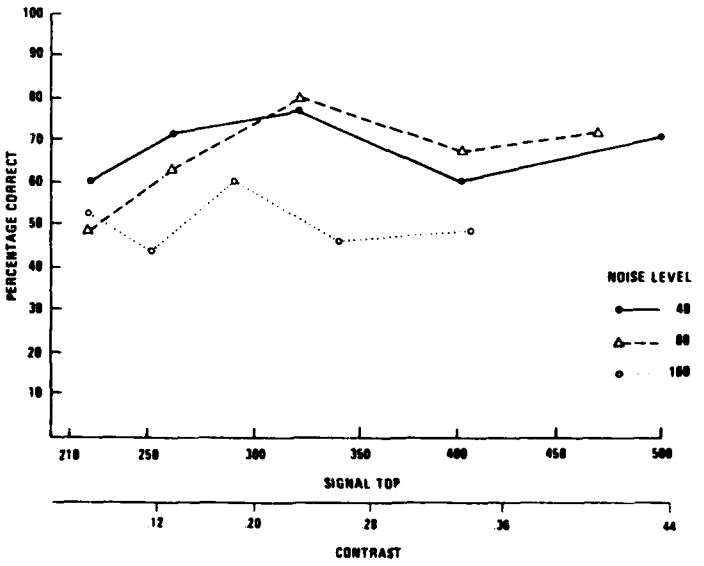

Figure 35. Percentage Correct Recognition Rate for FLIR 1, Target 3 as a Function of Target Contrast

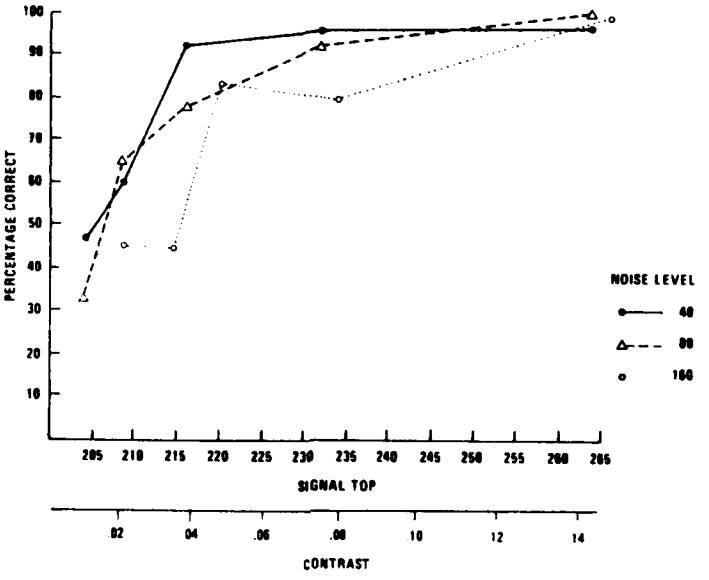

Figure 36. Percentage Correct Recognition Rate for FLIR 1, Target 4 as a Function of Target Contrast

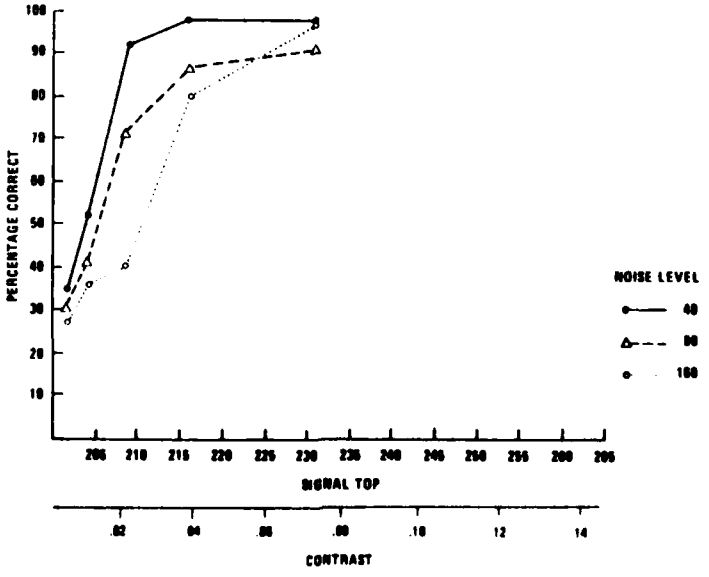

Figure 37. Percentage Correct Recognition Rate for FLIR 1, Target 5 as a Function of Target Contrast

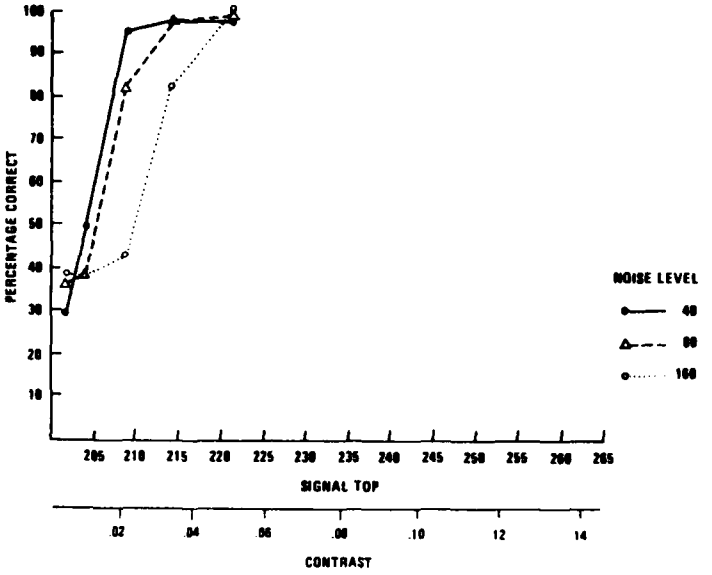

Figure 38. Percentage Correct Recognition Rate for FLIR 1, Target 6 as a Function of Target Contrast

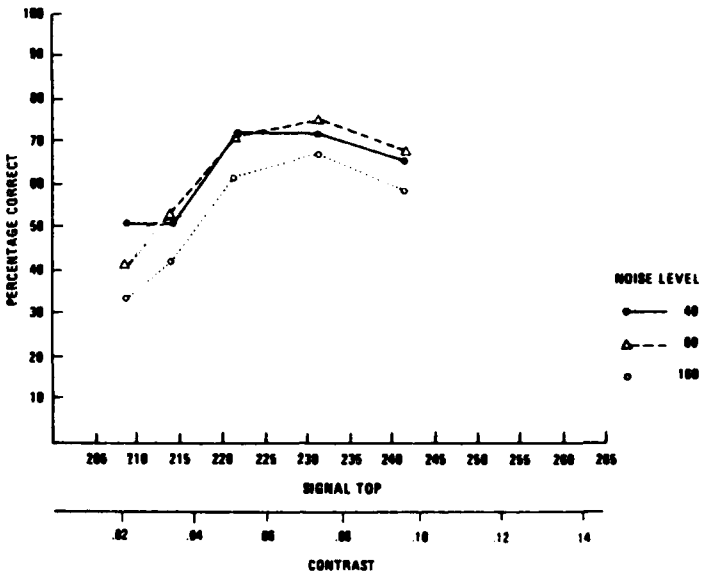

Figure 39. Percentage Correct Recognition Rate for FLIR 2, Target 2 as a Function of Target Contrast

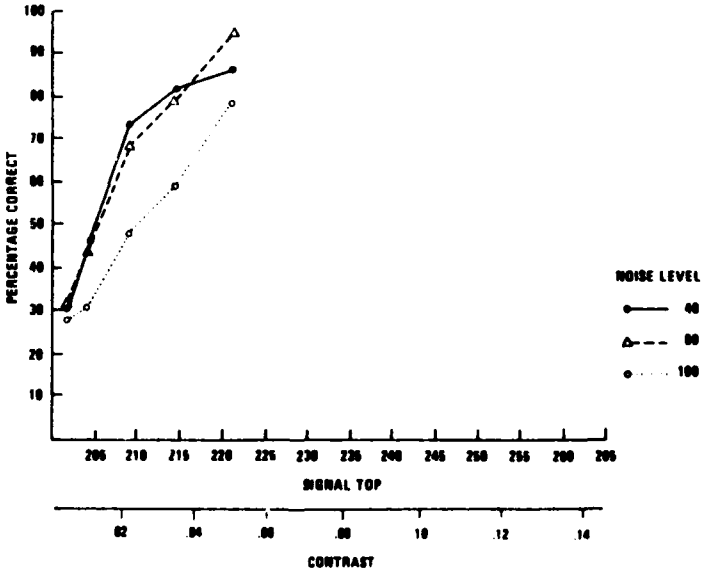

Figure 40. Percentage Correct Recognition Rate for FLIR 2, Target 3 as a Function of Target Contrast

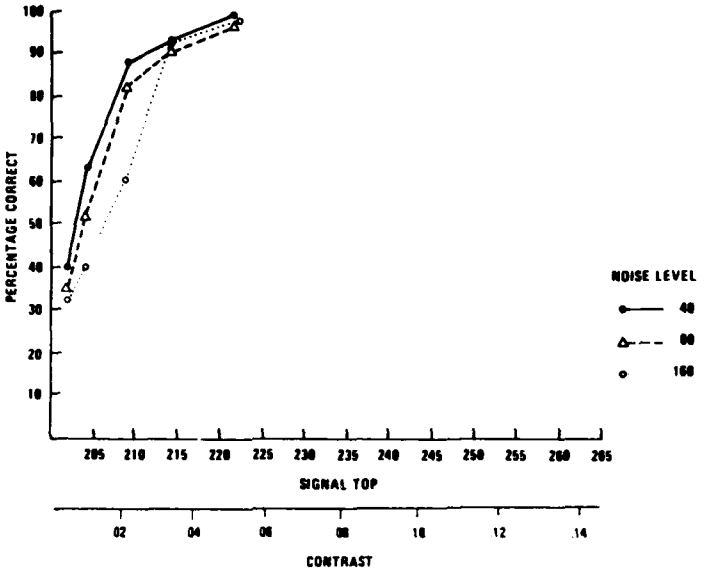

Figure 41. Percentage Correct Recognition for FLIR 2, Target 4 as a Function of Target Contrast

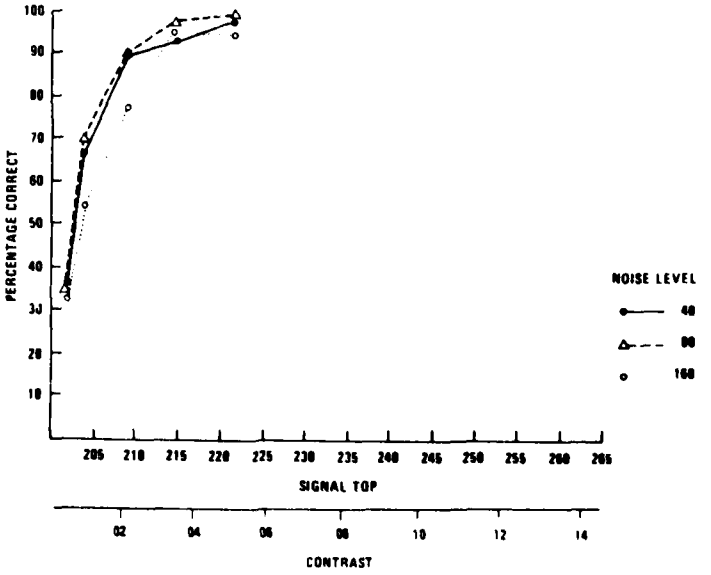

Figure 42. Percentage Correct Recognition for FLIR 2, Target 5 as a Function of Target Contrast

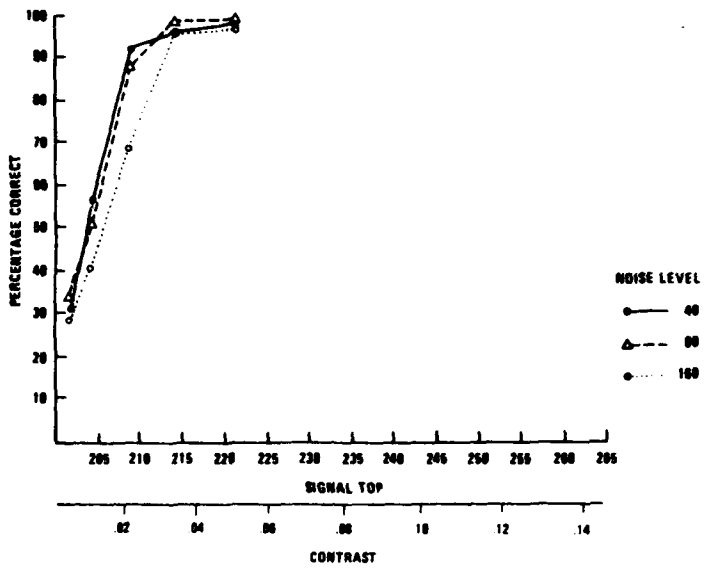

Figure 43. Percentage Correct Recognition for FLIR 2, Target 6 as a Function of Target Contrast

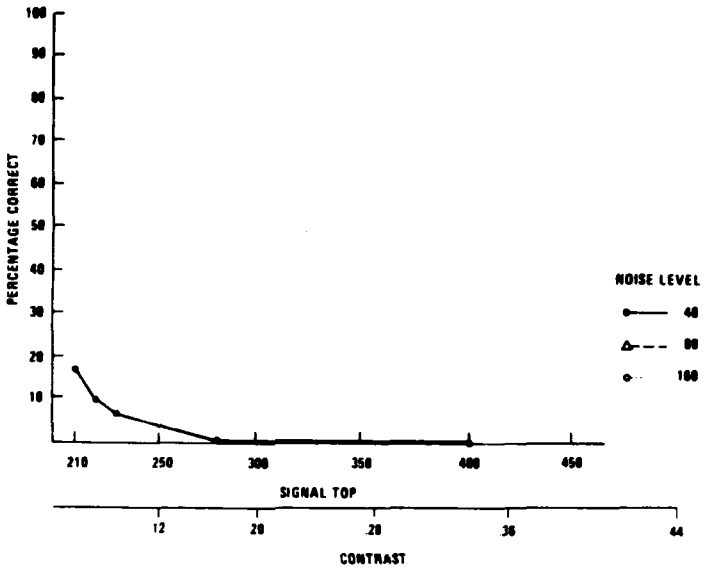

Figure 44. Percentage Correct Four-Bar Recognition Rate for FLIR 1, Target 2 as a Function of Target Contrast

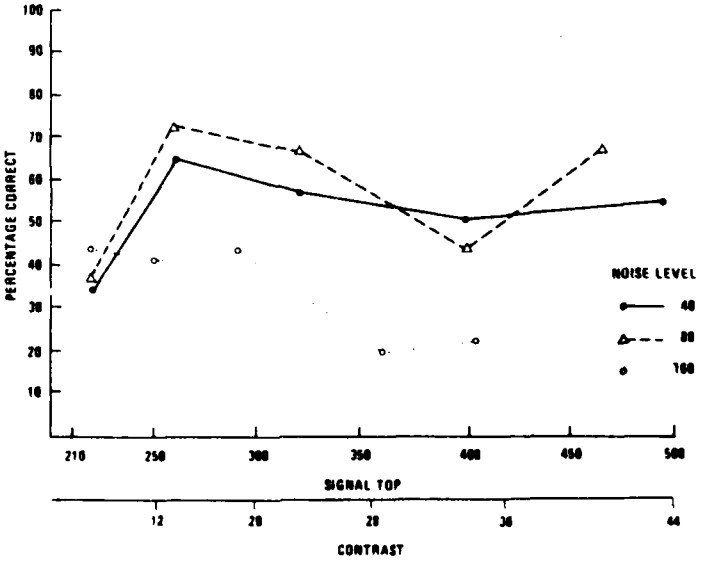

Figure 45. Percentage Correct Four-Bar Recognition Rate for FLIR 1, Target 3 as a Function of Target Contrast

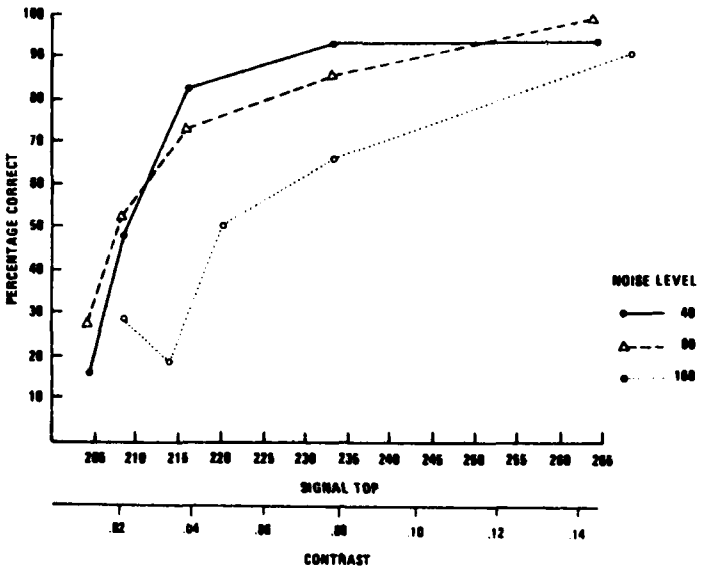

Figure 46. Percentage Correct Four-Bar Recognition Rate for FLIR 1, Target 4 as a Function of Target Contrast

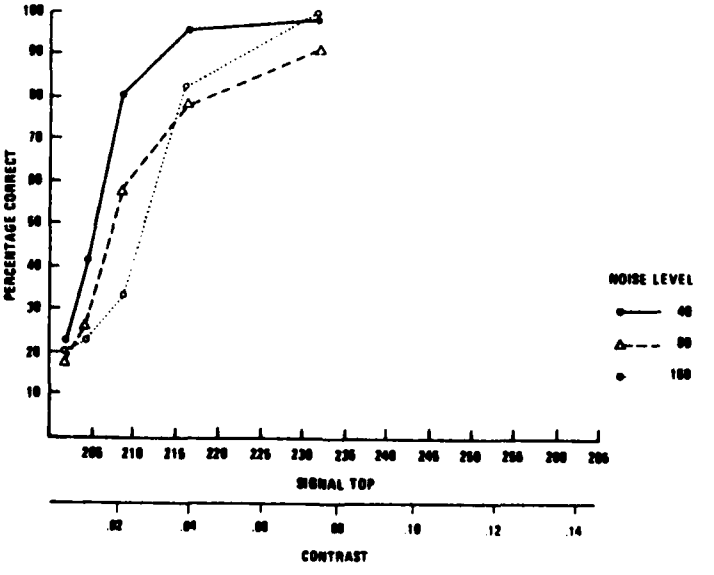

Figure 47. Percentage Correct Four-Bar Recognition Rate for FLIR 1, Target 5 as a Function of Target Contrast

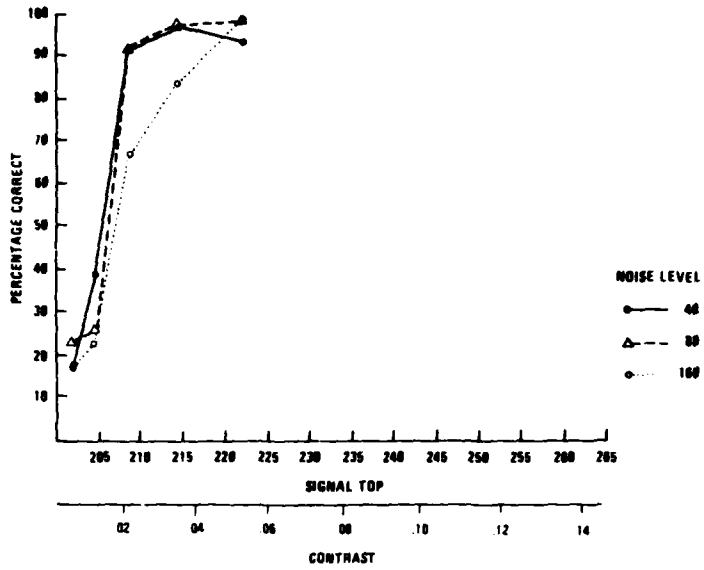

Figure 48. Percentage Correct Four-Bar Recognition Rate for FLIR 1, Target 6 as a Function of Target Contrast

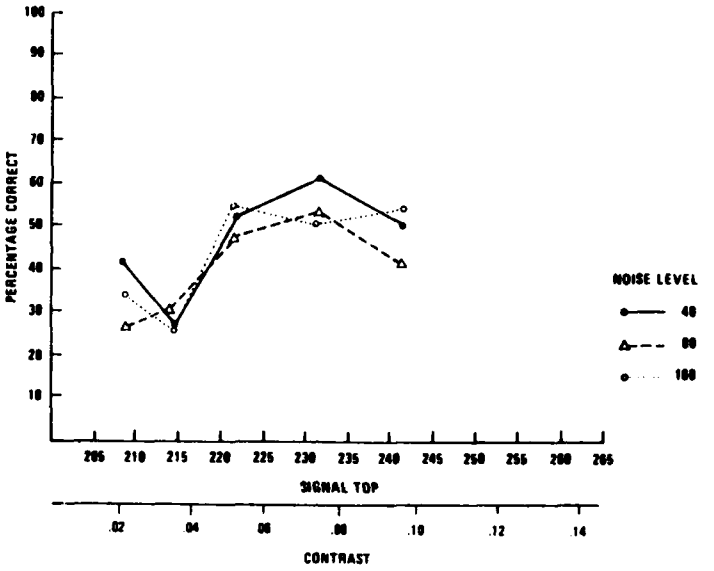

Figure 49. Percentage Correct Four-Bar Recognition Rate for FLIR 2, Target 2 as a Function of Target Contrast

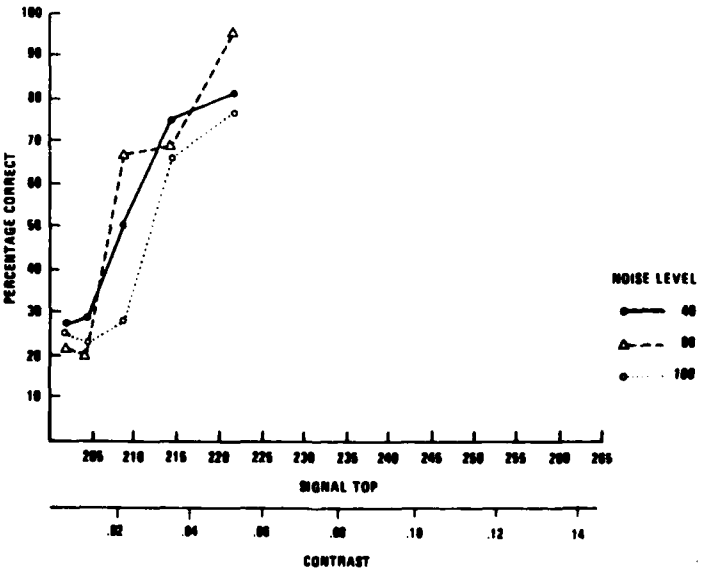

Figure 50. Percentage Correct Four-Bar Recognition Rate for FLIR 2, Target 3 as a Function of Target Contrast

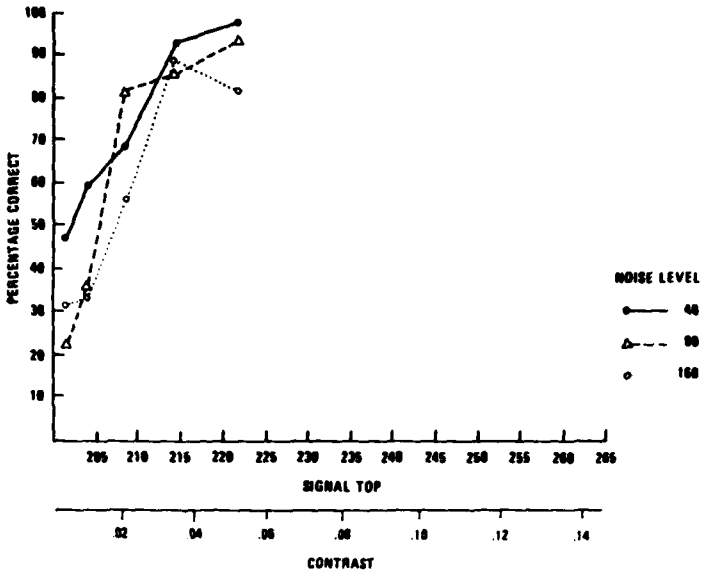

Figure 51. Percentage Correct Four-Bar Recognition Rate for FLIR 2, Target 4 as a Function of Target Contrast

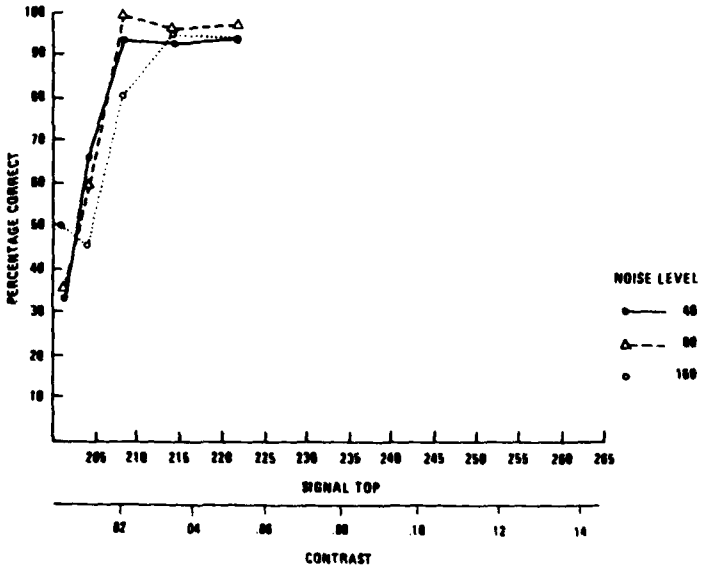

Figure 52. Percentage Correct Four-Bar Recognition Rate for FLIR 2, Target 5 as a Function of Target Contrast

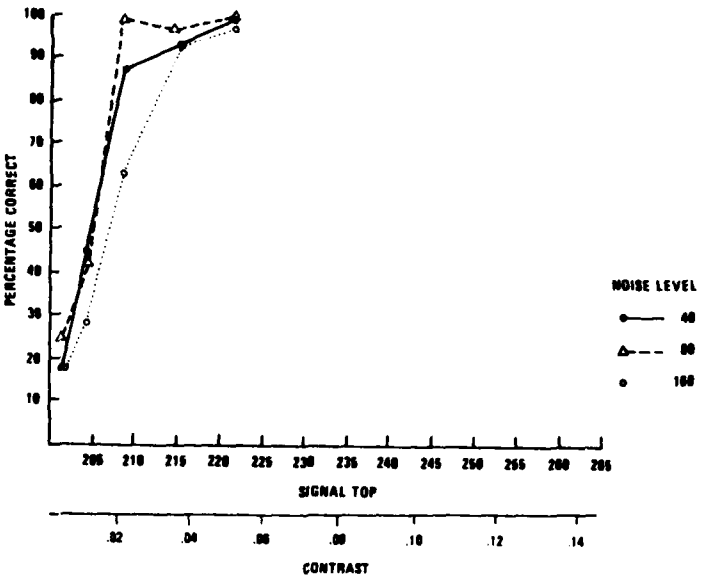

Figure 53. Percentage Correct Four-Bar Recognition Rate for FLIR 2, Target 6 as a Function of Target Contrast

Contrast thresholds for the detection task are summarized in Figures 56 and 57. The results are not completely straightforward for either FLIR 1 or FLIR 2. But again, thresholds were generally lower for FLIR 2.

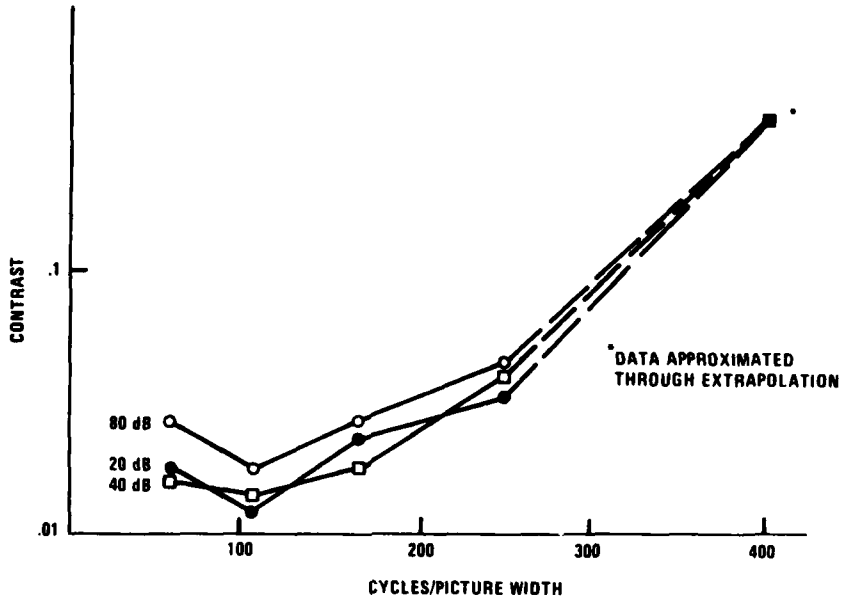

Figure 54. Contrast Threshold for Four-Bar Recognition as a Function of Target Size for FLIR 2

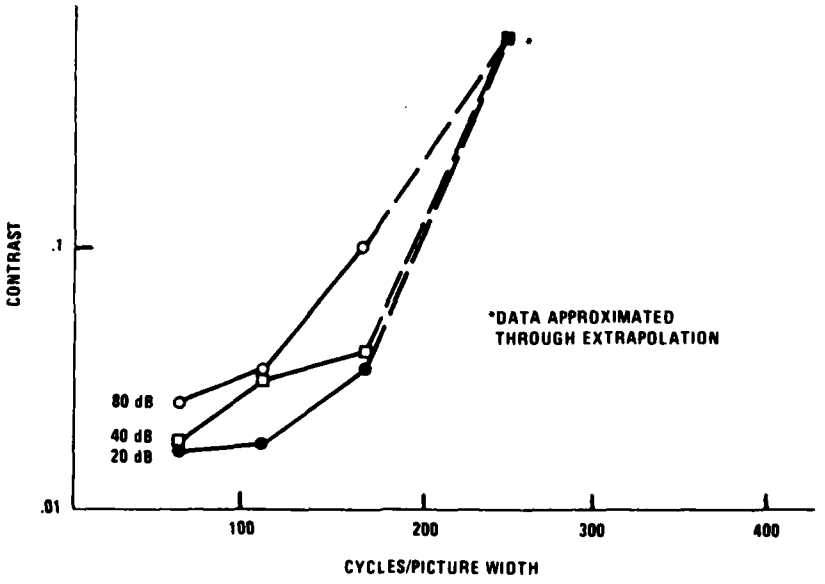

Figure 55. Contrast Threshold for Four-Bar Recognition as a Function of Target Size for FLIR 1

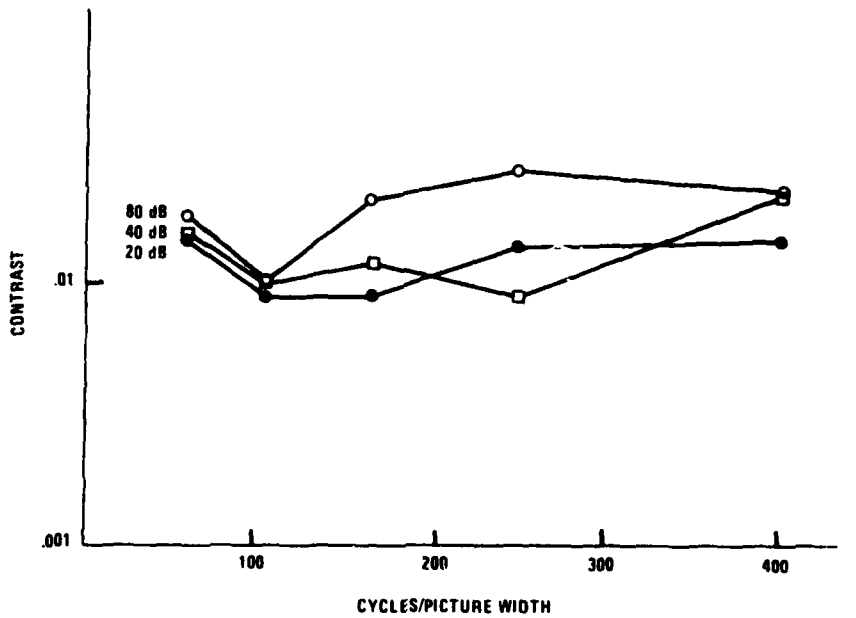

Figure 56. Contrast Threshold for Detection as a Function of Target Size for FLIR 2

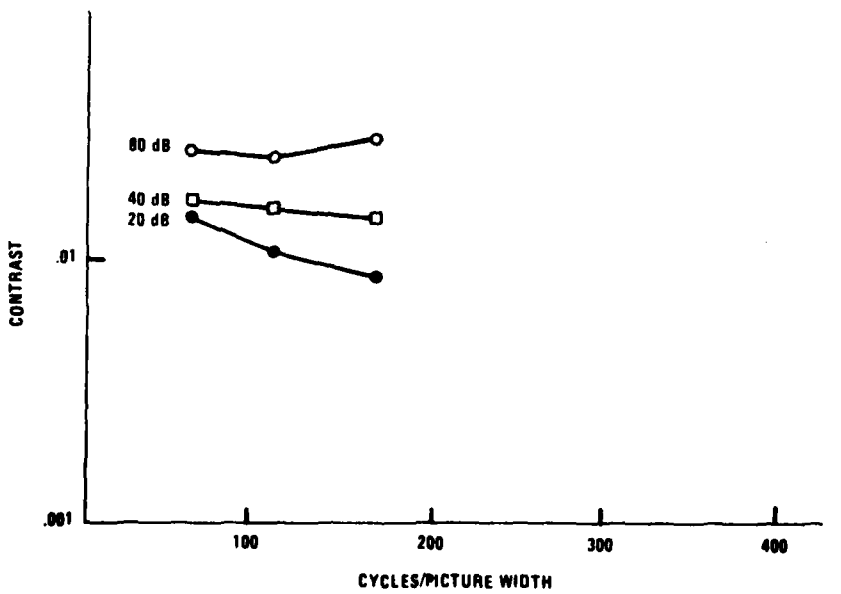

Figure 57. Contrast Threshold as a Function of Target Size for FLIR 1

Interestingly, both threshold functions for FLIR 2 display a U-shape non-monotonicity. Thresholds for the largest and smallest patterns were higher than thresholds for the second largest pattern. This finding is consistent with previous reports of the shape of contrast sensitivity functions for human observers. One such function is included for comparison (Figure 58).* The stimuli were square wave gratings in a 2 deg square field, displayed at a mean luminance level of 2.7 ft-L. The conditions are comparable with the present experiment.

Contrast thresholds for four-bar recognition were also used to obtain the MRT for FLIR 1 and FLIR 2. The MRT was calculated from:

$$MRT = \frac{\text{Peak Signal - Base Signal}}{\text{RMS Noise}} \times NE\Delta T(°K)$$

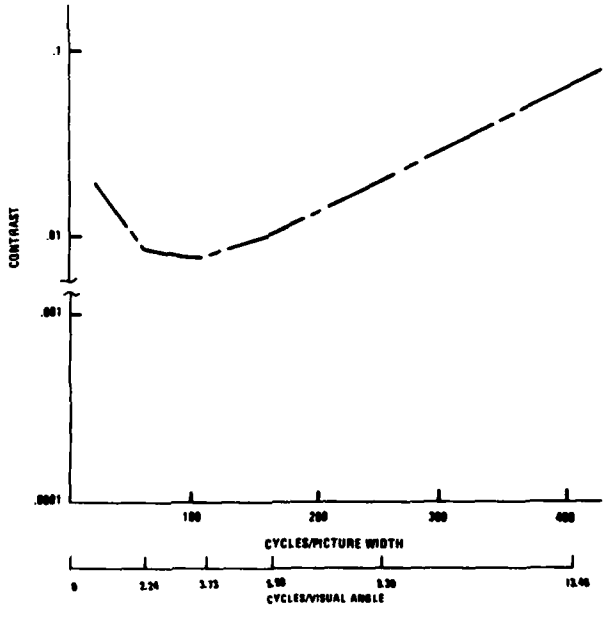

Figure 58. Contrast Threshold as a Function of Target Size

*Schober and Hilz, 1965.

where the signal and noise were measured in digital pixel values. NEΔT for FLIR 1 was obtained from NVL measurements (0.182K). A NVL predictive model was also used for FLIR 2.

The MRTs for each of the three noise levels in the FLIR 1 simulation are shown in Figure 59. The MRT prediction of the NVL model is also indicated in the figure. Figure 60 shows the three measured MRTs for FLIR 2 along with the MRT NVL prediction model. In both cases, the experimentally derived MRTs have a shape similar to the predicted MRTs but are shifted downward. This indicates that the simulations produced somewhat more sensitive MRTs than predicted. The measured MRTs do not show the continued downward trend with decreasing spatial frequency, as the models predict.

DISCUSSION

The MRT paradigm was adapted to digital image processing and standard psychophysical methods. Two FLIRs were simulated, one a first-generation FLIR that had been previously assessed by the NVL model and the other a second-generation FLIR.

Detection and recognition performance were measured for 12 observers under three different noise conditions. Four-bar and solid square targets of various sizes were used, and a contrast threshold was determined for each target size, noise level, and FLIR.

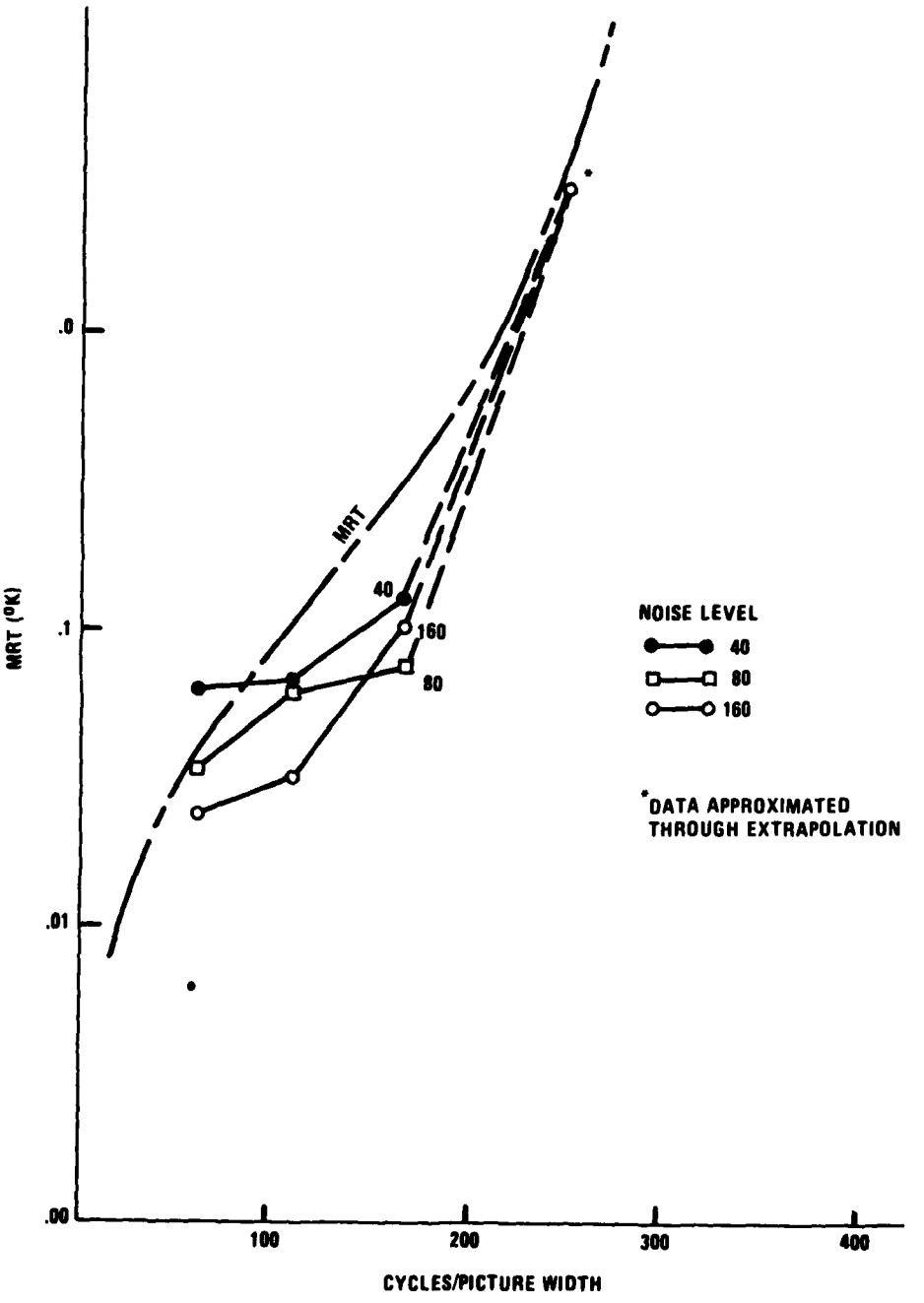

Figure 59. Analysis: Comparison of NVL MRT Prediction to Subject Data, FLIR 1

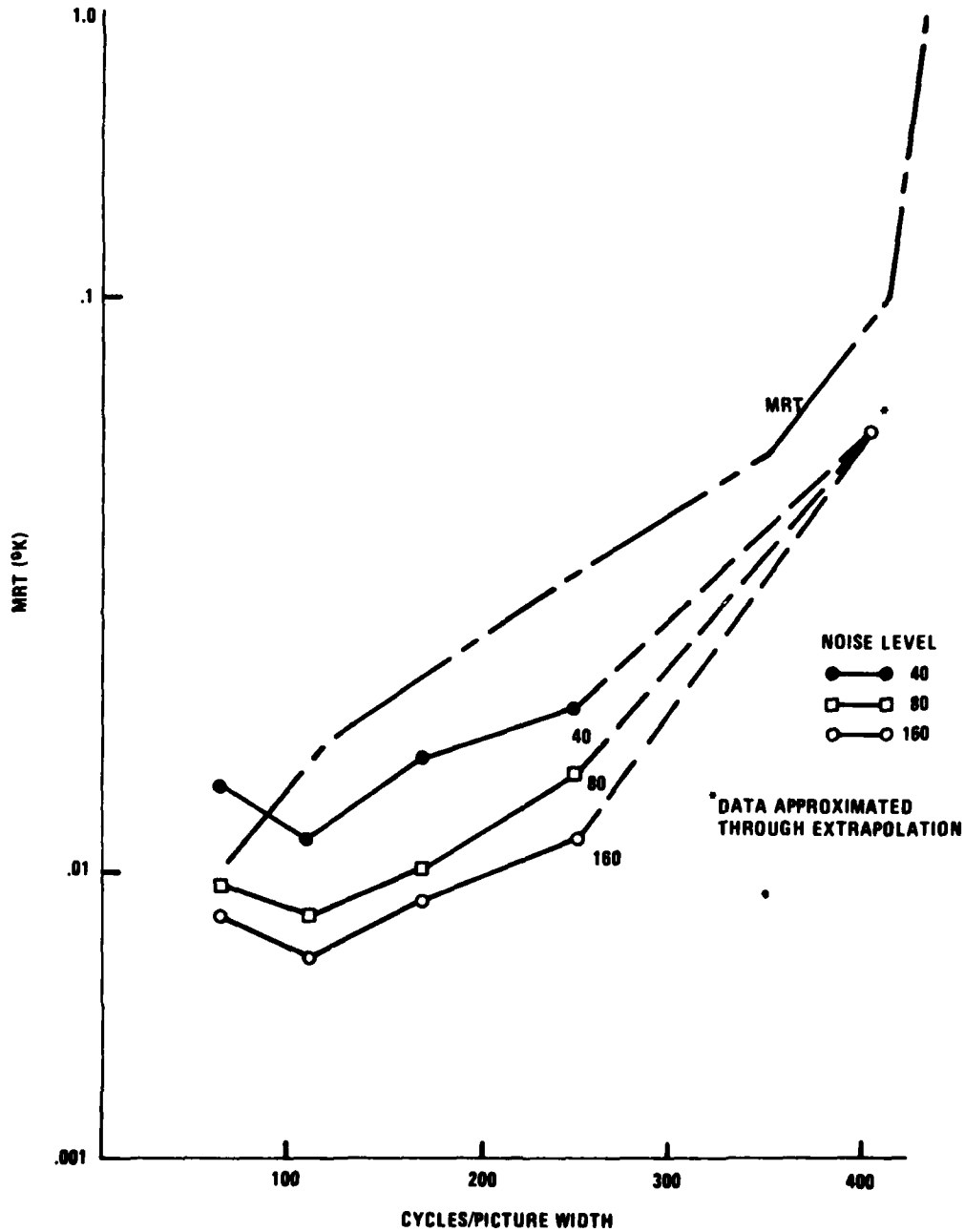

Figure 60. Analysis: Comparison of NVL MRT Prediction to Subject Data, FLIR 2

Figure 61 compares the four-bar recognition results (averaged across noise levels) with a contrast sensitivity function reported for similar viewing conditions by Schober and Hilz.* The recognition curves for FLIR 2 are similar in shape to the CSF. The upward translation of the FLIR 2 curve may be due to higher luminance level (10 vs 2.7 ft-L) or to differences in threshold criterion (75% correct in the present experiment). The similarity in shape was not wholly expected since the CSF measures detection threshold while the FLIR data represents recognition data. This may be due to the fact that mean luminance is kept constant in CSF experiments but was not in the present case. Instead, the target consisted of a luminance added to a constant background. Detection of the target becomes a luminance increment judgment which has different characteristics from pattern resolution as measured by the CSF. However, recognition in the present experiment requires resolution of the four-bar target as distinct from the solid square. Such a judgment may be quite similar to that demanded in standard CSF measures, which require discrimination of a bar target from a homogeneous field of the same average luminance.

The difference between the shapes of the FLIR 1 and FLIR 2 recognition curves may reflect many factors. Among them would be the possibility that the MTF of the visual system is superior to that of FLIR 1, so that the recognition performance becomes limited by the display rather than by the eye. This limitation would be less significant in the case of FLIR 2. Another way of putting the problem is to say that FLIR 1 is aperture-limited whereas FLIR 2 is noise-limited.

---

*Schober and Hilz, 1965.

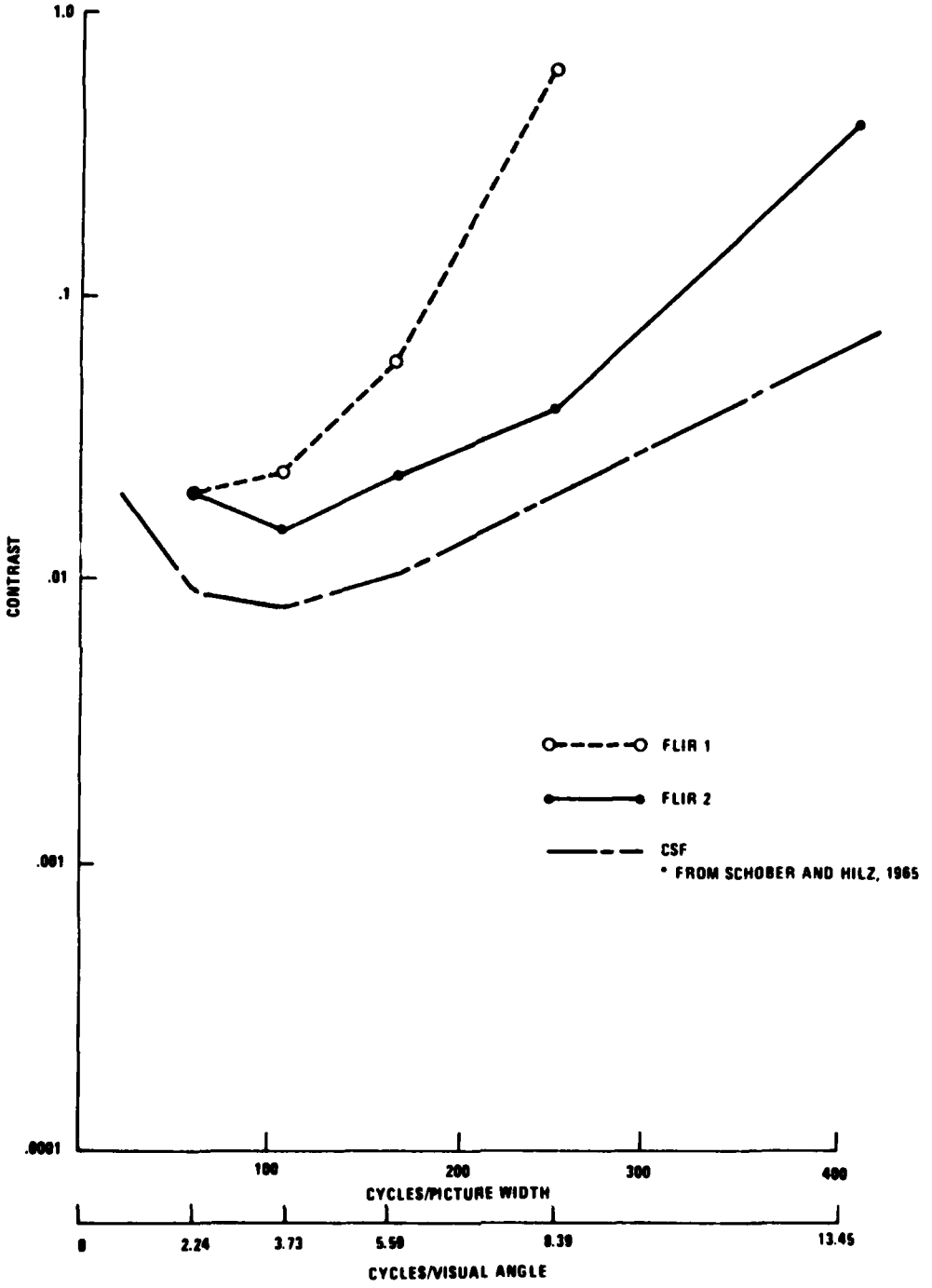

Figure 61. Analysis: Comparison of Contrast Sensitivity Function with Subject Data

MRTs were derived from the recognition data, and a comparison of Figures 59 and 60 indicates that MRTs were substantially lower for FLIR 2 than for FLIR 1.

As expected, both MRTs tended to decrease with increasing target size (decreasing spatial frequency). This trend was not maintained for the largest target sizes, especially in the case of FLIR 2.

The effect of different noise levels was again somewhat different for the two FLIRs. MRTs decreased with increasing RMS noise for FLIR 2. This tendency was also observed for larger target sizes with FLIR 1, but not for smaller targets.

The MRTs derived from recognition performance were compared with MRTs based on the NVL model.* The NVL prediction incorporates a variety of hardware parameters such as detector sensitivity, field of view, and scan velocity, as well as observer variables such as the signal-to-noise ratio required for target resolution, visual system MTF, and temporal integration time of the eye. The present experiment simulates the hardware parameters and measures the observer's performance directly.

The experimental results for FLIR 1 differ from the NVL prediction, particularly in the middle range of spatial frequencies (100 to 200 cycles/PW). The sensitivity in this range reflects the size of the detector IFOV.

---

*Ratches, et al., 1975.

The results for FLIR 2 differ from the NVL prediction at all spatial frequencies. For spatial frequencies greater than 100 cycles/PW, the shape of the curve is similar to that predicted. Over this range, the experimental data and model may be described as differing by some frequency independent factor. One such factor could result from the use of forced-choice procedures which sometimes yield lower thresholds than the method-of-limits.*

More important, however, is the frequency-dependent difference that is particularly apparent in the FLIR 2 data (see Figure 60). Experimental MRTs show an upturn at lower spatial frequencies while the predicted MRT continues to decrease.

A likely explanation for this discrepancy is that the normal contrast sensitivity function on which the visual system MTF is based is characterized by maximum sensitivity (minimum threshold) at intermediate target spatial frequencies. However, the NVL prediction models this MTF with a negative exponential function, which is adequate at higher spatial frequencies but does not exhibit the required non-monotonicity.

Such a discrepancy is usually dismissed as insignificant since the higher spatial frequencies are presumed to be of greater significance for most visual tasks. Recent evidence† suggests that a two-octave band of frequencies centered at approximately twice the fundamental frequency of an object may be the most important for recognition. The importance of this observation for modeling thermal viewing systems awaits further investigation.

---

*Swets, 1964.

†Ginsburg, 19.

The effect of different noise levels differed from NVL predictions. Noise in the present experiement was added to both target and background so as to maintain a constant signal-to-noise ratio and NEΔT. The three different rms noise levels simulate a FLIR operating with different amounts of gain. Since signal-to-noise and NEΔT are the only noise parameters in the model, it was predicted that the changes in noise level would not change MRT. It was expected that the three noise levels representing a constant NEΔT differing only in gain should serve as replications with $\Delta T/rms = K$.

Several explanations of this discrepancy are possible. The first is that the noise effect is not significant but merely results from experimental variability. However, the differences between the lowest and highest rms noise results exceeded two standard errors of the estimated $\dot{T}$. In addition, the ordering of T's for different noise levels was consistent throughout the entire range of spatial frequencies for FLIR 2 and much of FLIR 1.

Another possibility is that the higher noise levels took the simulation out of the range of linear operation. However, the documentation that preceded the experiment verified that the system operated linearly over the entire range of luminances used in the experiment.

A more likely explanation is that the differences reflect the non-linear operation of the visual system. In particular, the addition of noise to both target and background increased the mean luminance of the display field, and visual sensitivity generally improves with higher luminance.* However, the effect is generally smaller than that observed here.

*Patel, 1966.

The present results can be compared with a previous study by Decker* which had similar goals. Decker simulated a FLIR display with videotaped, closed-circuit television imagery. He derived MRTs from both forced-choice and method-of-limits bar recognition thresholds for a variety of FLIR/noise viewing conditions. The experimental MRTs were compared with several models including that of the NVL. Decker found that his data fit the NVL prediction in terms of shape (frequency independent) but also required the inclusion of a multiplicative constant to improve the fit. Some of Decker's data indicates the low spatial frequency non-monotoncity, particularly at low noise levels. This agrees well with the results reported here. However, Decker reported consistently higher MRTs than the NVL prediction, whereas the MRTs reported here are lower.

The results of this experiment indicate that FLIR imagery and the MRT measurement paradigm can be successfully simulated using digital image processing and standard psychophysical techniques. This approach to FLIR display assessment has several advantages over traditional methods using target slides, TV camera, and CRT monitor. It allows greater flexibility in the type of target, FLIR sensor, and viewing conditions being simulated while assuring precise control of the important parameters. These include simulation of the MTF, the noise of the FLIR, and the raster effects, as well as the linearity of the entire system. Furthermore, the extensive calibration and documentation discussed in Appendix B attest to the reliability and stability of the simulation.

---

*Decker, 1976.

Several additional advantages are realized by using relatively naive observers in a standard psychophysical experiment. Criterion problems associated with the traditional method of limits are reduced using the forced-choice procedure.*

Few special qualifications other than good eyesight are required of the observer, and little prior training is needed for stable results.

We conclude that the advantages of these techniques are such that they may be profitably extended to other types of FLIR targets and, perhaps, other subject populations.

*Swets, 1964.

APPENDIX A

INSTRUCTIONS TO SUBJECTS

During the experiment you will be asked to view a series of patterns on the TV screen in front of you. The patterns will consist of either a solid square or four vertical bars, displayed against a background of visual noise similar to the "snow" sometimes seen on a TV. You may also notice horizontal lines, but these are irrelevant.

The contrast (or visibility) of the patterns will vary from trial to trial. The noisiness of the background and size of the pattern will remain constant for a block of 50 trials, then change.

On each trial the pattern, either bars or square, will appear in one of two positions on the screen: right or left of center. The distance from the center of the pattern to the center of the screen will remain constant throughout the experiment. The pattern will be presented for about five seconds followed by a one second interval during which you are to respond.

Your task will be to determine where on the screen the pattern appears and to judge which shape, bars or square, is presented. The appropriate responses should be marked on the answer sheets. If you are unsure about either position or shape, please indicate your best guess. Remember, you must mark an answer, even if you do not think you saw the pattern.

Prior to each block of 50 trials you will see clearly visible examples of the bars and square "displayed" on the screen. Pay close attention to these patterns since they will be identical in size and shape to the subsequent patterns.

There will be a total of 34 blocks with rest periods after every few blocks. The first four blocks will be for practice only.

Since many of the patterns will be very faint, you will have to attend carefully to the TV screen.

In addition to the $25 payed for your participation, there will be a $10 bonus for the one who performs best.

Do you have any questions?

APPENDIX B

CALIBRATION AND DOCUMENTATION

Prior to the experiment, the performance of the Model 70 imaging system was carefully examined. Four levels of information were available (see Figure B-1):

1) Computer Memory--The image is represented in computer memory by a 512 x 512 array of digital pixel values. A listing of these values, ranging from 0 to 511, documents the input to the digital-to-analog converter.

2) Video Signal--The D/A converts values to analog video signals, ranging from 0.0 to 0.7 V. Selected horizontal video lines, corresponding to rows of the digital array, can be displayed on an oscilloscope. A photograph of the video signal being applied to the TV display.

3) TV Display--The resulting luminance pattern ranges from 0.2 to 25.0 ft-L. A photometric scan across the face of the TV monitor documents the luminance profile of the display.

4) Finally, a photograph of the TV display indicates the appearance of the generated image.

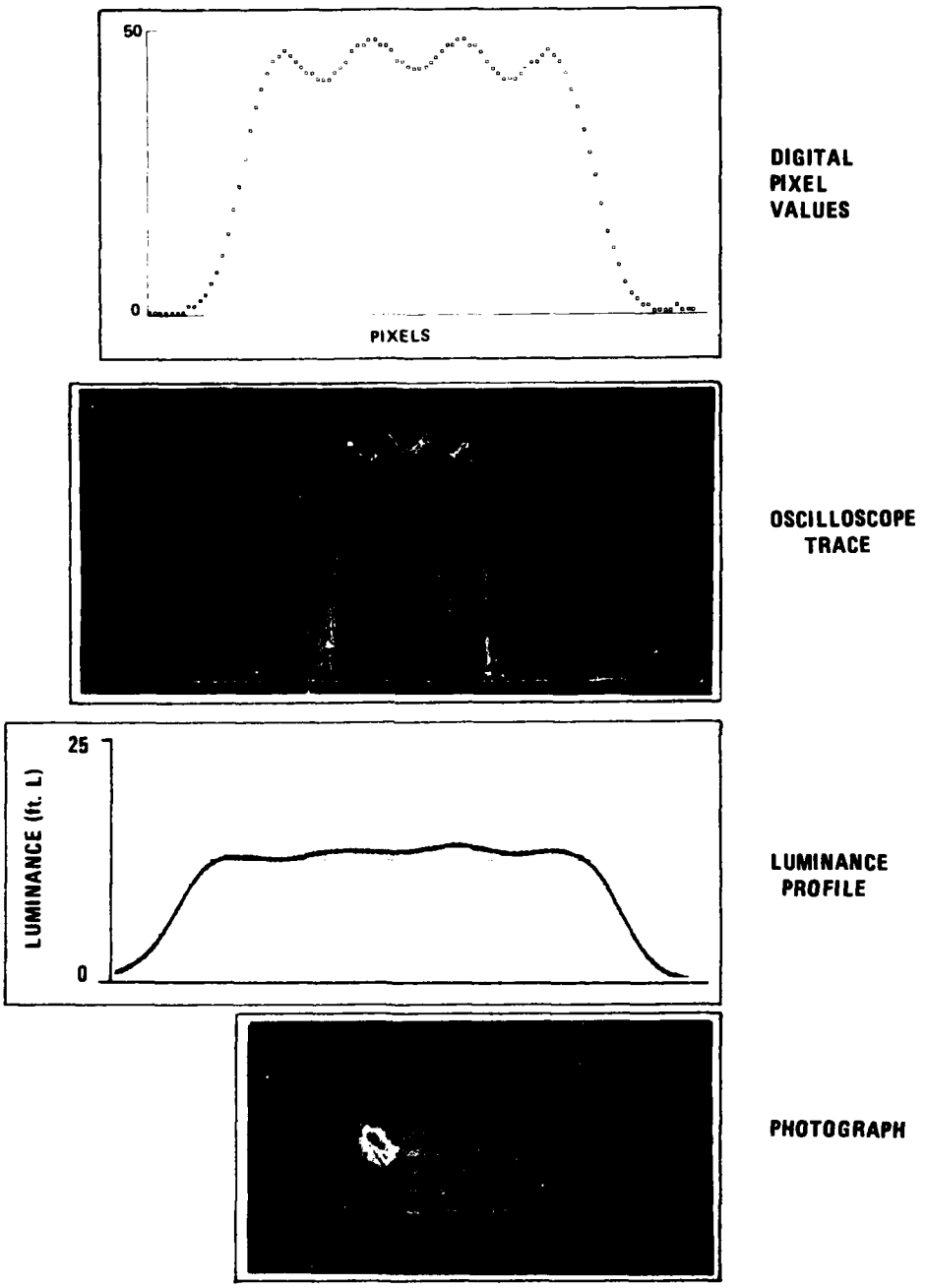

Figure B-1. Information Flow Through FLIR Simulation: FLIR 1 Four-Bar Target

DISPLAY CHARACTERISTICS

The uniformity of the TV display was assessed by setting all of the pixel values to the same level. Photometric measurements were made with a Gamma Scientific photometer calibrated against a Gamma Scientific standard 100 ft-L source. The measurements indicated that screen luminance varied less than ± 6%. Within the area used during the experiment, variability was reduced to less than ± 3%. Periodic checks over a four-hour interval revealed less than ± 3% drift in the display luminance.

Linearity of the display response was determined by measuring the video transfer function (VTF). This function relates output luminance to input voltage. The contrast and gain settings on the display were adjusted to produce the desired range of luminance (0.2 ft-L to 25 ft-L) for the given range of video signal voltages (0.0 to 0.7 V). Luminances were measured with the photometer for 32 equally spaced voltage steps. It is apparent from Figure B-2 that the VTF of the display is nonlinear.

One advantage of digital image generation is that undesirable characteristics of the system can be modified by appropriate program changes. In the present case, we were able to compensate for the nonlinearity of the VTF by supplying a set of conversion values in the program that produced a linear relation between digital pixel value and output luminance. This was accomplished by empirically mapping the 512 pixel values into unequal voltage steps that yielded equally spaced luminance levels. This produced a nonlinear relation between pixel values and voltages, but a linear relation between pixel values and luminance. The relationships after compensation are illustrated in Figure B-3.

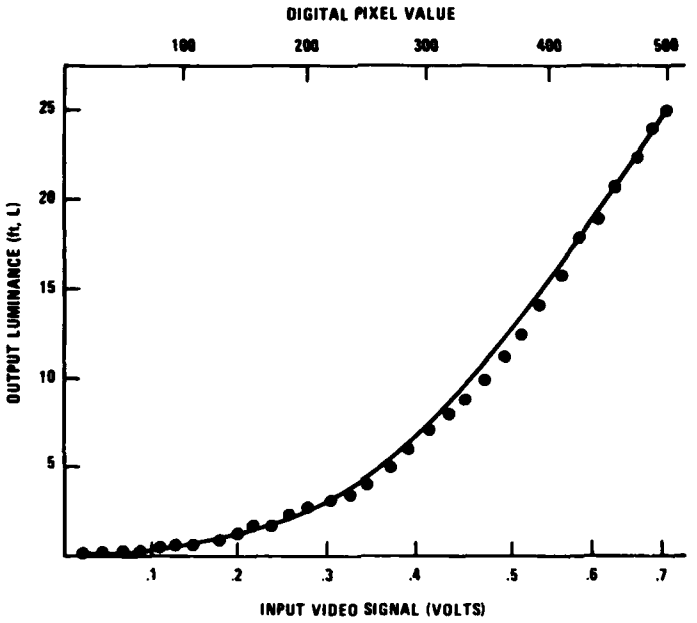

Figure B-2. Video Transfer Function of the Display System

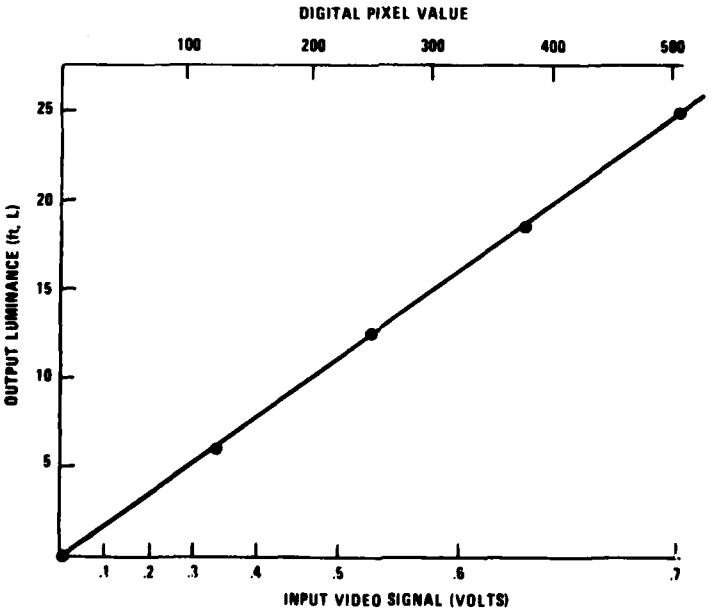

Figure B-3. Linearized Video Transfer Function

It is apparent from the above discussion that the intermediate stage of digital-to-analog conversion is essentially transparent to the Model 70 user; that is, once the digital values are calibrated to luminance levels, one can largely ignore the transformations that intervene. Nevertheless, they are included here for the sake of completeness.

With the display operating in a linear relation to pixel value, the system modulation transfer function (MTF) can be used as an indicator of image quality.* The MTF in the horizontal direction was derived from the square wave response (SqWR) measured at the display. Grid patterns were generated by the computer (pixel values of 0 and 511 for bright and dark bars, respectively) over a range of bar widths from 1 to 10 pixels. A luminance profile was obtained by scanning the display horizontally with a masked slit microphotometer. The slit was vertically oriented. Its width was less than one half the dimension of the narrowest bar and its height exceeded four raster lines. A representative luminance profile and corresponding oscilloscope tracing showing D/A output are reproduced in Figure B-4. The MTF was derived from the SqWR by the standard series expansion† and is given in Figure B-5. There was no significant roll-off in the range of bar widths used in the experiment (3-30 pixels/bar width).

---

*Strictly speaking, MTF techniques assume linearity, shift invariance, and continuous response of the system. The slight nonuniformity of the display violates the first assumption, and digital pixel values violate the third.

†Coltman, 1954.

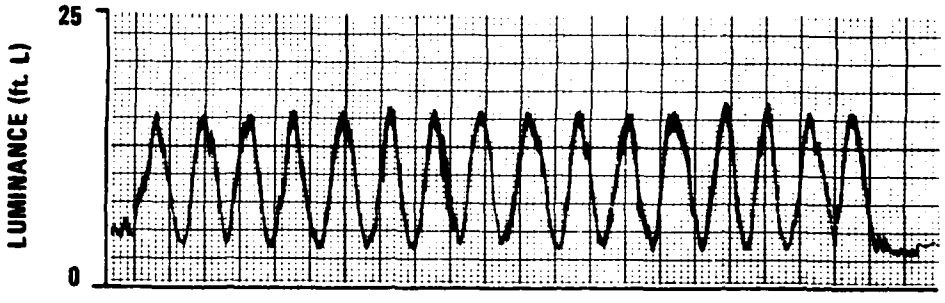

a. Luminance Profile

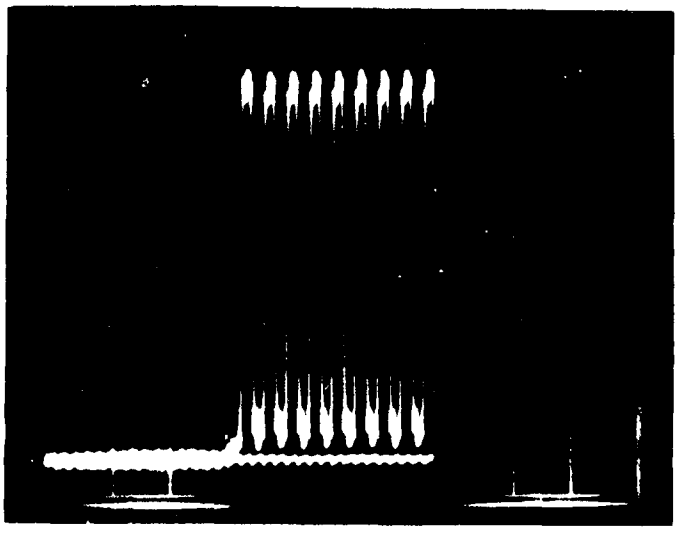

b. Oscilloscope Tracing

Figure B-4. Representative Luminance Profile and Oscilloscope Tracing of Grid Patterns to Measure the System's MTF

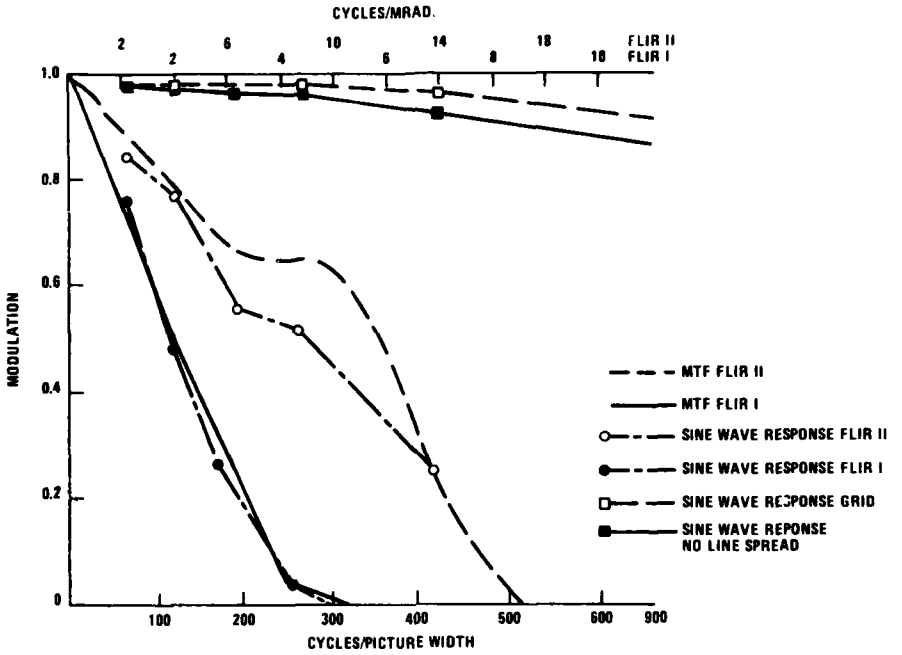

Figure B-5. MTF of FLIRs 1 and 2 Comparing Sine and Square Wave Response Measures

TARGET CHARACTERISTICS

Oscilloscope records, luminance profiles, and display photographs were also obtained for the four-bar target patterns. For the first set, no line spread function was applied to the target (see Figures B-6 to B-11. The MTF was obtained in the same fashion as above and is also shown in Figure B-5. As expected, the MTF derived from targets corresponds closely with that derived from the grid pattern. The slight discrepancy at higher spatial frequencies may reflect increased light scatter due to higher dark bar luminance (pixel values of 200 instead of 0) used during these measurements.

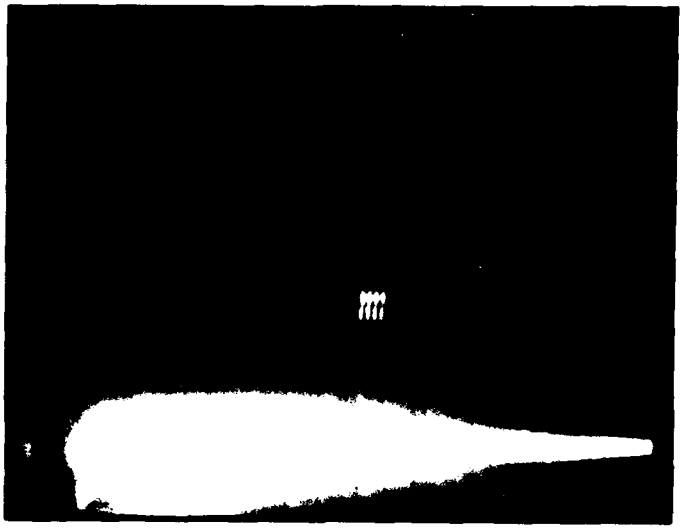

a. Oscilloscope Tracing

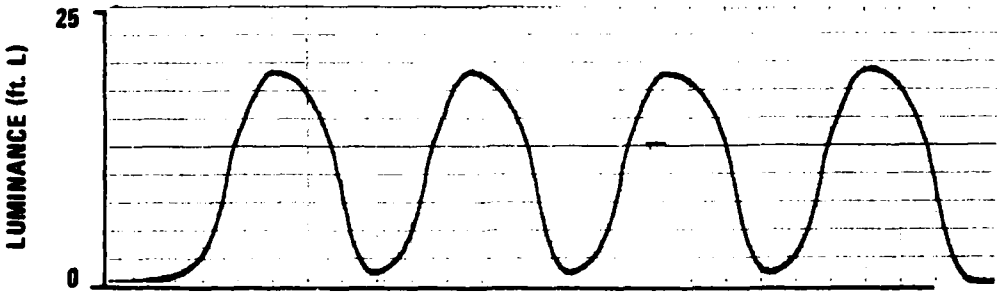

b. Luminance Profile

Figure B-6. No Point Spread Function Documentation for Target 1

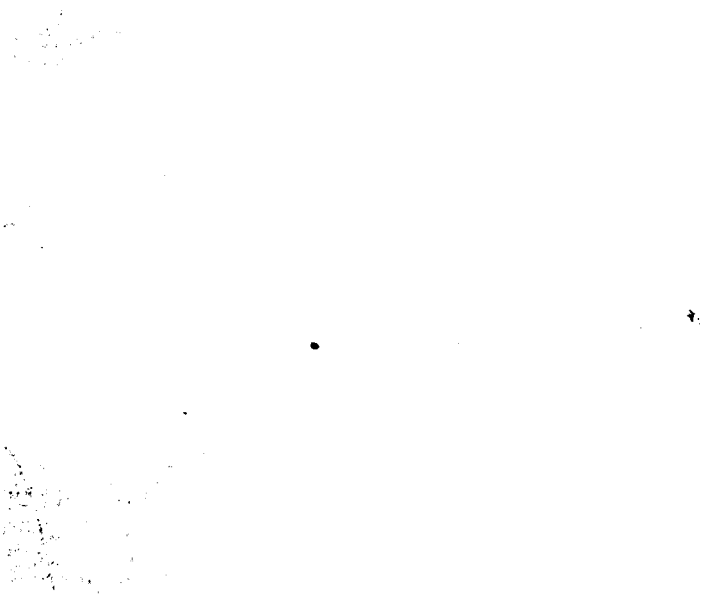

c. Photograph

Figure B-6. No Point Spread Function Documentation for Target 1 (concluded)

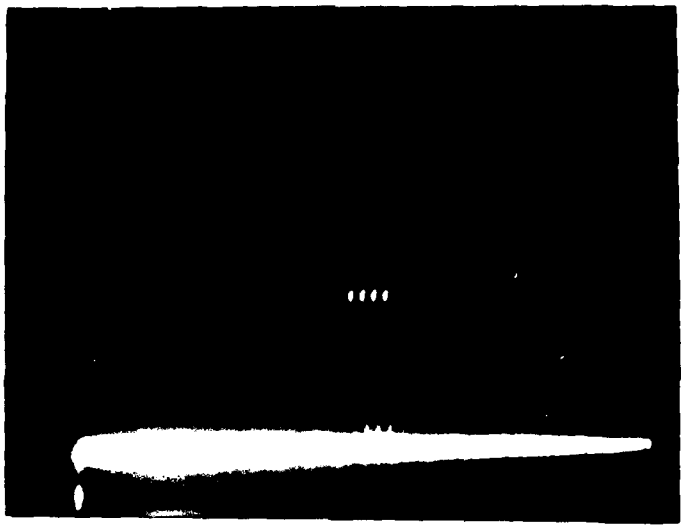

a. *Oscilloscope Tracing*

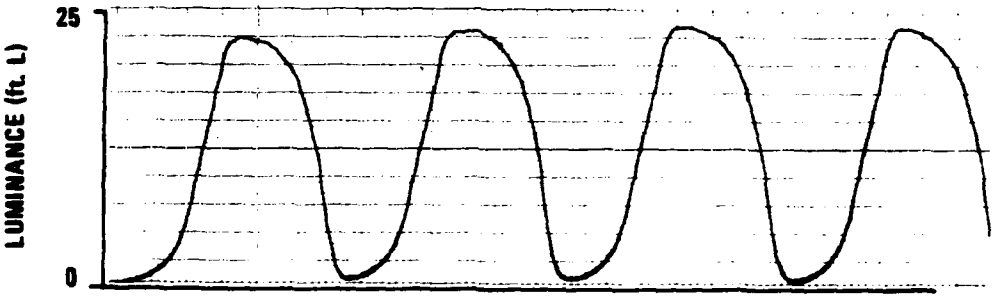

b. Luminance Profile

Figure B-7. No Point Spread Function Documentation for Target 2

c. Photograph

Figure B-7. No Point Spread Function Documentation for Target 2 (concluded)

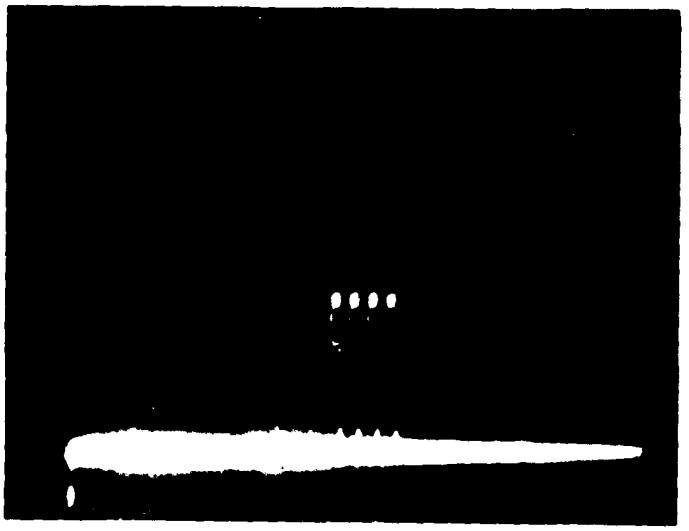

a. Oscilloscope Tracing

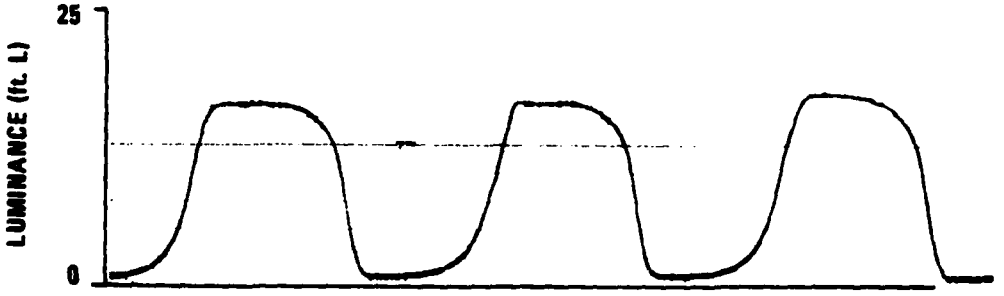

b. Luminance Profile

Figure B-8. No Point Spread Function Documentation for Target 3

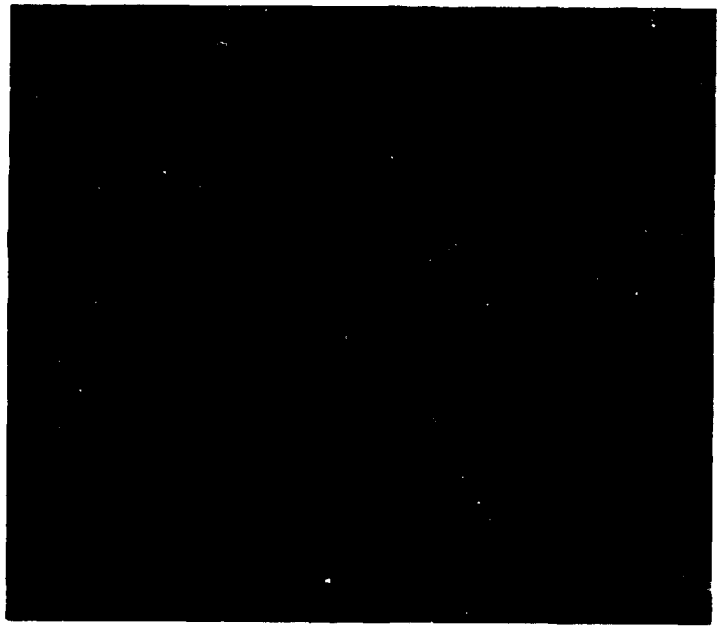

c. Photograph

Figure B-8. No Point Spread Function Documentation for Target 3 (concluded)

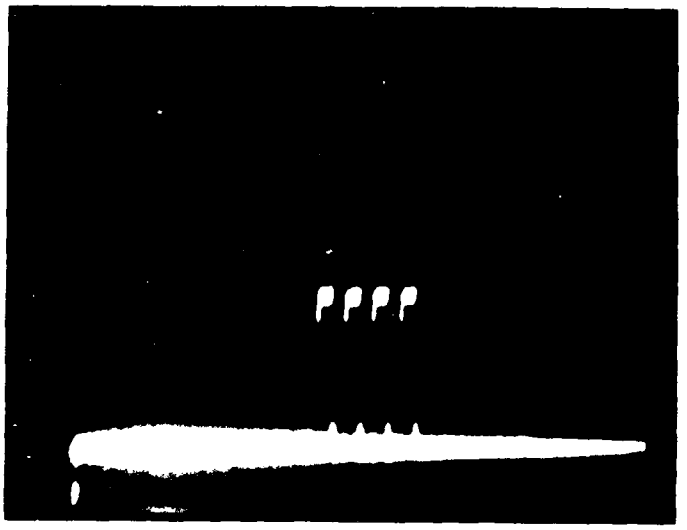

a. Oscilloscope Tracing

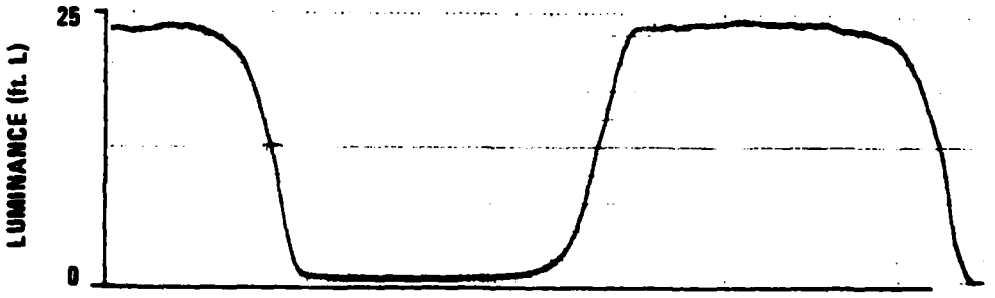

b. Luminance Profile

Figure B-9. No Point Spread Function Documentation for Target 4

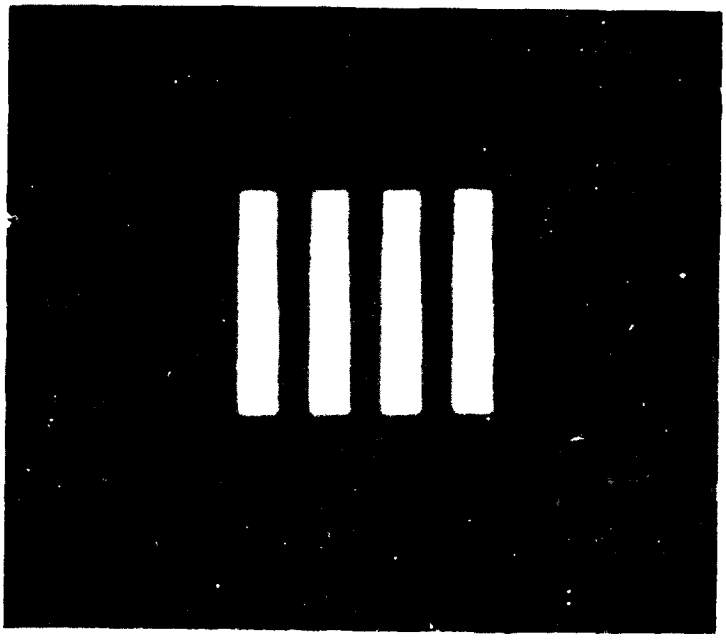

c. Photograph

Figure B-9. No Point Spread Function Documentation for Target 4 (concluded)

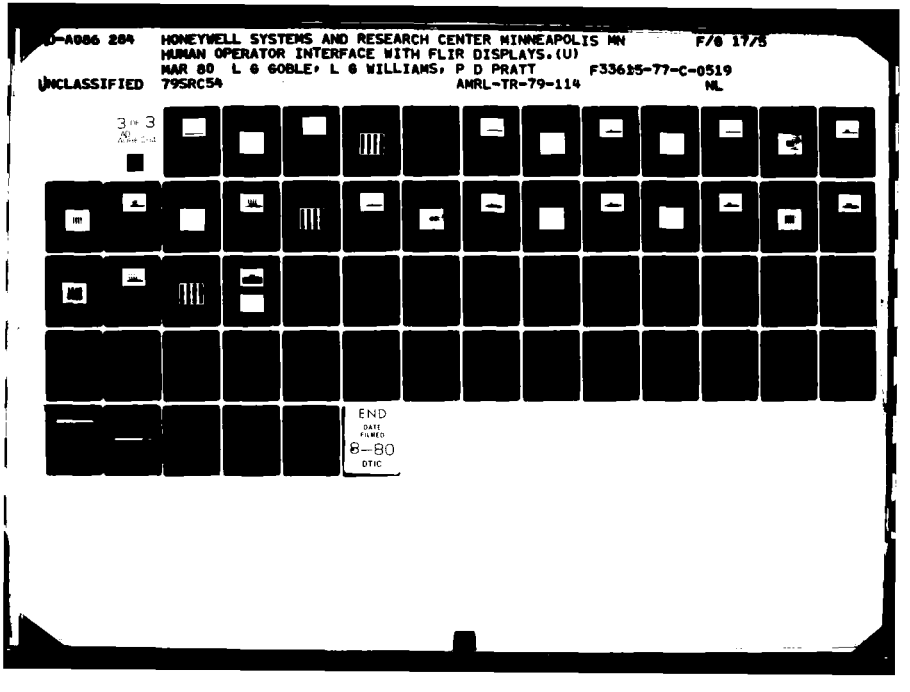
D-A086 284
HONEYWELL SYSTEMS AND RESEARCH CENTER MINNEAPOLIS MN
F/G 17/5
HUMAN OPERATOR INTERFACE WITH FLIR DISPLAYS.(U)
MAR 80 L G GOBLE, L G WILLIAMS, P D PRATT
F33615-77-C-0519
UNCLASSIFIED
79SRC54
AMRL-TR-79-114
NL
3 OF 3
END
DATE FILMED
8-80
DTIC

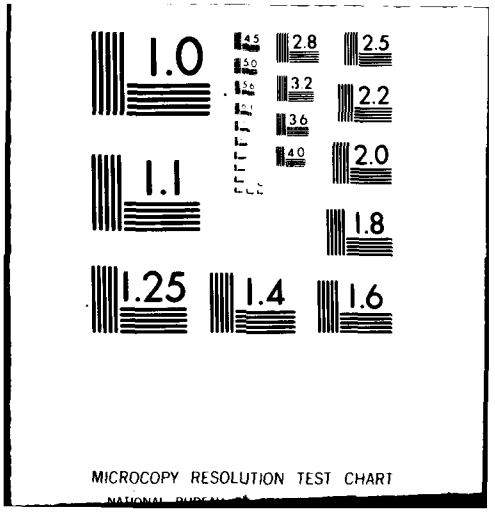
1.0
1.1
1.25
1.4
1.6
1.8
2.0
2.2
2.5
2.8
3.2
3.6
4.0
4.5
5.0
5.6
MICROCOPY RESOLUTION TEST CHART

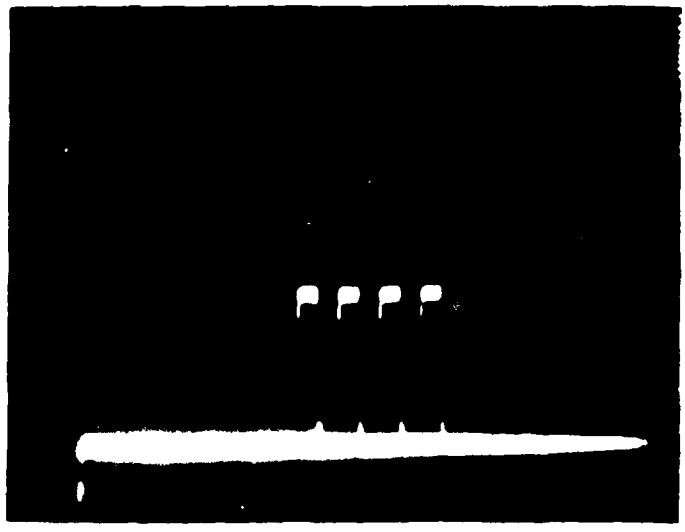

a. Oscilloscope Tracing

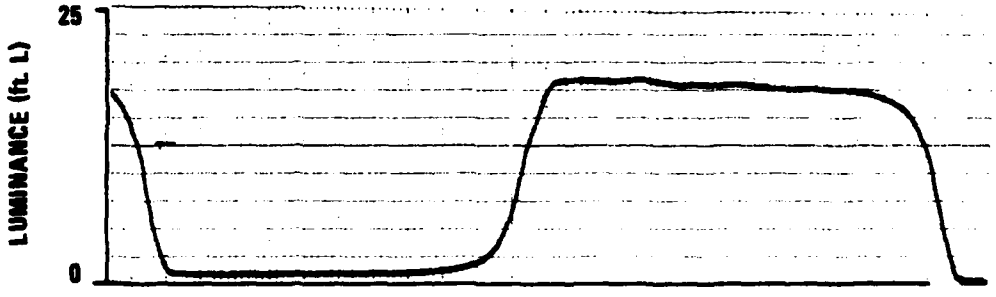

b. Luminance Profile

Figure B-10. No Point Spread Function Documentation for Target 5

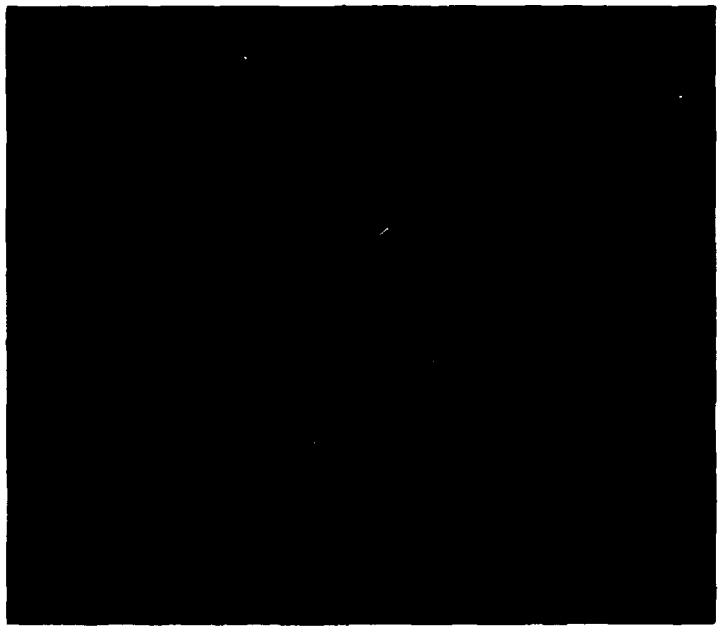

c. Photograph

Figure B-10. No point Spread Function Documentation for Target 5 (concluded)

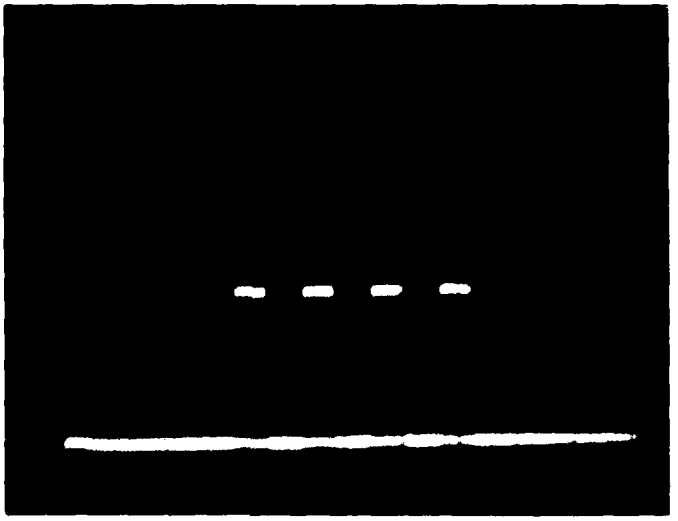

a. Oscilloscope Tracing

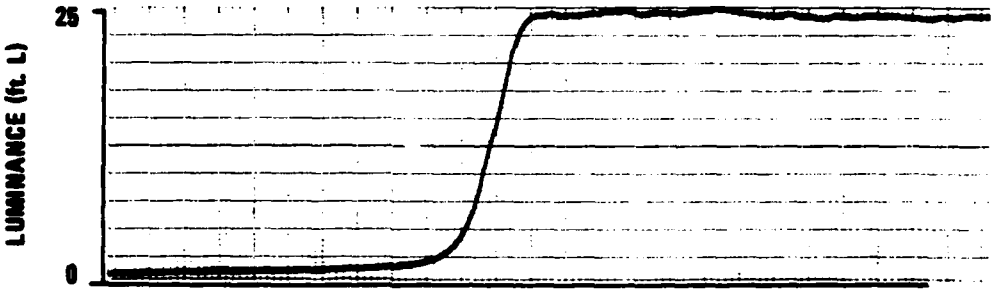

b. Luminance Profile

Figure B-11. No Point Spread Function Documentation for Target 6

c. Photograph

Figure B-11. No point Spread Function Documentation for Target 6 (concluded)

For the second set of records, the line spread function derived for FLIR 1 was applied to each target (see Figures B-12 to B-17). The MTF obtained from the SqWR is compared with the MTF of the FLIR being simulated (obtained from product specifications) in Figure B-5. The two MTFs agree quite closely, indicating that the simulation is valid.

The third set of records is for the FLIR 2 (see Figures B-18 to B-23), and the MTF derived from the SqWR is again compared with product specifications in Figure B-5. The MTF and sine wave response agree at higher and lower spatial frequencies. For intermediate frequencies, the sine wave response was somewhat less than expected.

NOISE CHARACTERISTICS

A representative oscilloscope recording of the four-bar target in noise is provided in Figure B-24. Figure B-25 shows the appearance of such a display. Since the noise was dynamic and the response of the photometer/strip chart recorder relatively slow, no luminance profile was obtained.

The three noise levels used in the experiment were verified using the tangential method.* The noise signal from the digital-to-analog converter was applied to both channels of a dual beam oscilloscope. The two noise traces were positioned adjacent to one another. When the noise signal was removed, the separation of the two traces indicated twice the RMS noise level. It was determined that the three noise levels: 40, 80, and 160 (digital pixel values) corresponded to 0.033V, 0.065V, and 0.130V RMS, as expected

---

*Franklin and Halley, 1973.

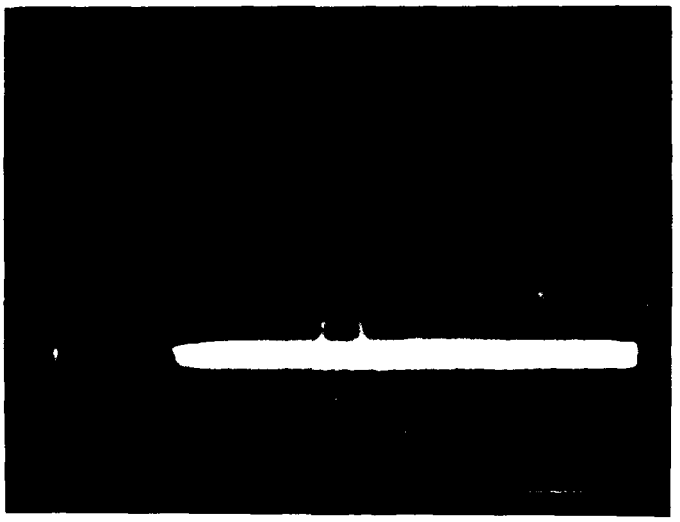

a. Oscilloscope Tracing

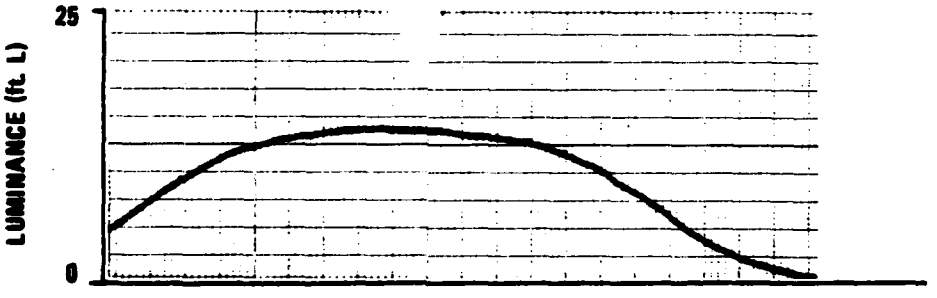

b. Luminance Profile

Figure B-12. FLIR 1 Documentation for Target 1

c. Photograph

Figure B-12. FLIR 1 Documentation for Target 1 (concluded)

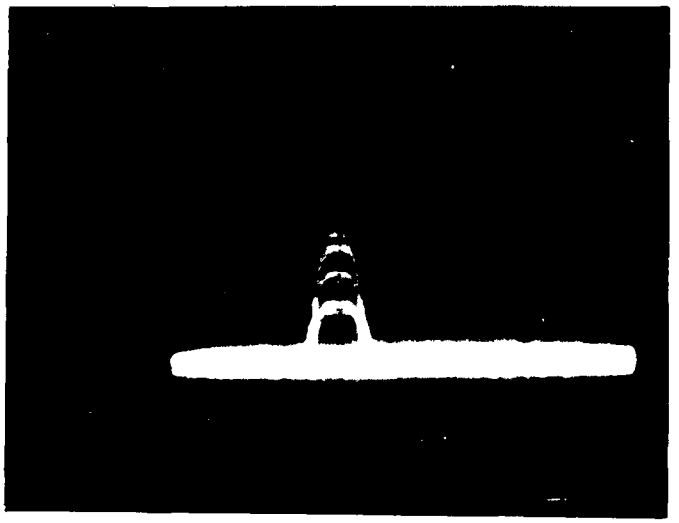

a. Oscilloscope Tracing

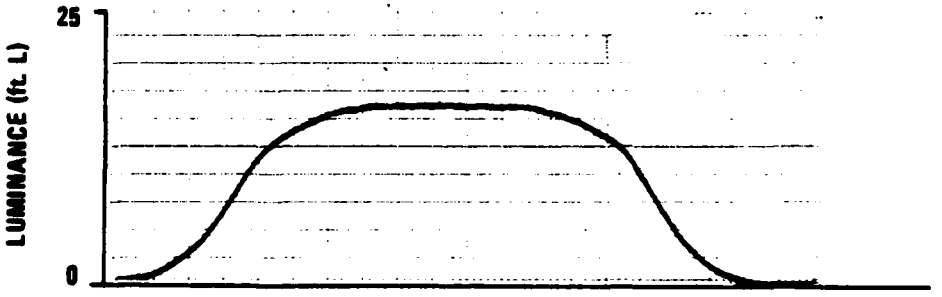

b. Luminance Profile

Figure B-13. FLIR 1 Documentation for Target 2

c. Photograph

Figure B-13. FLIR 1 Documentation for Target 2 (concluded)

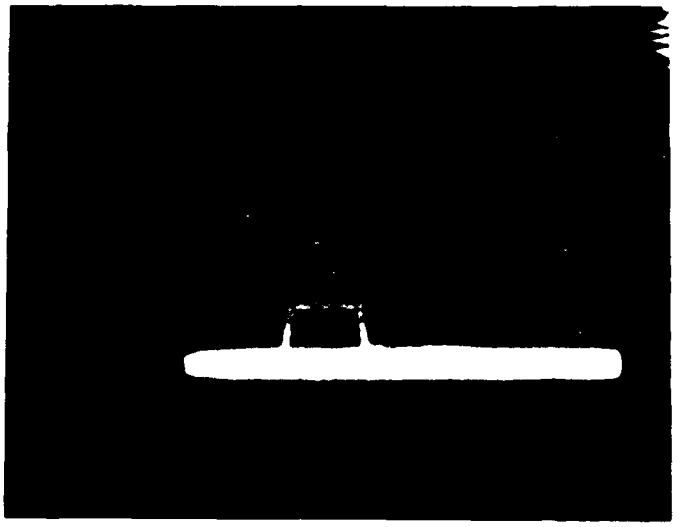

a. Oscilloscope Tracing

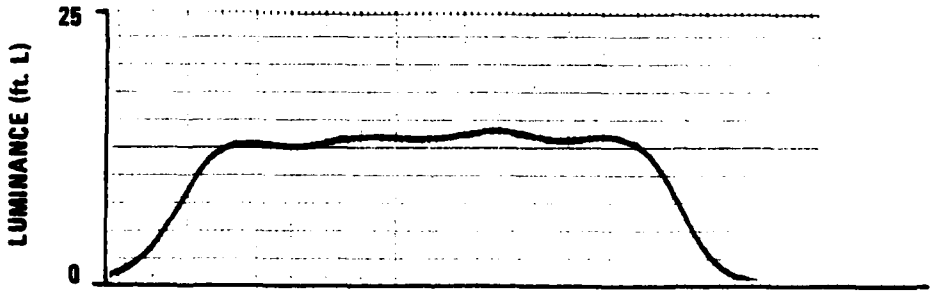

b. Luminance Profile

Figure B-14. FLIR 1 Documentation for Target 3

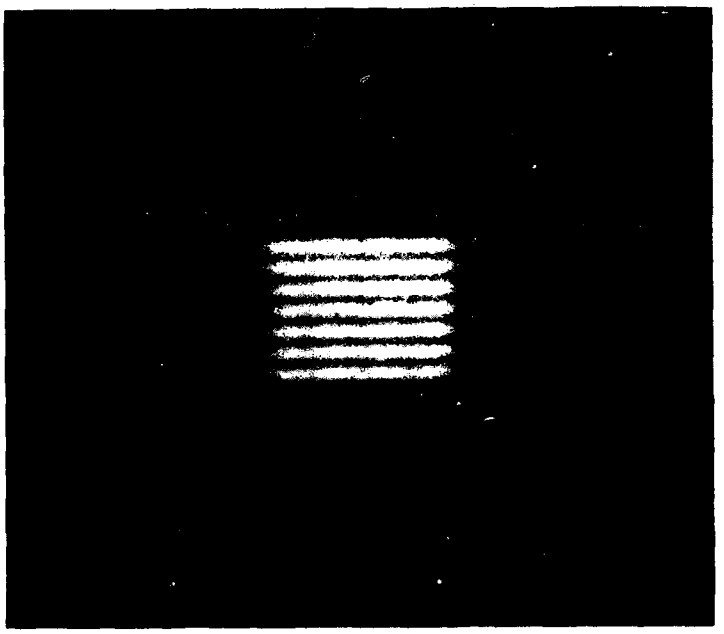

c. Photograph

Figure B-14. FLIR 1 Documentation for Target 3 (concluded)

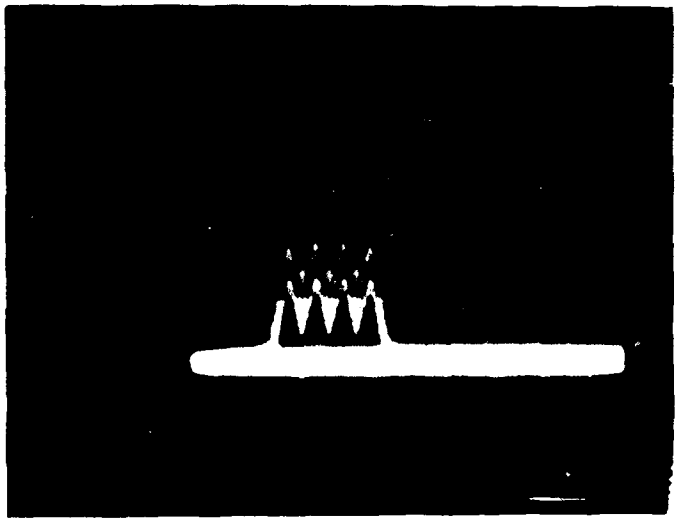

a. Oscilloscope Tracing

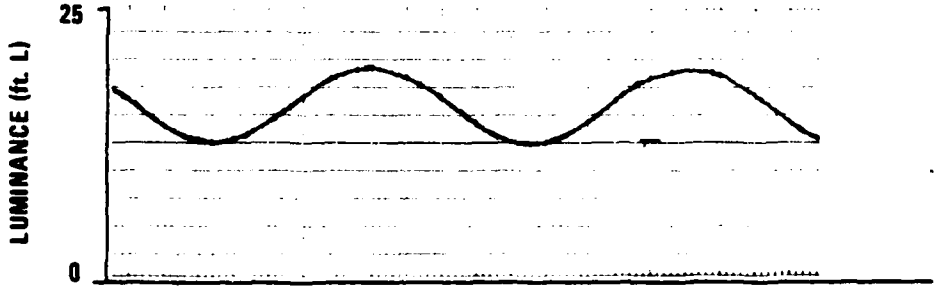

b. Luminance Profile

Figure B-15. FLIR 1 Documentation for Target 4

c. Photograph

Figure B-15. FLIR 1 Documentation for Target 4 (concluded)

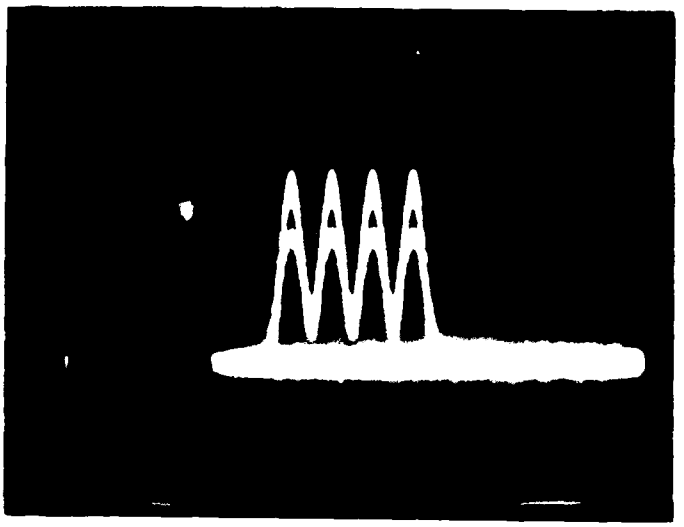

a. Oscilloscope Tracing

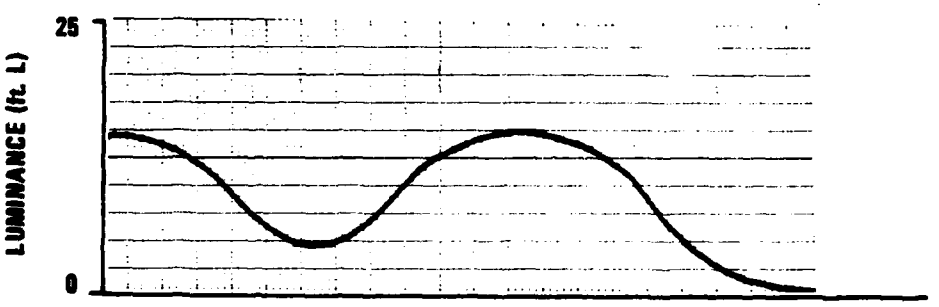

b. Luminance Profile

Figure B-16. FLIR 1 Documentation for Target 5

c. Photograph

Figure B-16. FLIR 1 Documentation for Target 5 (concluded)

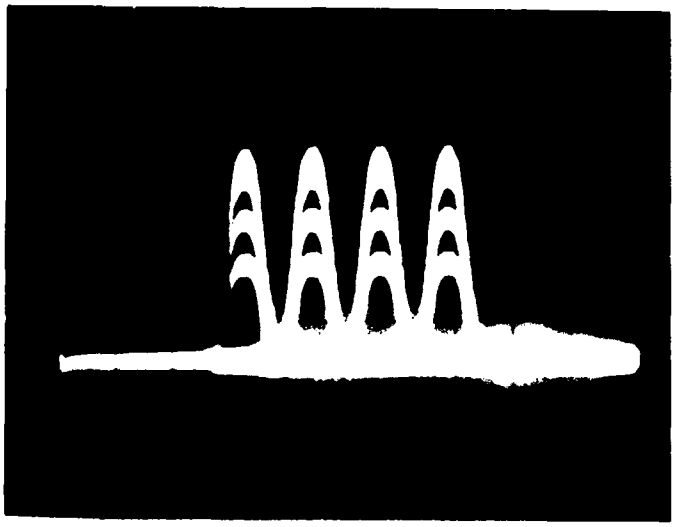

a. Oscilloscope Tracing

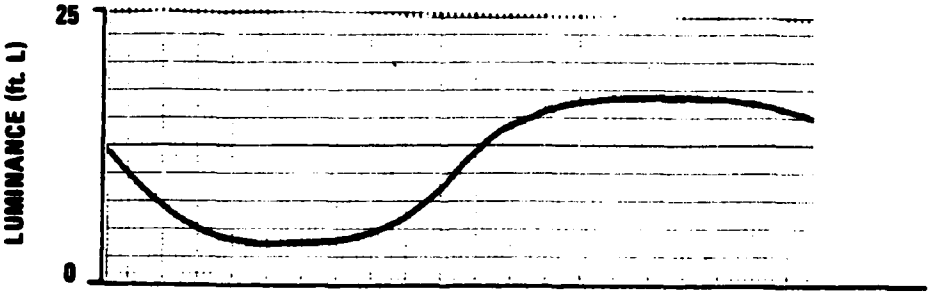

b. Luminance Profile

Figure B-17. FLIR 1 Documentation for Target 6

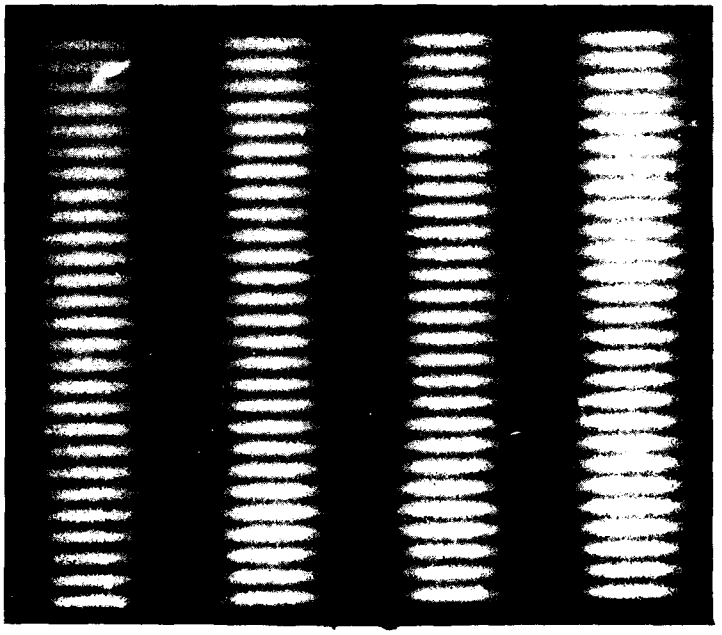

c. Photograph

Figure B-17. FLIR 1 Documentation for Target 6 (concluded)

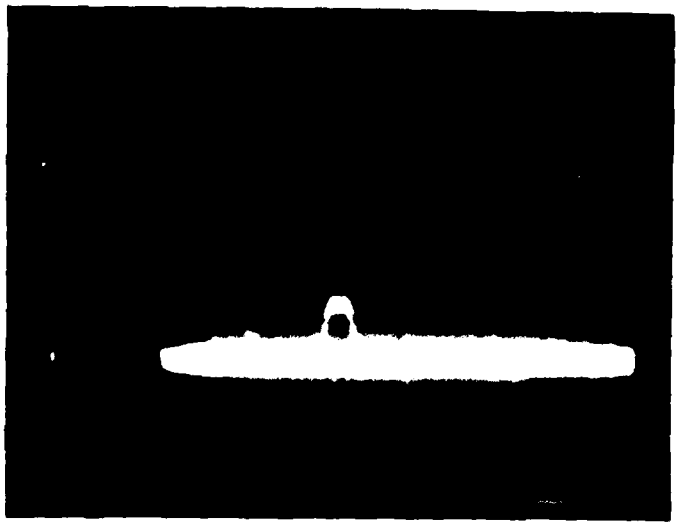

a. Oscilloscope Tracing

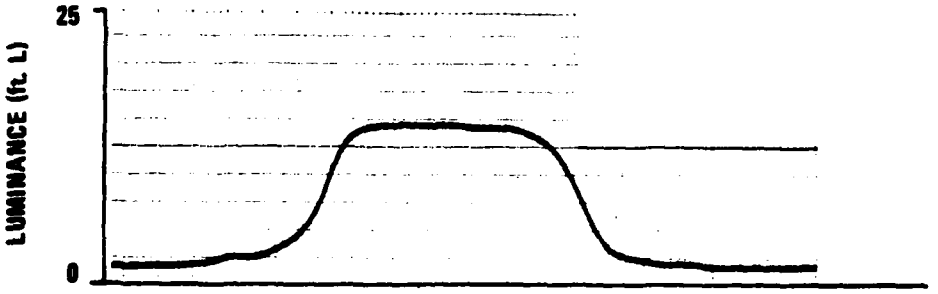

b. Luminance Profile

Figure B-18. FLIR 2 Documentation for Target 1

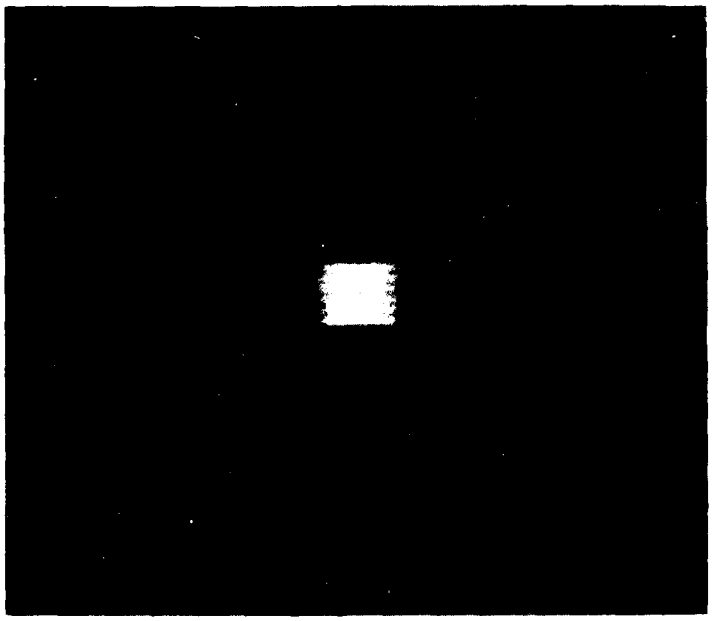

c. Photograph

Figure B-18. FLIR 2 Documentation for Target 1 (concluded)

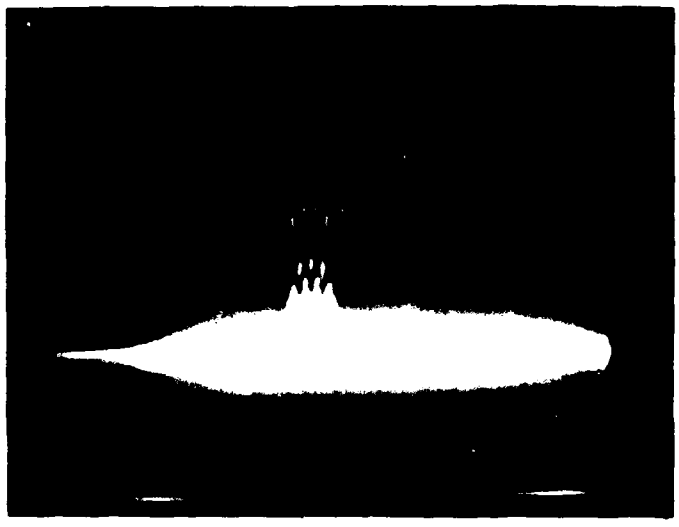

a. Oscilloscope Tracing

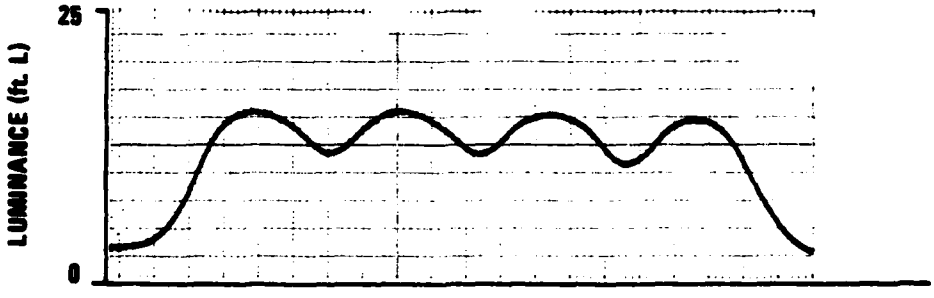

b. Luminance Profile

Figure B-19. FLIR 2 Documentation for Target 2

c. Photograph

Figure B-19. FLIR 2 Documentation for Target 2 **(concluded)**

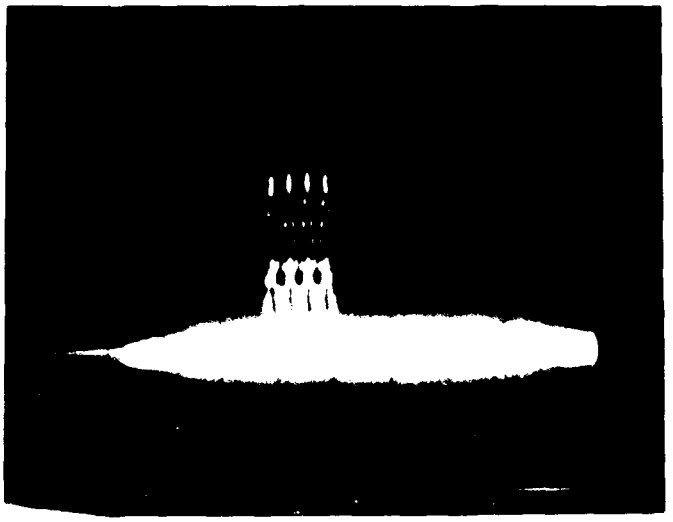

a. Oscilloscope Tracing

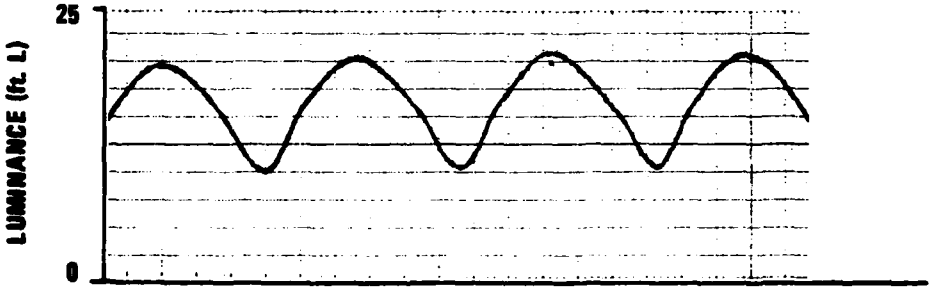

b. Luminance Profile

Figure B-20. FLIR 2 Documentation for Target 3

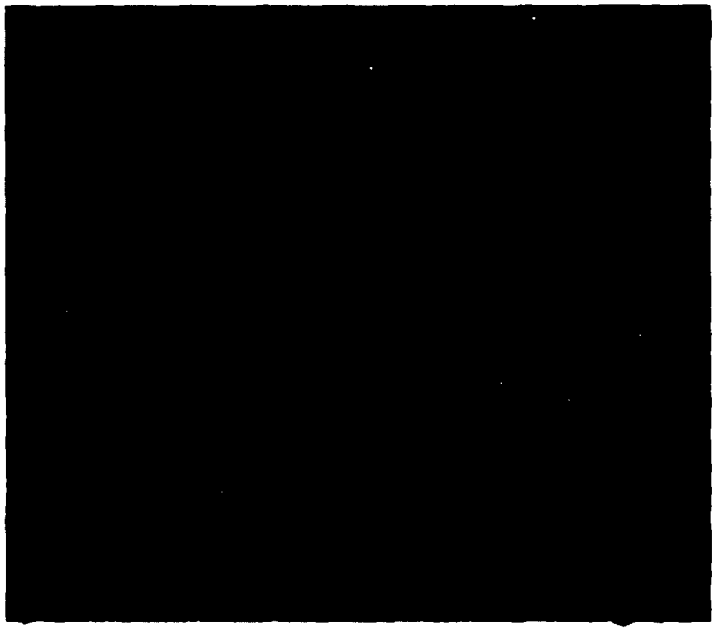

c. Photograph

Figure B-20. FLIR 2 Documentation for Target 3 **(concluded)**

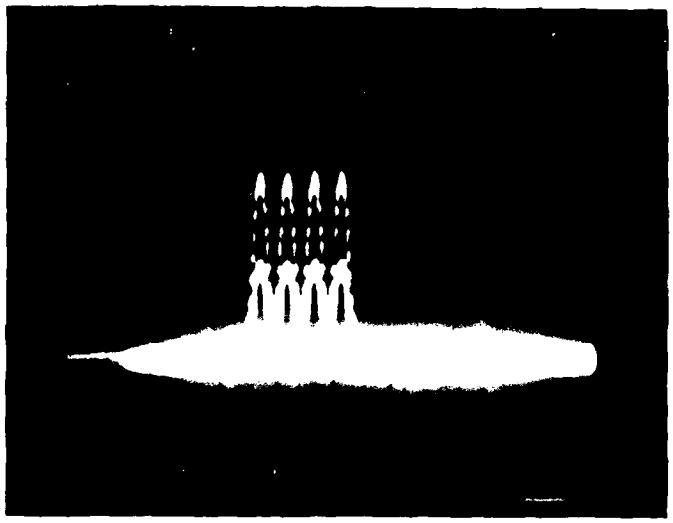

a. Oscilloscope Tracing

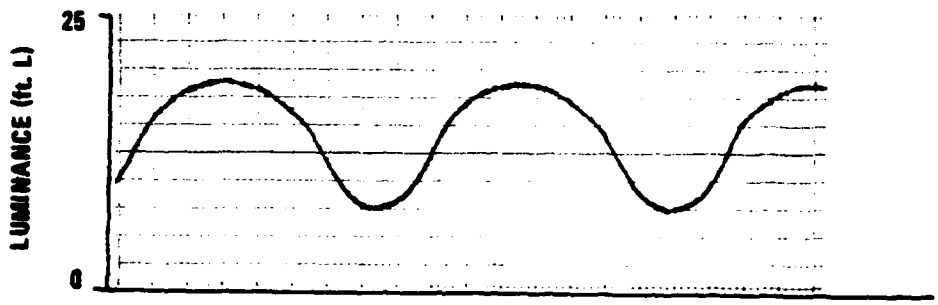

b. Luminance Profile

Figure B-21. FLIR 2 Documentation for Target 4

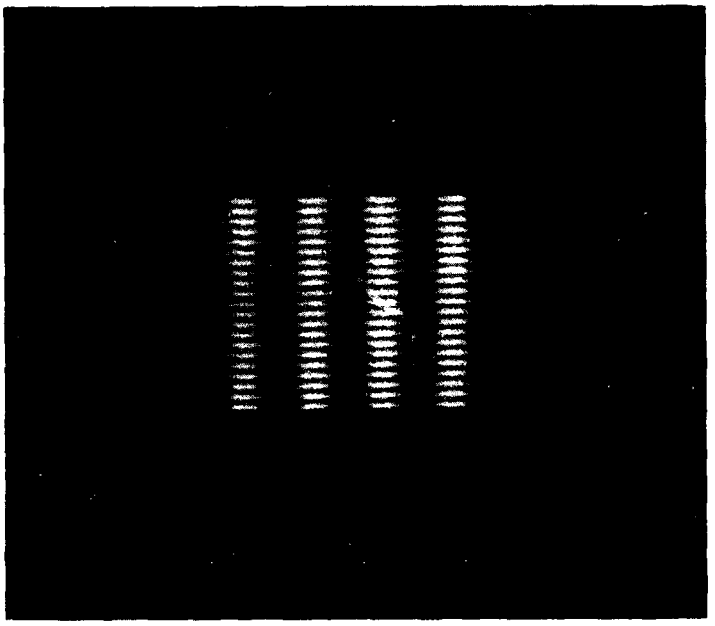

c. Photograph

Figure B-21. FLIR 2 Documentation for Target 4 (concluded)

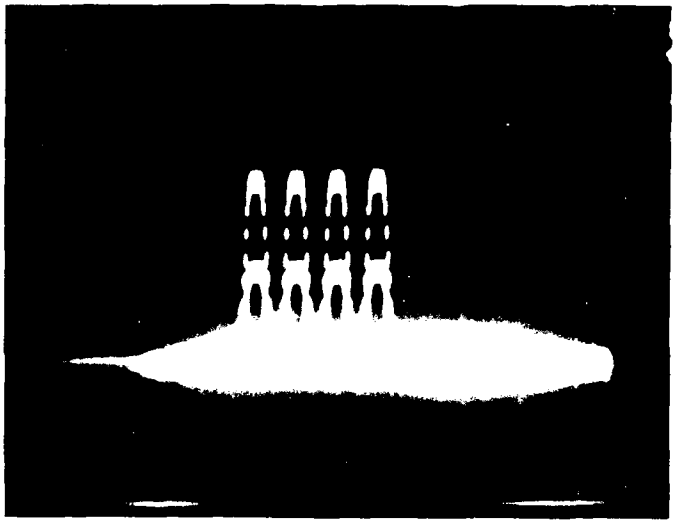

a. Oscilloscope Tracing

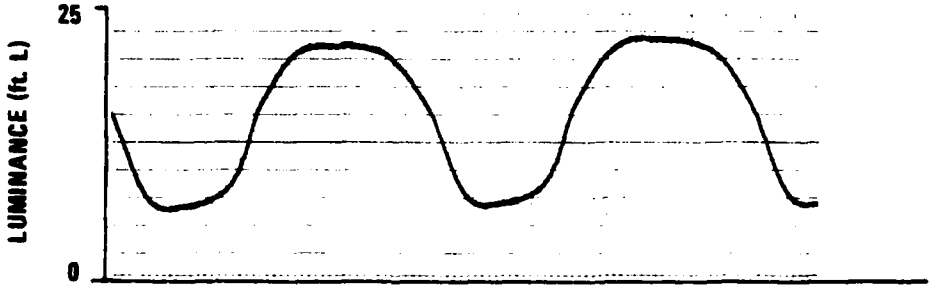

b. Luminance Profile

Figure B-22. FLIR 2 Documentation for Target 5

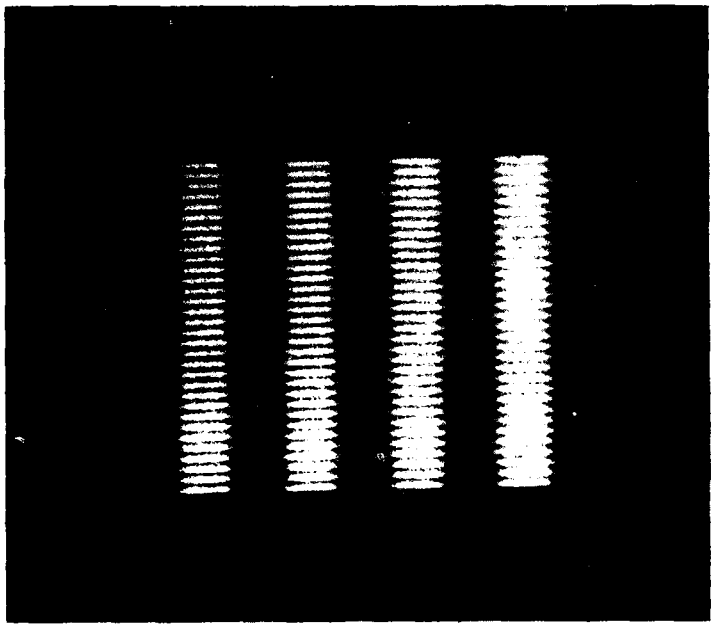

c. Photograph

Figure B-22. FLIR 2 Documentation for Target 5 (concluded)

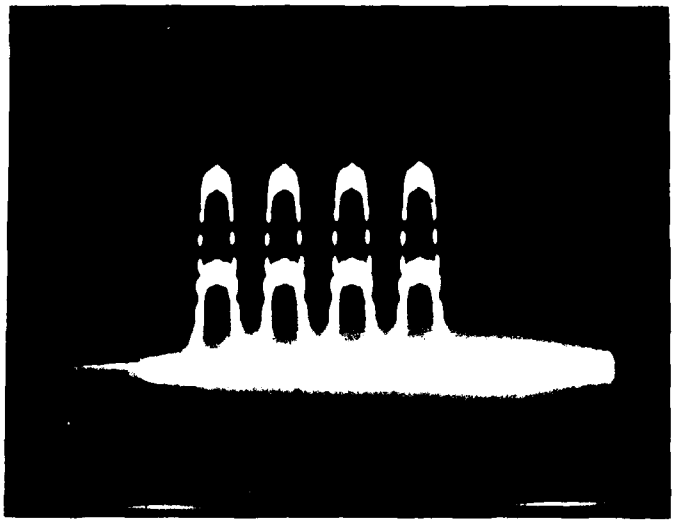

a. Oscilloscope Tracing

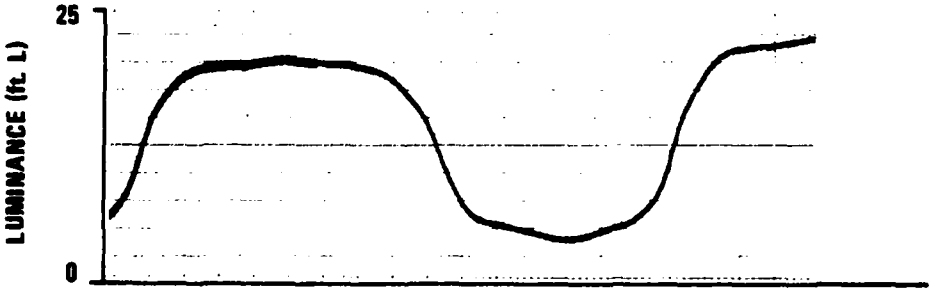

b. Luminance Profile

Figure B-23. FLIR 2 Documentation for Target 6

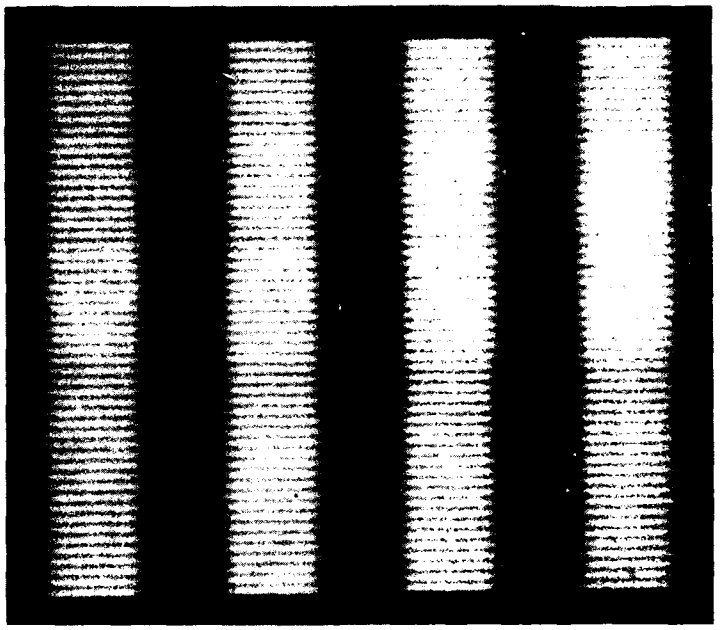

c. Photograph

Figure B-23. FLIR 2 Documentation for Target 6 (concluded)

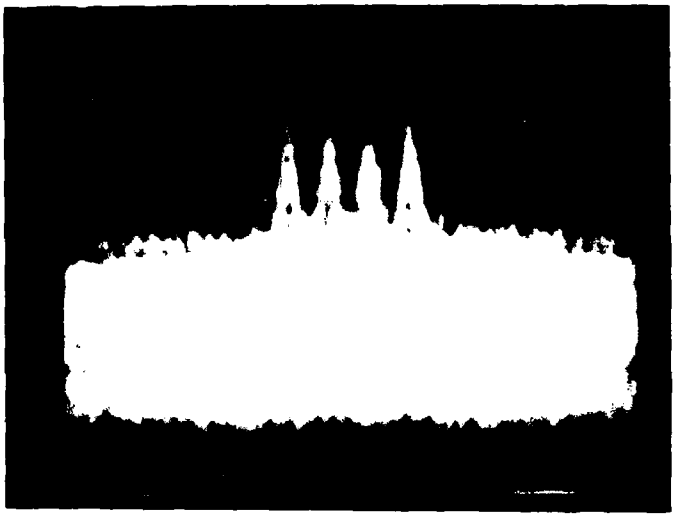

Figure B-24. Representative Oscilloscope Recording for a Four-Bar Target (Number 5) in Noise (160)

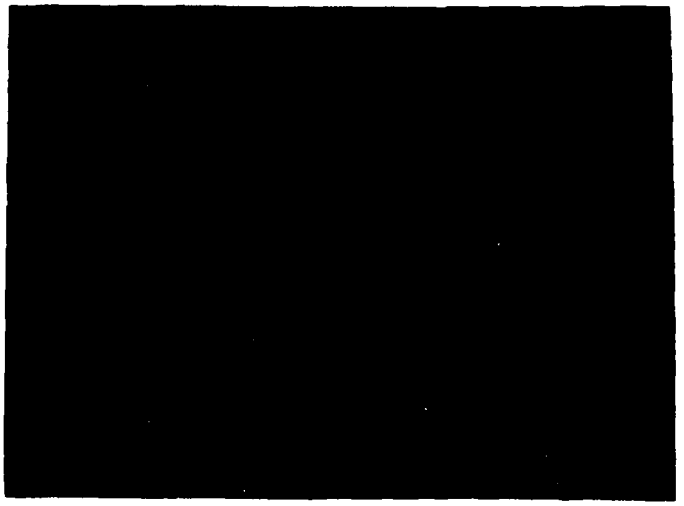

Figure B-25. Photograph of Four-Bar Target (Number 2) in Noise (200)

The tangential method and the simulation itself depended on a Gaussian distribution of noise levels. This was also verified by obtaining the list of digital pixel values stored in computer memory that determined noise signal. The distribution of pixel values was found not to deviate significantly from the assumed Guassian distribution.

APPENDIX C

INDIVIDUAL SUBJECT DATA

Each cell of the following tables represents the number of correct responses out of 10 trials, unless otherwise specified, for both four-bar and square targets. Both signal top (digital value) and target contrast are indicated for the five luminance levels under each noise condition. Target contrast was calculated as follows:

$$\text{target contrast} = \frac{\text{signal top - signal base (200)}}{\text{signal top + signal base}}$$

TABLE C-1. FLIR 1: DETECTION--TARGET 2

	Noise Level 40					Noise Level 80					Noise Level 160				
	1	2	3	4	5	1	2	3	4	5	1	2	3	4	5
Signal Top:	210	220	240	280	400										
Target Contrast:	0.024	0.048	0.091	0.167	0.333										
Subjects A	7	10	9	10	10										
B	9	10	10	10	10										
C	8	10	10	10	10										
D	10	10	10	10	10										
E															
F															
G															
H															
I															
J															
K															
L															
Mean $\bar{x}$	85.00	100.00	97.50	100.00	100.00										

TABLE C-2. FLIR 1: DETECTION--TARGET 3

	Noise Level 40					Noise Level 80					Noise Level 160				
	1	2	3	4	5	1	2	3	4	5	1	2	3	4	5
Signal Top:	220	260	320	400	495	220	260	320	400	465	220	250	290	340	405
Target Contrast:	0.048	0.130	0.231	0.333	0.424	0.048	0.130	0.231	0.333	0.398	0.048	0.111	0.184	0.259	0.339
Subjects A	10					10					6/9				
B	10					10					9/9				
C	10					10					9/9				
D	10					10					9/9				
E	10	10	10	10	10	10	10	10	10	10	9	10	10	10	10
F	10	10	10	10	10	10	9	10	10	10	9	10	10	10	10
G	10	10	10	10	10	10	10	10	10	10	9	10	10	10	10
H	10	10	9	9	8	10	10	8	9	10	7	10	8	10	8
I	10	9	10	10	10	9	10	10	10	10	9	10	10	10	10
J	10	10	10	10	10	10	10	9	10	9	10	10	10	10	10
K	9	10	10	10	10	10	10	10	10	10	10	10	10	8	10
L	10	10	10	10	10	10	10	10	10	10	9	9	9	9	10
Mean $\bar{x}$	99.17	98.75	98.75	98.75	97.50	99.17	98.75	96.25	98.75	98.75	90.56	98.75	96.25	96.25	97.50

TABLE C-3. FLIR 1: DETECTION--TARGET 4

		Noise Level 40					Noise Level 80					Noise Level 60				
		1	2	3	4	5	1	2	3	4	5	1	2	3	4	5
Signal Top:		204	208	216	232	264	204	208	216	232	264	208	214	220	234	264
Target Contrast:		0.010	0.020	0.038	0.074	0.138	0.010	0.020	0.038	0.074	0.138	0.020	0.034	0.048	0.078	0.138
Subjects	A	6/9	8/11	10	9/9	11/11	6/9	10/11	9/9	11/11	10	8	7	9/9	10/11	10
	B	7/9	11/11	10	9/9	11/11	9/9	11/11	9/9	11/11	10	8	9	9/9	11/11	10
	C	7/9	11/11	10	9/9	11/11	4/9	10/11	9/9	11/11	10	5	5	8/9	11/11	10
	D	6/9	10/11	10	9/9	11/11	4/9	10/11	9/9	11/11	10	9	7	9/9	10/11	10
	E															
	F	7	8	10	10		6	8	10	10		7	10		10	
	G	7	9	10	10		5	9	10	10		7	7		10	
	H															
	I	10	10	10	10		4	7	6	7		5	8		10	
	J															
	K															
	L															
Mean $\bar{x}$		75.56	90.52	100.00	100.00	100.00	57.94	87.53	94.29	95.17	100.00	70.00	75.70	97.22	94.57	100.00

TABLE C-4. FLIR 1: DETECTION--TARGET 5

	Noise Level 40					Noise Level 80					Noise Level 160				
	1	2	3	4	5	1	2	3	4	5	1	2	3	4	5
Signal Top:	202	204	208	216	232	202	204	208	216	232	202	204	208	216	232
Target Contrast:	0.005	0.010	0.020	0.038	0.074	0.005	0.010	0.020	0.038	0.074	0.005	0.010	0.020	0.038	0.074
Subjects A	3	8	10	10	10	3/9	8/11	8/9	11/11	10		7	8	10/11	9/9
B	4	7	10	10	10	8/9	9/11	7/9	11/11	10		6	8	11/11	9/9
C	2	5	9	10	10	0	1/11	8/9	11/11	9		8	5	11/11	9/9
D	6	8	10	10	10	4/9	8/11	9/9	11/11	10		5	6	11/11	9/9
E	8	9	10	10	10	8	8	10	10	10	8	6	5	10	10
F	2	6	9	10	10	3	7	10	10	10	4	6	5	10	10
G	8	9	10	10	10	8	6	9	10	10	5	3	7	10	10
H	6	9	7	10	10	6	5	6	10	9	7	5	6	6	10
I	8	8	10	10	10	5	4	10	10	10	6	8	6	10	10
J	3	9	10	10	10	4	8	7	5	8	5	6	8	10	10
K	4	5	10	10	10	3	8	7	5	5	5	6	9	9	10
L	7	8	10	10	10	5	5	9	10	10	5	3	8	10	10
Mean $\bar{x}$	50.85	75.83	95.83	100.00	100.00	48.89	62.28	86.38	91.67	92.50	56.25	57.50	67.50	95.08	100.00

TABLE C-5. FLIR 1: DETECTION--TARGET 6

	Noise Level 40					Noise Level 80					Noise Level 160				
	1	2	3	4	5	1	2	3	4	5	1	2	3	4	5
Signal Top:	202	204	208	214	222	202	204	208	214	222	202	204	208	214	222
Target Contrast:	0.005	0.010	0.020	0.034	0.052	0.005	0.010	0.020	0.034	0.052	0.005	0.010	0.020	0.034	0.052
Subjects A	5	7	10/11			4	6	9				5	3	9/9	
B	7	4	11/11			6	6	10				7	6	9/9	
C	1	7	11/11			3	6	8				2	4	9/9	
D	8	5	11/11			6	7	10				7	5	9/9	
E	6	4	10	10	10	8	5	9	10	10	8	6	6	10	10
F	3	7	10	10	10	3	6	10	10	10	5	7	7	10	10
G	5	7	10	10	10	7	5	10	10	10	7	6	8	10	10
H	8	5	9	9	10	7	6	7	10	10	6	8	3	7	10
I	8	9	9	10	9	6	6	9	10	10	4	4	7	9	10
J	4	2	10	10	10	7	5	9	9	10	5	6	8	10	10
K	3	6	8	10	9	7	5	8	10	10	6	6	7	10	10
L	8	6	10	10	10	4	4	9	10	10	7	8	8	9	10
Mean $\bar{x}$	55.00	60.00	95.91	98.75	97.50	56.67	55.83	90.00	98.75	100.00	60.00	60.00	60.00	95.83	100.00

TABLE C-6. FLIR 1: RECOGNITION--TARGET 2

	Noise Level 40					Noise Level 80					Noise Level 160				
	1	2	3	4	5	1	2	3	4	5	1	2	3	4	5
Signal Top:	210	220	240	290	400										
Target Contrast:	0.024	0.048	0.091	0.180	0.333										
Subjects A	6	7	6	5	4										
B	5	5	7	4	5										
C	6	5	7	5	4										
D	6	5	7	4	4										
E															
F															
G															
H															
I															
J															
K															
L															
Mean $\bar{x}$	57.50	55.00	67.50	45.00	42.50										

TABLE C-7. FLIR 1: RECOGNITION--TARGET 3

	Noise Level 40					Noise Level 80					Noise Level 160				
	1	2	3	4	5	1	2	3	4	5	1	2	3	4	5
Signal Top:	220	260	320	400	495	220	260	320	400	495	220	250	290	340	405
Target Contrast:	0.048	0.130	0.231	0.333	0.424	0.048	0.130	0.231	0.333	0.424	0.048	0.130	0.231	0.333	0.424
Subjects A	5					5					6/9				
B	5					5					5/9				
C	5					5					7/9				
D	5					5					5/9				
E	5	9	9	7	10	6	9	9	9	10	5	4	6	4	4
F	6	5	6	6	4	8	4	8	5	7	4	6	7	4	5
G	8	8	8	9	9	6	9	10	10	10	5	4	6	6	8
H	7	7	5	5	7	2	6	5	7	8	5	2	4	6	6
I	8	5	8	7	9	6	6	7	6	4	6	5	7	4	4
J	3	7	7	3	4	3	6	9	5	3	4	5	9	4	3
K	8	7	9	1	4	2	5	7	6	6	5	4	6	3	3
L	7	9	9	10	10	6	8	9	7	10	3	5	3	5	6
Mean $\bar{x}$	60.00	71.25	76.25	60.00	71.25	49.17	63.75	80.00	68.75	72.50	52.13	43.75	60.00	45.00	46.25

TABLE C-8. FLIR 1: RECOGNITION--TARGET 4

	Noise Level 40					Noise Level 80					Noise Level 160				
	1	2	3	4	5	1	2	3	4	5	1	2	3	4	5
Signal Top:	204	208	216	232	264	204	208	216	232	264	204	208	216	232	264
Target Contrast:	0.010	0.020	0.038	0.074	0.138	0.010	0.020	0.038	0.074	0.138	0.010	0.020	0.038	0.074	0.138
Subjects A	4/9	6/11	9	9/9	11/11	2/9	6/11	7/9	10/11	10	6	5	7/9	7/11	10
B	5/9	6/11	10	8/9	11/11	5/9	11/11	9/9	11/11	10	7	5	8/9	10/11	10
C	5/9	10/11	10	9/9	11/11	4/9	8/11	6/9	11/11	10	4	5	7/9	11/11	10
D	4/9	7/11	10	9/9	10/11	2/9	7/11	8/9	11/11	10	5	4	8/9	6/11	10
E															
F	4	6	8	10		4	5	7	10		1	7		10	
G	3	4	9	10		2	6	9	10		5	2		5	
H															
I	6	6	9	9		3	6	5	6		4	3		10	
J															
K															
L															
Mean $\bar{x}$	47.14	60.57	92.86	96.98	97.73	33.49	65.84	77.62	92.30	100.00	45.71	44.29	83.33	79.87	100.00

TABLE C-9. FLIR 1: RECOGNITION--TARGET 5

		Noise Level 40					Noise Level 80					Noise Level 160				
		1	2	3	4	5	1	2	3	4	5	1	2	3	4	5
Signal Top:		202	204	208	216	232	202	204	208	216	232	202	204	208	216	232
Target Contrast:		0.005	0.010	0.020	0.038	0.074	0.005	0.010	0.020	0.038	0.074	0.005	0.010	0.020	0.038	0.074
Subjects	A	2	4	9	9	10	2/9	5/11	6/9	7/11	10		3	4	9/11	9/9
	B	3	6	9	10	10	5/9	6/11	7/9	11/11	10		4	6	11/11	9/9
	C	1	3	8	10	10	0	1/11	8/9	10/11	9		1	4	10/11	9/9
	D	2	7	8	10	10	3/9	6/11	7/9	11/11	10		2	5	11/11	9/9
	E	6	8	10	10	10	5	6	10	10	10	3	10	4	8	10
	F	2	4	9	10	9	2	4	6	10	10	1	3	1	9	10
	G	6	7	9	10	10	3	5	5	10	10	4	1	6	8	10
	H	5	5	7	10	10	5	4	5	10	9	5	3	4	2	8
	I	4	5	8	10	10	4	3	10	10	10	3	6	4	7	10
	J	6	7	10	10	10	1	4	5	4	7	1	5	3	7	10
	K	2	2	8	10	10	2	5	4	4	5	2	4	6	9	10
	L	3	5	10	10	10	3	3	8	10	10	4	1	2	9	10
Mean $\bar{x}$		35.00	52.50	92.08	99.17	99.17	30.00	41.97	70.09	86.21	91.67	28.75	35.83	40.83	80.73	98.33

TABLE C-10. FLIR1: RECOGNITION--TARGET 6

	Noise Level 40					Noise Level 80					Noise Level 160				
	1	2	3	4	5	1	2	3	4	5	1	2	3	4	5
Signal Top:	202	204	208	214	222	202	204	208	214	222	202	204	208	214	222
Target Contrast:	0.005	0.010	0.020	0.034	0.052	0.005	0.010	0.020	0.034	0.052	0.005	0.010	0.020	0.034	0.052
Subjects A	5	4	10/11			3	3	7				3	2	9/9	
B	3	3	11/11			4	4	10				5	5	9/9	
C	0	7	11/11			2	5	8				2	3	9/9	
D	3	5	11/11			3	5	8				5	4	9/9	
E	3	4	10	10	10	5	4	9	10	10	6	4	6	10	10
F	3	6	9	10	10	3	4	10	10	10	3	3	4	10	10
G	2	6	10	10	10	3	4	10	10	10	6	2	4	10	10
H	4	4	9	9	10	3	3	5	9	9	2	7	2	3	10
I	5	7	8	9	9	4	5	9	10	10	3	2	5	9	10
J	2	2	10	10	10	6	4	9	9	10	1	5	5	9	10
K	0	6	8	10	9	5	5	6	10	10	4	4	7	10	10
L	4	5	10	10	10	3	1	9	10	10	6	3	4	9	10
Mean $\bar{x}$	28.33	49.17	95.08	97.50	86.25	36.67	39.17	83.33	97.50	98.75	38.75	37.50	42.50	83.33	100.00

TABLE C-11. FLIR 2: DETECTION--TARGET 2

	Noise Level 40					Noise Level 80					Noise Level 160				
	1	2	3	4	5	1	2	3	4	5	1	2	3	4	5
Signal Top:	208	214	222	232	242	208	214	222	232	242	208	214	222	232	242
Target Contrast:	0.020	0.034	0.052	0.074	0.095	0.020	0.034	0.052	0.074	0.095	0.020	0.034	0.052	0.074	0.095
Subjects A	7/9	10/11	8/9	11/11		7	9	9/9	11/11						
B	9/9	10/11	9/9	11/11		9	10	9/9	11/11						
C	7/9	10/11	9/9	11/11		5	9	9/9	11/11						
D	9/9	10/11	9/9	11/11		9	8	9/9	9/11						
E	9	5	8	7	6	8	8	10	10	10	7	9	9	10	10
F						7	10	10	10	9	4	8	10	9	10
G						8	9	10	10	10	9	9	10	9	10
H	4	9	9	9	9	5	10	9	10	8	7	8	8	9	9
I						8	9	10	10	10	7	9	9	10	10
J	9	9	10	10	10	9	9	10	10	10	8	7	10	10	10
K	9	9	10	10	10	5	8	10	10	10	8	9	10	10	10
L	6	10	10	10	10	7	9	10	10	10	9	9	10	10	10
Mean $\bar{x}$	80.62	88.08	95.43	95.56	90.10	72.50	90.00	99.17	98.48	96.23	73.75	85.00	95.00	96.25	98.75

TABLE C-12. FLIR 2: DETECTION--TARGET 3

	Noise Level 40					Noise Level 80					Noise Level 160				
	1	2	3	4	5	1	2	3	4	5	1	2	3	4	5
Signal Top:	202	204	208	214	222	202	204	208	214	222	202	204	208	214	222
Target Contrast:	0.005	0.010	0.020	0.034	0.052	0.005	0.010	0.020	0.034	0.052	0.005	0.010	0.020	0.034	0.052
Subjects A	5	8	9	10	10	5/9	10/11	9/9	11/11	9		3/9	9	11/11	9/9
B	5	7	10	10	10	2/9	9/11	9/9	11/11	10		4/9	6	11/11	9/9
C	3	7	10	9	10	2/9	6/11	8/9	11/11	9		2/9	6	11/11	8/9
D	6	4	10	10	10	5/9	6/11	8/9	11/11	10		5/9	4	7/11	8/9
E	3	5	8	10	10						5	6	5	6	7
F	3	9	6	9	10	6	8	9	8	10	5	6	8	10	10
G	7	8	10	10	10	3	8	8	9	10	5	3	7	9	10
H	6	7	7	9	9						5	8	6	8	9
I	6	7	10	10	9	7	7	8	10	10	6	6	7	9	9
J	8	7	9	10	8						6	6	6	10	10
K	3	5	7	8	9						4	4	7	8	10
L	8	5	8	10	10						6	7	5	8	10
Mean $\bar{x}$	52.50	67.50	86.67	95.83	95.83	45.08	75.97	89.68	95.71	97.14	52.50	51.30	63.33	86.97	93.98

TABLE C-13. FLIR 2: DETECTION--TARGET 4

		Noise Level 40					Noise Level 80					Noise Level 160				
		1	2	3	4	5	1	2	3	4	5	1	2	3	4	5
Signal Top:		202	204	208	214	222	202	204	208	214	222	202	204	208	214	222
Target Contrast:		0.005	0.010	0.020	0.034	0.052	0.005	0.010	0.020	0.034	0.052	0.005	0.010	0.020	0.034	0.052
Subjects	A	3	5/9	10/11	9	10	6/9	8/11	9/9	11/11	10		5	7	10	10
	B	7	7/9	11/11	10	10	5/9	9/11	9/9	11/11	10		9	10	10	10
	C	5	8/9	11/11	10	10	2/9	9/11	9/9	11/11	10		9	7	9	10
	D	8	6/9	11/11	10	10	6/9	8/11	9/9	11/11	10		7	5	10	10
	E	7	10	9	10	10	9	9	9	10	10	8	6	7	10	10
	F	7	9	8	10	10	5	5	9	10	10	2	9	10	9	10
	G	8	7	10	10	10	5	6	7	7	9	4	2	9	9	10
	H	5	6	9	10	10	6	4	8	9	10	7	6	4	9	1
	I	9	6	9	9	10	6	7	9	9	10	7	7	9	9	1
	J	6	10	9	10	10	6	6	10	9	10	5	6	8	10	10
	K	5	8	7	10	10	7	7	7	8	10	6	7	7	10	10
	L	2	7	10	10	10	6	8	10	10	10	7	5	10	10	10
Mean $\bar{x}$		60.00	76.57	91.74	98.33	100.00	59.26	69.09	90.83	93.33	99.17	57.50	65.00	73.33	95.83	100.00

TABLE C-14. FLIR 2: DETECTION--TARGET 5

	Noise Level 40					Noise Level 80					Noise Level 160				
	1	2	3	4	5	1	2	3	4	5	1	2	3	4	5
Signal Top:	202	204	208	214	222	202	204	208	214	222	202	204	208	214	222
Target Contrast:	0.005	0.010	0.020	0.034	0.052	0.005	0.010	0.020	0.034	0.052	0.005	0.010	0.020	0.034	0.052
Subjects A	3/9	5	9	8	9/11	6/9	9	11/11	9/9	11/11		6	10	11/11	9/9
B	4/9	9	10	9	11/11	4/9	9	10/11	8/9	11/11		7	10	11/11	9/9
C	3/9	9	10	9	11/11	3/9	9	11/11	9/9	11/11		8	10	11/11	9/9
D	7/9	8	9	9	11/11	7/9	7	11/11	9/9	11/11		7	9	10/11	9/9
E	4	9	10	10	10	7	9	10	10	10	7	9	9	10	10
F	6	6	9	10	10	6	9	9	10	10	5	4	10	10	10
G	8	8	10	10	10	6	5	10	10	9	5	10	10	10	10
H	4	8	9	9	9	3	9	7	9	10	6	7	7	10	9
I	8	8	9	10	10	8	8	10	10	10	8	6	8	7	8
J	3	6	9	10	10	8	10	10	10	10	7	5	7	10	9
K	7	6	7	10	10	7	6	8	10	10	4	6	8	10	10
L	3	8	10	10	10	5	10	10	10	10	6	9	8	10	10
Mean $\bar{x}$	51.54	75.00	92.50	95.00	96.89	60.19	75.00	94.24	98.24	99.17	60.00	70.00	88.33	96.74	96.67

TABLE C-15. FLIR 2: DETECTION--TARGET 6

	Noise Level 40					Noise Level 80					Noise Level 160				
	1	2	3	4	5	1	2	3	4	5	1	2	3	4	5
Signal Top:	202	204	208	214	222	202	204	208	214	222	202	204	208	214	222
Target Contrast:	0.005	0.010	0.020	0.034	0.052	0.005	0.010	0.020	0.034	0.052	0.005	0.010	0.020	0.034	0.052
Subjects A	3	6	8/9	10/11	10							4	8	10	10
B	6	9	9/9	11/11	10							6	10	10	10
C	4	8	9/9	11/11	10							5	9	10	10
D	5	5	8/9	11/11	10							5	7	9	10
E	6	8	10	10	10	4	5	9	10	10	5	5	9	10	10
F	3	4	10	10	10	6	6	10	10	10	3	8	5	10	10
G	6	4	10	10	10	5	5	10	10	10	4	6	8	10	10
H	5	7	9	10	9	4	7	9	9	10	8	9	8	10	10
I	5	5	10	9	10	6	8	7	10	10	6	4	9	10	9
J	8	4	10	9	10	3	6	9	10	10	7	7	8	10	10
K	6	5	8	10	10	6	7	8	10	9	2	5	9	10	10
L	6	6	10	10	10	4	7	10	10	10	5	3	8	10	10
Mean $\bar{x}$	52.50	59.17	95.65	97.58	99.17	47.50	63.75	90.00	98.75	98.75	50.00	55.83	81.67	99.17	99.17

TABLE C-16. FLIR 2: RECOGNITION--TARGET 2

	Noise Level 40					Noise Level 80					Noise Level 160				
	1	2	3	4	5	1	2	3	4	5	1	2	3	4	5
Signal Top:	208	214	222	232	242	208	214	222	232	242	208	214	222	232	242
Target Contrast:	0.020	0.034	0.052	0.074	0.095	0.020	0.034	0.052	0.074	0.095	0.020	0.034	0.052	0.074	0.095
Subjects A	6/9	5/11	4/9	7/11		5	5	5/9	7/11						
B	6/9	6/11	8/9	8/11		7	7	9/9	9/11						
C	5/9	6/11	6/9	6/11		4	6	7/9	7/11						
D	8/9	8/11	9/9	9/11		4	6	8/9	9/11						
E	6	2	8	6	5	3	5	6	6	9	6	6	7	6	7
F						3	3	10	7	5	1	2	6	6	5
G						3	5	7	4	6	2	4	6	7	7
H	2	5	7	8	7	4	5	6	4	5	5	4	4	6	4
I						7	5	7	5	4	3	7	8	6	5
J	3	4	5	8	9	3	5	5	8	9	3	2	6	8	8
K	4	7	7	8	3	3	5	6	8	3	1	3	7	7	5
L	3	5	9	9	9	2	6	7	9	9	6	5	6	8	6
Mean $\bar{x}$	50.86	50.81	73.33	73.64	66.00	40.00	52.50	71.85	75.83	90.00	33.75	41.25	62.50	67.50	58.75

TABLE C-17. FLIR 2: RECOGNITION--TARGET 3

	Noise Level 40					Noise Level 80					Noise Level 160				
	1	2	3	4	5	1	2	3	4	5	1	2	3	4	5
Signal Top:	202	204	208	214	222	202	204	208	214	222	202	204	208	214	222
Target Contrast:	0.005	0.010	0.020	0.034	0.052	0.005	0.010	0.020	0.034	0.052	0.005	0.010	0.020	0.034	0.052
Subjects A	4	3	6	5	8	4/9	5/11	5/9	4/11	8		3/9	5	7/11	7/9
B	3	6	9	9	10	2/9	5/11	7/9	11/11	10		3/9	6	10/11	9/9
C	2	6	10	8	10	0	4/11	7/9	11/11	9		0	4	9/11	6/9
D	4	1	10	10	10	3/9	3/11	7/9	11/11	10		4/9	4	5/11	8/9
E	1	4	7	10	10						2	3	3	4	5
F	2	4	4	4	8	4	3	4	5	10	4	3	5	5	10
G	5	6	8	10	10	2	4	7	9	10	1	1	1	6	8
H	5	6	7	9	8						4	5	6	5	6
I	3	6	8	10	9	5	5	8	9	10	5	4	4	6	9
J	4	5	9	9	8						1	5	3	9	8
K	1	3	5	5	3						2	2	6	3	6
L	2	4	6	10	10						3	2	5	6	9
Mean $\bar{x}$	30.00	46.67	74.17	82.50	86.67	30.00	39.42	67.41	80.91	95.41	27.50	30.09	47.50	60.15	78.61

TABLE C-18. FLIR 2: RECOGNITION--TARGET 4

	Noise Level 40					Noise Level 80					Noise Level 160				
	1	2	3	4	5	1	2	3	4	5	1	2	3	4	5
Signal Top:	202	204	208	214	222	202	204	208	214	222	202	204	208	214	222
Target Contrast:	0.005	0.010	0.020	0.034	0.052	0.005	0.010	0.020	0.034	0.052	0.005	0.010	0.020	0.034	0.052
Subjects A	3	5/9	9/11	7	10	2/9	6/11	7/9	10/11	10		4	6	10	9
B	5	5/9	11/11	10	10	5/9	8/11	9/9	11/11	9		7	9	10	10
C	4	8/9	11/11	10	10	1/9	7/11	9/9	11/11	10		7	7	9	9
D	6	7/9	11/11	9	10	4/9	7/11	9/9	11/11	10		5	3	10	10
E	5	9	9	10	10	5	8	8	10	10	5	4	4	10	10
F	5	6	7	10	10	3	4	9	10	10	2	4	7	9	10
G	3	5	10	10	10	4	5	7	7	9	3	1	5	9	10
H	4	4	9	10	10	2	2	7	9	9	4	2	4	8	10
I	5	4	8	9	10	3	6	7	9	10	7	6	7	9	9
J	3	9	9	10	10	4	3	10	9	10	3	2	8	10	10
K	4	6	5	8	10	3	5	5	6	10	2	3	6	8	10
L	1	7	10	10	10	5	5	9	10	10	1	4	7	10	10
Mean $\bar{x}$	40.00	64.81	87.65	94.17	100.00	35.28	52.88	83.19	90.76	97.50	33.75	40.83	60.83	93.33	97.50

TABLE C-19. FLIR 2: RECOGNITION--TARGET 5

	Noise Level 40					Noise Level 80					Noise Level 160				
	1	2	3	4	5	1	2	3	4	5	1	2	3	4	5
Signal Top:	202	204	208	214	222	202	204	208	214	222	202	204	208	214	222
Target Contrast:	0.005	0.010	0.020	0.034	0.052	0.005	0.010	0.020	0.034	0.052	0.005	0.010	0.020	0.034	0.052
Subjects A	2/9	2	9	8	9/11	3/9	7	10/11	9/9	11/11		4	6	11/11	9/9
B	4/9	9	10	9	11/11	4/9	9	10/11	9/9	11/11		5	10	11/11	9/9
C	3/9	9	10	9	11/11	2/9	9	11/11	9/9	11/11		8	10	11/11	9/9
D	5/9	8	9	9	9/11	4/9	6	11/11	9/9	11/11		3	8	10/11	9/9
E	0	9	10	10	10	1	7	10	10	10	3	8	7	10	10
F	5	6	9	10	10	5	6	8	10	10	2	2	8	10	10
G	6	7	10	9	10	3	3	9	10	10	3	8	10	10	10
H	2	7	8	9	9	1	6	7	9	10	4	7	6	9	9
I	3	6	8	10	10	6	7	9	9	10	5	5	7	7	7
J	6	5	9	10	10	3	9	10	10	10	3	4	7	10	9
K	4	5	6	10	10	4	6	8	10	10	2	5	8	10	10
L	2	8	10	10	10	4	9	10	10	10	5	7	6	10	10
Mean $\bar{x}$	36.30	67.50	90.00	94.17	97.65	34.54	70.00	90.98	98.33	100.00	33.75	55.00	77.50	95.91	95.83

TABLE C-20. FLIR 2: RECOGNITION--TARGET 6

	Noise Level 40					Noise Level 80					Noise Level 160				
	1	2	3	4	5	1	2	3	4	5	1	2	3	4	5
Signal Top:	202	204	208	214	222	202	204	208	214	222	202	204	208	214	222
Target Contrast:	0.005	0.010	0.020	0.034	0.052	0.005	0.010	0.020	0.034	0.052	0.005	0.010	0.020	0.034	0.052
Subjects A	2	4	6/9	10/11	9							3	5	10	10
B	3	9	9/9	11/11	10							6	9	10	10
C	2	8	9/9	11/11	10							4	9	10	10
D	3	5	8/9	11/11	10							3	7	9	10
E	3	7	10	10	10	3	5	9	10	10	4	4	8	9	10
F	3	9	10	10	10	4	5	10	10	10	3	6	5	10	10
G	3	4	10	10	10	3	5	10	10	10	1	5	7	10	10
H	3	6	9	10	9	4	2	8	9	10	2	5	5	10	10
I	4	4	9	8	10	4	8	7	10	10	4	3	7	10	9
J	6	3	10	8	10	0	5	9	10	10	3	3	5	10	10
K	3	4	8	10	10	5	4	8	10	9	1	4	9	10	10
L	2	5	10	10	10	3	6	10	10	10	4	2	5	8	8
Mean $\bar{x}$	30.88	56.67	92.96	95.91	98.33	32.50	50.00	88.75	98.75	98.75	27.50	40.00	67.50	96.67	97.50

BIBLIOGRAPHY

Baker, C. A. and Nicholson, R. M. "Raster Scan Parameters and Target Identification," 1967 Proceedings, National Aerospace Electronics Conference, Dayton, OH, May 1967, 285-290.

Baldwin, W. J. "Evaluation of Background Suppression Techniques for 3-5 Micrometer Solid State Imagers," Contract No. DAAK02-73-C-0048 Final Report, General Electric, Syracuse, NY, May 1974.

Barbe, D. F. "Charge-Coupled Device and Charge-Injection Device Imaging," IEEE Journal of Solid State Circuits, SC-11(1), 1976, 109-114.

Biberman, L. M. "A Guide for the Preparation of Specifications for Real-Time Thermal Imaging Systems," IDA Paper P-676, Institute for Defense Analyses, Science and Technology Division, Arlington, VA, January 1971.

Biberman, L. M. "Fallacy and Fact of Sampled Imagery Displays," Human Factors, 16(3), 1974, 286-299.

Biberman, L. M. "Effect of Weather at Hannover, Federal Republic of Germany, on Performance of Electro-Optical Imaging Systems, Part 1: Theory, Methodology and Data Base." Paper P-1123, Institute for Defense Analyses, Arlington, VA, August 1976.

Bower, F.H. "CCD Fundamentals," Military Electronics/Counter-Measures, 4(2), 1978, 16-17, 28-29, 32, 34.

Charman, W. N. and Olin, A. "Image Quality Criteria for Aerial Camera Systems," Photographic Science and Engineering, 9(6), 1965, 385-397.

Coluccio, T. L., MacLeod, S., and Maier, J. J. "Effect of Image Contrast and Resolution on Photointerpreter Target Detection and Identification," Journal of the Optical Society of America, 59(11), 1969, 1478-1481.

Corsi, C. "Infrared Detector Arrays by New Technologies," Proceedings of the IEEE, 63(1), 1975, 14-26.

Decker, P. R. "An Experimental Investigation of the Minimum Resolvable Temperature (MRT) Difference Test and Comparison with Mathematical Models," Report No. NWC TP 5890, Naval Weapons Center, China Lake, CA, July 1976.

Dyall, W. T. "Televiewers: What Do You Mean By High Resolution?" Electro-Optical Systems Design, 10 (March), 1978, 26-29.

Erickson, R. A. "Line Criteria in Target Acquisition with Television," Human Factors, 20(5), 1978, 573-588.

Farrell, R. J. and Booth, J. M. Design Handbook for Imagery Interpretation Equipment. Boeing Aerospace Company, Seattle, WA, 1975.

Ginsburg, A. P. "Relating Detection and Identification of Snellen Letters to the Spatial Filtering Characteristics of the Human Visual System," Paper presented to the Annual Meeting of the Aerospace Medical Association, Washington, DC, May 1979.

Hanson, T. G., Jones, D., Macek, A. J., Peters, G. L., Sandvig, J. H. "Research on Visual Display Integration for Advanced Fighter Aircraft," Report No. AMRL, Aerospace Medical Research Laboratory, Air Force Systems Command, Wright-Patterson AFB, Dayton, OH, July 1978.

Hirshberg, I. "The Charge-Coupled Technology Bursts through Imaging Limits," Optical Spectra, 9(11), 1975, 28-33.

Hollanda, P. A., Scott, F., and Harabedian, A. "The Informative Value of Sampled Images as a Function of the Number of Scan Lines Per Scene Object and the Signal-to-Noise Ratio," Photographic Science and Engineering, 14(6), 1970, 407-412.

Hudson, R. D., Jr. and Hudson, J. W. "The Military Applications of Remote Sensing by Infrared," Proceedings of the IEEE, 63(1), 1975, 104-128.

Humes, J. M. and Bauerschmidt, D. K. "Low Light Level TV Viewfinder Simulation Program; Phase B - The Effects of Television System Characteristics upon Operator Target Recognition Performance," Technical Report AFAL-TR-68-271, Autonetics Division of North American Rockwell Corporation, November 1968.

Johnson, J. "Analysis of Image Forming Systems," Proceedings of the Image Intensifier Sympsium, October 1958, 249-273.

[redacted]

Jones, D. B., Freitag, M., and Collyer, S. C. Air-to-Ground Target Acquisition Source Book: A Review of the Literature. Martin-Marietta Corporation, Orlando, FL, September 1974. Sponsored by the Office of Naval Research, Arlington, VA.

Klass, P. J. "Infrared Systems Commonality Pressed," Aviation Week and Space Technology, September 3, 1973, 17.

Kruse, P. W. "Future FLIR Technology," Internal paper, Corporate Research Center, Honeywell, Inc., Bloomington, MN, December 1976. Honeywell Proprietary.

Levinstein, H. and Mudar, J. "Infrared Detectors in Remote Sensing," *Proceedings of the IEEE*, 63(1), 1975, 6-14.

Levinstein, H. "Infrared Detectors," Physics Today, 30(11), 1977, 23-28.

Lewis, T. T. "The Future of CIDs and CCDs," Interview in Electro-Optical Systems Design, 10(8), 1978, 76-77.

Lloyd, J. M. "State-of-the-Art for Thermal Imagery," Optical Engineering, 14(1), 1975, 50-56. (a)

Lloyd, J. M. Thermal Imaging Systems. New York: Plenum Press, 1975. (b)

Maldonato, E. D. "Forward Looking Infrared Simulation," Report No. TN-39, Department of the Navy, Naval Training Equipment Center, Orlando, FL, July 1974.

Mengers, P. "Low Contrast Imaging," Electro Optical Systems Design, 10(10), 1978, 20-26.

Miller, B. "FLIR Gaining Wider Acceptance," Aviation Week and Space Technology, May 7, 1973, 42-49. (a)

Miller, B. "Cost Reductions Key to Wider FLIR Use," Aviation Week and Space Technology, May 21, 1973, 48-53. (b)

Miller, J. Personal Communication, 1979.

Mortensen, C. A. "PROTOCOL for Human Operator Interface with FLIR Display Tests, Internal paper, Electro-Optical Center, Honeywell, Inc., Lexington, MA, December 1978.

Narendra, P. M., Tack, D. H., and Joseph, J. D. "Image Enhancement Algorithms, Analysis, and Implementation," Part I of Final Report on Automated Image Enhancement Techniques for Second Generation FLIR, Contract No. DAAG53-76-C-0915, Systems and Research Center, Honeywell, Inc., Minneapolis, MN, December 1977.

Patel, A. S. "Spatial Resolution by the Human Visual System: The Effect of Mean Retinal Illuminance," Journal of the Optical Society of America, 56(5), 1966, 689-694.

"Poise Sensor Design Evaluation Study," Contract No. DAAG53-76-C-0213, Avionics Division, Honeywell, Inc., Minneapolis, MN, March 1977.

Pratt, P. Personal communication, 1975.

"Real-Time FLIR Image Enhancement," Internal paper, Systems and Research Center, Honeywell, Inc., Minneapolis, MN, July 1977.

Ratches, J. A., Lawson, W. E., Obert, L. P., Bergemann, R. J., Cassidy, T. W., and Swenson, J. M. "Night Vision Laboratory Static Performance Model for Thermal Viewing Systems," Report No. ECOM-7043, U.S. Army Electronics Command, Night Vision Laboratory, Fort Belvoir, VA, April 1975.

Rosell, F. A. "Levels of Visual Discrimination for Real Scene Objects vs. Bar Pattern Resolution for Aperture and Noise-Limited Imagery," Proceedings of the IEEE 1975 National Aerospace and Electronics Conference, NAECON '75, Dayton, OH, June 1975, 327-334.

Rosell, F. A. and Willson, R. H. "Recent Psychophysical Experiments and the Display Signal-to-Noise Ratio Concept," in L. M. Biberman (ed.), Perception of Displayed Information. New York: Plenum Press, 1973.

Sachs, F. A. "Solid State Imaging Systems," Electro-Optical Systems Design, 7(10), 1975, 34-38.

Sachs, F. A. "Which Solid State Imager: CID CCD?" Interview in Electro-Optical Systems Design, 10(8), 1978, 70-75.

Savoye, F. D. "Which Solid State Imager: CID CCD?" Interview in Electro-Optical Systems Design, 10(8), 1978, 70-75.

Scanlan, L. A. "Target Acquisition Model Development: Effect of Realistic Terrain," Technical Report P76-484, Hughes Aircraft Company, Culver City, CA, December 1976.

Schade, O. H. "Modern Image Evaluation and Television (The Influence of Electronic Television on the Methods of Image Evaluation)," Applied Optics, 3(1), 1964, 17-21.

Schnitzler, A. D. "Image-Detector Model and Parameters of the Human Visual System," Journal of the Optical Society of America, 61(11), 1973, 1357-1368.

Schober, H. A. W. and Hilz, R. "Contrast Sensitivity of the Human Eye for Square-Wave Gratings," Journal of the Optical Society of America, 55(9), 1965, 1086-1091.

Scott, F., Hollanda, P. A., and Harabedian, A. "The Informative Value of Sampled Images as a Function of the Number of Scans Per Scene Object," Photographic Science and Engineering, 14(1), 1970, 21-27.

Sendall, R. L. "Figures of Merit for IR Imaging Systems (U)," Proceedings of the Infrared Information Symposia, 15(3), January 1971, 59-68.

Sendall, R. L. and Rosell, F. A. "E/O Sensor Performance Analysis and Synthesis (TV/IR Comparison Study)," Final Report, AFAL-TR-72-374, Wright-Patterson AFB, Dayton, OH. April 1973.

Shanahan, D. "Effects of Television Bandwidth on Target Identification," Report No. NMC-TM-64-2, U.S. Naval Missile Center, Point Mugu, CA, April 1964 (AD/435746).

Snyder, H. L. "Image Quality and Observer Performance," in L. M. Biberman (ed.), Perception of Displayed Information. New York: Plenum Press, 1973.

Snyder, L. L. "Image Quality and Face Recognition on a Television Display," Human Factors, 16(3), 1974, 300-307.

Snyder, H. L., Keese, R. L., Beaman, W. S., and Aschenbach, J. R. "Visual Search and Image Quality," Report No. AMRL-TR-73-114, Aerospace Medical Research Laboratory, Wright-Patterson AFB, Dayton, OH, October 1974.

Snyder, H. L. "Visual Search and Image Quality: Final Report," Report No. AMRL-TR-76-89, Aerospace Medical Research Laboratory, Aerospace Medical Division, Air Force Systems Command, Wright-Patterson AFB, Dayton, OH, December 1976.

Swets, J. A. "Indices of Signal Detectability Obtained with Various Psychophysical Procedures," in John A. Swets (ed.) Signal Detection and Recognition by Human Observers. New York: John Wiley and Sons, 1964.

Task, H. L. "An Evaluation and Comparison of Several Measures of Image Quality for Television Displays," Report No. AMRL-TR-79-7, Aerospace Medical Research Laboratory, Aerospace Medical Division, Air Force Systems Command, Wright-Patterson AFB, Dayton, OH, January 1979.

Task, H. L., Pinkus, A. R., and Hornseth, J. P. "A Comparison of Several Televesion Image Quality Measures," Proceedings of the S. I. D., 19(3), 1978, 113-119.

Task, H. L. and Verona, R. W. "A New Measure of Television Display Quality Relatable to Observer Performance," Report No. AMRL-TR-76-73, Aerospace Medical Research Laboratory, Aerospace Medical Division, Wright-Patterson AFB, Dayton, OH, August 1976.

Tuer, T.W. "Thermal Imaging Systems Relative Performance: 3-4 um vs 8-12 um," Technical Report AFAL-TR-76-217, Science Applications, Inc., Ann Arbor, MI, January 1977.

Williams, L. G. and Erickson, J.M. "FLIR Operator Requirements Study," Final Report No. AFAL-TR-76-9, Air Force Avionics Laboratory, Wright-Patterson AFB, Dayton, OH, April 1976.

*U.S.Government Printing Office: 1980 — 657-084/536